

2-Quinoxalinol Based Schiff Base Ligands in Copper(II)-Mediated C-H Activation

by

Yuancheng Li

A dissertation submitted to the Graduate Faculty of
Auburn University
in partial fulfillment of the
requirements for the Degree of
Doctor of Philosophy

Auburn, Alabama
Aug 4th, 2012

Keywords: 2-Quinoxalinol, Schiff Base, Copper(II), Allylic Oxidation

Copyright 2012 by Yuancheng Li

Approved by

Anne E. V. Gorden, Chair, Associate Professor of Department of Chemistry and Biochemistry
Stewart Schneller, Professor of Department of Chemistry and Biochemistry
Michael Squillacote, Associate Professor of Department of Chemistry and Biochemistry
Christian Goldsmith, Associate Professor of Department of Chemistry and Biochemistry
Jack DeRuiter, Professor of Department of Pharmacal Sciences

Abstract

As environment and energy issues become of increasing concern, so too does our awareness of the impacts of chemical industry. Numerous successful attempts toward “green” or “greener” chemistry have been made. Among these, transition metal mediated homogeneous catalysis is of great interest to us because of its broad capability and fundamental importance.

In this dissertation, Cu(II) catalyzed allylic oxidation reactions are investigated. 2-quinoxalinol is introduced as the backbone to a series of new salen ligands to adjust the electronic properties of their Cu(II) complexes. The allylic oxidation of steroids is investigated using *tert*-butyl hydroperoxide (TBHP) as the oxidant. A variety of Δ^5 -steroidal substrates are selectively oxidized to the corresponding enones. Excellent yields are achieved (up to 99% under optimized conditions) while significantly reduced reaction time is required as compared to other current oxidation methods. In addition, simple olefin substrates are also oxidized using the same catalyst. Excellent yields are achieved (up to 99%) within a very short reaction time and with great tolerance for additional functional groups. Using the oxidation of simple alkenes as a probe, mechanistic studies are performed using Raman spectroscopy, cyclic voltammetry, and theoretical calculations. It is believed that the Cu(II) complex binds to TBHP to form the *tert*-butyl peroxy- Cu(II) complex that undergoes a homolytic cleavage of the O-O bond of the peroxy-. The resulting species will carry out the oxidations of substrates. Besides salen-type ligands, a tridentate Schiff base ligand with 2-quinoxalinol as backbone is also employed to the oxidation reaction. UV-Vis spectroscopy and cyclic voltammetry are employed to study the

electronic properties of such tridentate ligand bound Cu(II) complex. It has been found that the tridentate ligand bound Cu(II) complex exhibited different electronic properties from the tetradentate salen-type ligand bound Cu(II) complex. Theoretical calculation provides two different possible reaction pathways leading to the same product exist during the reaction when the tridentate ligand bound Cu(II) complex is used as catalyst. One of the pathways involves the homolytic cleavage of the O-O bond of the peroxy Cu(II) complex, while, the other pathway undergoes a direct H atom abstraction. The experimental results suggest the concurrence of two different reaction pathways.

Acknowledgments

First, I would love to express my sincere gratitude to my advisor, Dr. Anne E. V. Gordon, who has been mentoring me since I started my graduate study at Auburn University. She is not only an excellent supervisor in science, but also a very good friend in life. This dissertation would not be accomplished without her guidance and persistent help.

I would also like to thank my committee members, Dr. Stewart Schneller, Dr. Michael Squillacote, Dr. Christian Goldsmith, and Dr. Jack DeRuiter, for their help with my research, publications, and dissertation. Especially during the writing of this dissertation, they have been continuously supportive when I was overwhelmed by all kinds of things.

In addition, my deepest appreciation also belongs to my beloved wife and collaborator. Thank you!

Last but not least, I want to thank the department of chemistry and biochemistry, and all the faculties, lab-mates, and colleagues that helped me. I have learnt a lot during my study at Auburn, and I believe I will benefit from this experience through my life.

Adapted with permission from Li, Yuancheng; Wu, Xianghong; Lee, Tae Bum; Isbell, Eleanor, K.; Parish, Edward J.; Gorden, Anne E. V. *J. Org. Chem.*, **2010**, 75 (5), 1807-1810. Copyright (2010) American Chemical Society. Li, Yuancheng; Lee, Tae Bum; Wang, Tanyu; Gamble, Audrey V.; Gorden, Anne E. V. *J. Org. Chem.*, **2012**, 77 (10), 4628-4633. Copyright (2012) American Chemical Society.

Table of Contents

Abstract.....	ii
Acknowledgments.....	iv
List of Tables	vii
List of Figures.....	viii
List of Schemes.....	x
Chapter 1 Introduction.....	1
Chapter 2 Salqu Cu(II) Catalyzed Allylic Oxidation of Δ^5 -Steroids.....	15
Chapter 3 Oxidation of Simple Olefins Using a Salqu Cu(II) Complex	30
Chapter 4 2-Quinoxalinol Based Tridentate Schiff Base Ligand in Cu(II) Mediated Allylic Oxidation.....	49
Chapter 5 Conclusion and Future Work	70
Chapter 6 Experimental Section	76
References	137

List of Tables

Table 2.1 Oxidation of steroids using optimized condition.....	20
Table 2.2 Oxidation of steroids using further optimized conditions	25
Table 2.3 Calculations of free energies of model radicals.....	29
Table 3.1 Cu(II) Salqu Catalyzed Allylic Oxidation of Olefins	38
Table 4.1 Tridentate Cu(II) Complex 3 Catalyzed Allylic Oxidation of Olefins	54

List of Figures

Figure 1.1 Jacobsen's catalyst.....	5
Figure 1.2 CuSalen and tetrahydrosalen CuSalen ^{red}	11
Figure 1.3 Structures of 2-quinoxalinol, diamino-2-quinoxalinol, salqu-imine, asymmetric salqu ligand, complex 2, complex 1, complex 3.	13
Figure 2.1 Complex 1 and complex 2.....	17
Figure 2.2 Isolated yields with reaction time and isolated yields with oxidant ratio.....	18
Figure 2.3 Resonance structures of 7-radical species (upper) and 4-radical species (lower).....	27
Figure 3.1 Cu(II) salqu complex 1 and complex 2	32
Figure 3.2 Cu(II) Effects of oxidant ratio and solvents on reaction yields.....	34
Figure 3.3 Cu(II) Resonance Raman spectroscopy of Cu(II) salqu with TBHP	41
Figure 3.4 Cyclic voltamogram of Cu(II) salqu with supporting electrolyte 0.1 M tetrabutyl ammonium tetrafluoroborate in 5 mL CH ₂ Cl ₂ and 1 mM ferrocene internal standard, reference Ag/AgCl, counter electrode Pt gauze (A = 0.77 cm ²), and the working electrode was a glassy carbon disk (d = 0.3 cm, A = 0.071 cm ²)	43
Figure 3.5 Cu(II) Spin density of [LCu(III)] ⁺ with 0.0004 a.u. isosurface density (L = salen and salqu).....	45
Figure 4.1 Structures of complex 1 (catalyst for allylic oxidation), complex 2 (catalyst for benzylic oxidation), complex 3, and diamino-2-quinoxalinol	51
Figure 4.2 UV-vis spectra of salqu ligand, salqu Cu(II) complex 1, and tridentate Cu(II) complex 3.....	56
Figure 4.3 Cyclic voltamogram of salqu ligand with supporting electrolyte 0.04 M tetrabutyl ammonium tetrafluoroborate in 5 mL CH ₂ Cl ₂ , reference Ag/AgCl, counter electrode Pt gauze (A = 0.77 cm ²), and the working electrode was a glassy carbon disk (d = 0.3 cm, A = 0.071 cm ²). Scan rate = 100 mV/s	58

Figure 4.4 MS spectrum of reaction solution using regular TBHP as the oxidant under $^{18}\text{O}_2$ atmosphere	69
Figure 5.1 Structures of complex 1 (catalyst for allylic oxidation), complex 2 (catalyst for benzylic oxidation), complex 3, and diamino-2-quinoxalinol	71

List of Schemes

Scheme 1.1 Consensus Mechanism for the Oxidation Reaction Catalyzed by GOase	10
Scheme 2.1 Further optimization of reaction conditions	23
Scheme 3.1 Decomposition of <i>tert</i> -Butyl Peroxy Ether under Basic Condition	36
Scheme 3.2 Possible Reaction Pathways of LCu(II)OO <i>t</i> Bu.....	42
Scheme 3.3 Postulated Catalytic Cycle for Allylic Oxidation Catalyzed by Cu(II) Salqu.....	46
Scheme 4.1 Synthesis of 2-Quinoxalinol Based Tridenate Schiff Base Ligand.....	53
Scheme 4.2 Calculated Reaction Pathway 1 for Allylic Oxidation using Complex 3 as the Catalyst	60
Scheme 4.3 Calculated Reaction Pathway 2 for Allylic Oxidation using Complex 3 as the Catalyst	64

Chapter 1

Introduction

As we as a society are becoming increasingly conscious of the environmental impacts of chemical industry, how to make the best use of limited natural resources is of tremendous concern. One of the contributions from chemists is the proposal of the concept of “green chemistry”. Green chemistry, also known as environmentally benign chemistry or sustainable chemistry, is the philosophy of chemical research and engineering that encourages the design of products and processes that minimize the use and generation of hazardous substances.¹ The term “green chemistry” was first coined in 1991 by the chemist Paul Anastas. In 1998, Paul Anastas and John Warner developed the “12 principles of green chemistry”.¹ These principles have served as guidelines for chemists to achieve the goal of lowering the ecological footprint of industry and covered concepts including: designing processes to be atom economical (i.e, maximizing the amount of raw material that ends up in the product) using more environmentally friendly or less toxic chemicals whenever possible, including solvents; designing more energy efficient processes (e.g. eliminating purification steps), using catalytic rather than stoichiometric reagents, and reducing wastes produced instead of remediating them afterwards.¹

Great strides have been made towards the goal of “green” or “greener” chemistry since people realized its importance. Numerous successful outcomes related to the media

in which chemical reactions are performed are well documented.²⁻¹⁷ For example, the applications of ionic liquids as chemical reaction environments have been extensively investigated and characterized.³⁻⁵ Unlike conventional industrial solvents, most of which are volatile organic compounds (VOCs), ionic liquids are salts in the liquid state, and thus provide little/no vapor pressure. Hence, the replacement of traditional solvents by ionic liquids can prevent the emission of VOCs, a major source of environmental pollution.³ In addition, ionic liquids can dissolve enzymes,¹⁸ and form versatile biphasic systems for separations.¹⁹ Ionic liquids can also be highly conducting.²⁰ These extraordinary physical and chemical properties enable ionic liquids to be excellent media for a variety of organic and inorganic reactions.²¹⁻²³ Another driving force behind the research towards the application of ionic liquids relies on their diversity. There are at least one million binary ionic liquids, and 1018 ternary ionic liquids that are potentially applicable to chemical processes,² however, only about 600 molecular solvents are currently in use.² Such a large combination allows for the design and adjustment of ionic liquids for the optimization of the reaction yields, region/chemo-selectivity, substrate solubility, product separation, and even enantioselectivity.^{2,24} Ionic liquids are not always “green”, as the starting materials used to produce them can be extremely toxic.²⁴ Consequently, while we can benefit from ionic liquids, extra care must be taken to avoid risk.

Another approach to “green” media is to use water as reaction solvent. As a solvent, water has many unique properties, such as high heat capacity, a high dielectric constant, extensive hydrogen bonding, and a wide range of reaction temperature.^{17,25,26} Many accomplishments have been made for using water as a solvent or as a cosolvent in chemical reactions. Water has been proven to enhance the rates and to affect the

selectivity of a wide range of organic reactions, such as Diels-Alder reactions,²⁷⁻³³ 1,3-dipolar cycloadditions,³⁴⁻⁴³ azodicarboxylates cycloadditions,²⁷ Claisen rearrangement,^{27,44} Passerini and Ugi reactions,⁴⁵⁻⁴⁸ nucleophilic substitution reactions,⁴⁹⁻⁵² carbon-carbon bond formation,^{39,53-55} bromination reactions,⁵⁶⁻⁵⁸ and certain oxidations and reductions.⁵⁹⁻⁶⁴ In spite of these advantages and accomplishments, water is still not commonly used in organic synthesis. One major issue that prevents water from being used widely is that most organic compounds do not dissolve in water to a significant extent requiring the use of cosolvents; however, the involvement of organic solvents can diminish or even cancel out the initial benefits brought by using water as solvent. Investigations are being undertaken to overcome this problem.¹⁷

Besides using alternative reaction media, one other strategy is to use little or no solvent. The benefits arising from solvent-free/high concentration processes include cost saving and a large reduction in reactor size. Many reactions have been successfully carried out under solvent-free condition, such as polymerizations,⁶⁵⁻⁶⁸ radical additions,^{65,69,70} ionic reactions,⁷¹⁻⁷⁷ solid-state reactions,⁷⁸⁻⁸¹ and photochemical reactions.^{78,82-84} The catalyst efficiency and enantioselectivity of enantioselective transformations are usually very sensitive to solvent.^{85,86} As a result, the optimizations that can be brought about by tuning solvent properties and concentrations are disabled under solvent-free conditions. Moreover, in solvent-free reactions, the medium will change as the reagents convert to products during the reaction processes. The impacts of the changes are currently unpredictable and this complicates their development and practical use.¹³ Reactions under solvent-free conditions can also be highly exothermic. The generated heat can also subsequently affect the reaction – in particular, the selectivity

for a specific product. Thus, it is crucial to attend to this type of reactions closely to keep them under control.¹³

In addition to altering the reaction media, another strategy toward “green” or “greener” chemistry is to improve the efficiency of reactions, and improve the overall yield of a desired product using fewer synthetic steps. This has numerous benefits, including the elimination of protection/deprotection steps during synthesis and the reduction of the amount of solvents needed for purification. One key strategy to improve overall reaction yields is through the addition of a catalyst. A catalyst is a compound that takes part in a reaction, leading to an increased reaction rate, but it is not consumed during the overall reaction.⁸⁷ Catalysts can be categorized into non-metallic based (organo-) and metallic based (organometallic or coordination compounds) catalyst systems. Among numerous types of catalytic strategies, transition metal mediated homogeneous catalysis is of great interest to us because of its broad capability and fundamental importance. In particular, my research focuses on the application of 2-quinoxalinol based Schiff base ligands in the copper-mediated catalysis.

A Schiff base is a compound containing the functional group of carbon-nitrogen double bond with the nitrogen connected to a non-hydrogen group. Due to their ease of preparation and the ability to form stable complexes with a wide array of metal ions,⁸⁸⁻⁹¹ Schiff base compounds have been extensively used as ligands in a wide range of fields, such as pharmaceuticals and biology.⁹²⁻⁹⁴ They also have played several key roles in catalysis. One of the most successful applications is in the enantioselective epoxidation as catalyzed by Jacobsen’s catalyst, (Figure 1.1) whose ligand bears two Schiff bases and

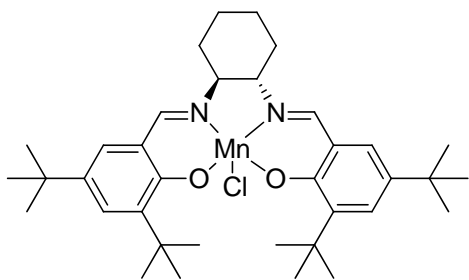


Figure 1.1. Jacobsen's catalyst

two phenolate units, forming a tetradentate chelating environment of the type [O, N, N, O]. This type of ligand is named salen, coming from its two precursors: salicylic aldehyde and ethylene diamine.⁹⁵

In catalysis, salen and related structures have proved effective metal catalyst ligand supports. Salen type ligands can form stable complexes with main group metals to help aid in catalytic transformations, providing solubility and modulating accessibility to the metal center. For example, salen-Al complexes can be used to facilitate Michael additions with excellent enantioselectivity.^{96,97} Other notable work has included the enantioselective formal hydration of α,β -unsaturated imides catalyzed by a salen-Al complex.⁹⁸ This conversion used to be quite challenging to accomplish in good yields in part due to the relative weakness of O-nucleophiles and the reversibility of the reaction.⁹⁸⁻

100

In addition to main group metals, numerous catalytic systems involving salen supported transition metals have been documented. Ti salen complexes have proved to be effective for asymmetric ring opening of epoxides.¹⁰¹ It has also been reported that Ti salen complexes can catalyze the asymmetric addition of KCN and Ac₂O to aldehydes to prepare cyanohydrin esters with excellent enantioselectivity.^{102,103} The products of this reaction are very useful intermediates, and are widely used in organic synthesis.¹⁰⁴⁻¹¹⁴ Ti salen complexes are also used as the catalysts in the enantioselective oxidation of cyclic dithioacetals¹¹⁵ and the enantioselective coupling of aryl aldehydes to form diol analogs.¹¹⁶ Cr salen complexes catalyze a wide range of enantioselective transformations, such as asymmetric ring opening,^{117,118} the allylation of aldehyde,¹¹⁹⁻¹²¹ and the aminolytic kinetic resolution (AKR) of epoxides.¹²² The coupling of CO₂ into aziridines

can be catalyzed by Cr salen complex as well,¹²³ leading to the 5-substituted oxazolidinone products that exhibits antibacterial activity and are widely used in the pharmaceutical industry.¹²⁴⁻¹²⁸

As noted above, Jacobsen's catalyst, i.e. Mn salen complex, is excellent for the asymmetric epoxidation of olefins.¹²⁹ This transformation is one of the most important reactions in organic chemistry and has been investigated extensively by many chemists.^{130,131} The resultant chiral epoxide products are versatile intermediates that can be further converted to many chiral synthetic building blocks.¹³²⁻¹³⁶ Ru salen complexes can be used to catalyze the oxidation of primary alcohols to aldehydes¹³⁷ and the asymmetric sulfimidations.¹³⁸⁻¹⁴⁰ The latter can be further used in the olefination of aldehydes to address the problems encountered in Wittig reaction.¹⁴¹⁻¹⁴³ Co salen complexes are capable of catalyzing a wide range of reactions, including asymmetric ring opening of epoxides,¹⁴⁴⁻¹⁴⁷ asymmetric intramolecular cyclopropanation,¹⁴⁸ enantioselective Baeyer-Villiger oxidation,¹⁴⁹ oxidation of alcohols to carboxylic acids and ketones,^{150,151} arylation ofazole heteroarenes,^{152,153} hydrolytic kinetic resolution (HKR) of terminal epoxides,¹⁵⁴ and enantioselective cyclopropanation.¹⁵⁵

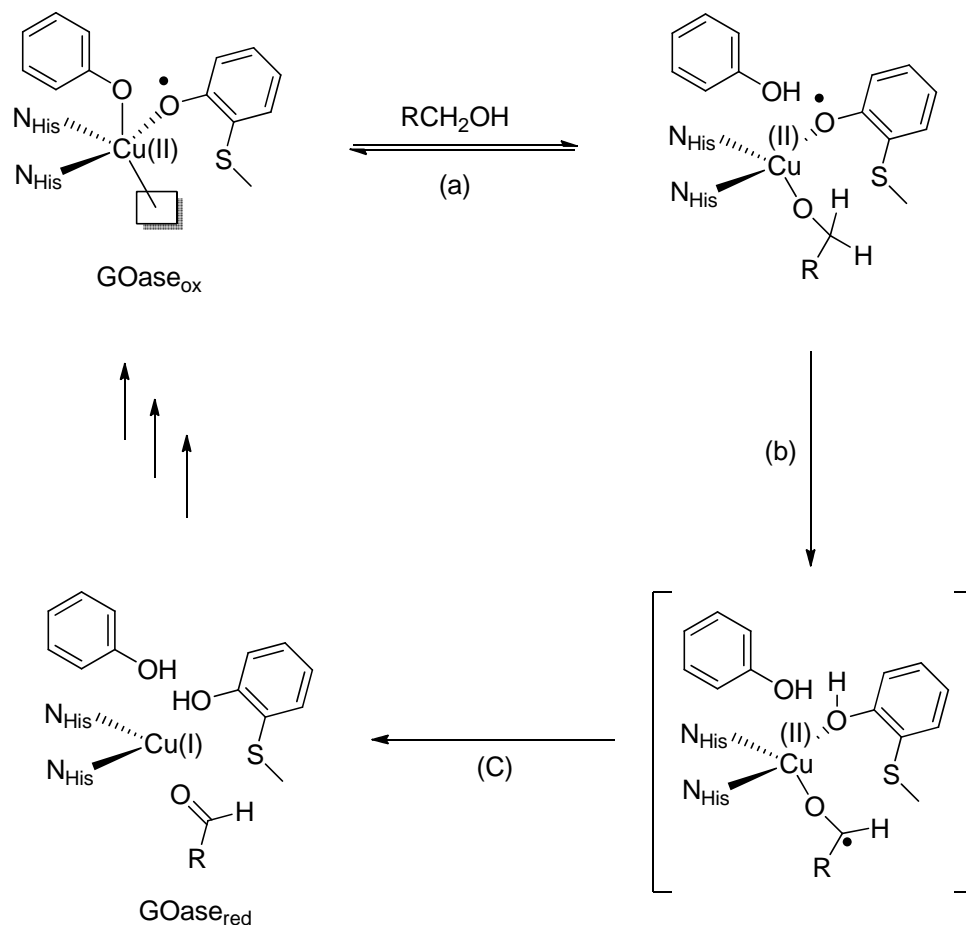
Among all the transition metals, copper is of particular interest to us. Copper is widely used in metalloenzymes for oxygen binding, activation, and reduction.¹⁵⁶ For instance, hemocyanin, an oxygen transport protein, uses two copper atoms to bind dioxygen reversibly.¹⁵⁷ Dopamine β -monooxygenase (D β M) is a copper-containing metalloenzyme that catalyze the oxidation of dopamine to norepinephrine. This enzyme is crucial to organism because of its role in controlling the levels of the neurotransmitters/hormones dopamine and norepinephrine.¹⁵⁸ Copper Amine Oxidases

(CAOs) are widely distributed in nature. They can be found in bacteria, yeast, plants, and mammals.^{159,160} The function of CAOs is to convert primary amines to aldehydes. In prokaryotes, CAOs allows the microorganisms to grow on primary amines as a nitrogen source via an oxidative release of ammonium ion; whereas in eukaryotes, they regulate biogenic amine levels through oxidative metabolism.¹⁵⁸ Galactose Oxidase is a fungal protein consisting of a single polypeptide chain with one copper atom per active center.^{161,162} It catalyzes the two-electron reduction of O₂ to hydrogen peroxide and the oxidation of primary alcohols to aldehydes.^{156,158} Tyrosinase, one of the most well-studied multicopper oxygenases, is ubiquitous among eukarya.¹⁶³ It contains a coupled binuclear copper active site that catalyzes the *ortho*-hydroxylation of monophenols and the subsequent two-electron oxidation of *ortho*-diphenols to *ortho*-quinones. Its numerous mutations play a wide range of physiological roles in different living systems.¹⁶⁴ Dopamine β -hydroxylase (*D β H*) and peptidylglycine α -hydroxylating monooxygenase (PHM) also have binuclear copper sites, although the two coppers are not coupled.^{156,158} One copper center is thought to be responsible for the hydrogen atom abstraction from the substrate, as the other copper provides one electron to form hydroperoxide.^{156,158} Another class of copper-containing metalloenzyme is monooxygenase, such as methane monooxygenase (pMMO) and ammonia monooxygenase (AMO). pMMO is a copper-containing membrane-bound metalloenzyme¹⁶⁵ that catalyzes the monooxygenation of methane to methanol in methanotrophic eubacteria.¹⁶³ AMO is a membrane-bound protein that catalyzes the monooxygenation of ammonia to hydroxylamine. This transformation is the first step of the oxidation of ammonia to nitrite, and is used by ammonia-oxidizing eubacteria to

produce energy.¹⁶³ In addition to ammonia, AMO can also catalyze the oxidation of a variety of hydrocarbons,¹⁶⁶ halogenated organic,¹⁶³ carbon monoxide,¹⁶³ and thioethers.¹⁶⁷

To better understand these functions of the enzymes, copper salen complexes have been studied as functional mimics.¹⁶⁸⁻¹⁷⁰ It has been demonstrated that salen Cu(II) complexes are models for galactose oxidase (GOase).^{169,170} GOase is responsible for the aerobic oxidation of primary alcohols to aldehydes in living system.¹⁷¹ The oxidation reaction involves a copper atom and a cysteine-modified tyrosine residue. It is commonly believed that the oxidized form of enzyme (GOase_{ox}) contains a Cu(II)-tyrosine radical. This reactive intermediate binds primary alcohols in an exchangeable fashion, followed by hydrogen abstraction and electron transfer from the alcoholic substrate to Cu center leading to the formation of aldehyde product and the reduced form of enzyme (GOase_{red}). (Scheme 1.1) In the investigation of using salen Cu(II) complex (Figure 1.2) as model for GOase, the oxidizing half-reaction (oxidation of primary alcohols into aldehydes) is successfully duplicated.¹⁶⁹ This study also showed that salen is a non-innocent ligand in its Cu(II) complex. The oxidation of the Cu-salen complex resulted in a metal-base product [Cu(III)Salen]⁺ in the solid state; however, a temperature-dependent equilibrium existed in solution between high-valent metal form [Cu(III)Salen]⁺ and ligand-radical form [Cu(II)Salen•]⁺, in which the [Cu(III)Salen]⁺ form is stabilized at low temperature.¹⁷⁰ In addition, investigations with the reduced tetrahydrosalen Cu(II) species [CuSalen^{red}]⁺ suggested that this oxidized complex existed as a temperature-independent species [Cu(II)Salen^{red}]⁺ in solution. In the oxidation of benzyl alcohol to benzaldehyde, [CuSalen^{red}]⁺ exhibited faster reactivity compared to [CuSalen]⁺, even though [CuSalen]⁺ is a much stronger oxidant.¹⁶⁸ The conflicting results might stem from the more

Scheme 1.1. Consensus Mechanism for the Oxidation Reaction Catalyzed by GOase.



(a) Binding of primary alcohol to the Cu(II) center and subsequent deprotonation by the axial tyrosine ligand. (b) Hydrogen abstraction by the organic radical cofactor, resulting in a ketyl radical intermediate. (c) Electron transfer from the bound radical substrate to the Cu(II) center, leading to the formation of Cu(I) and aldehyde product.

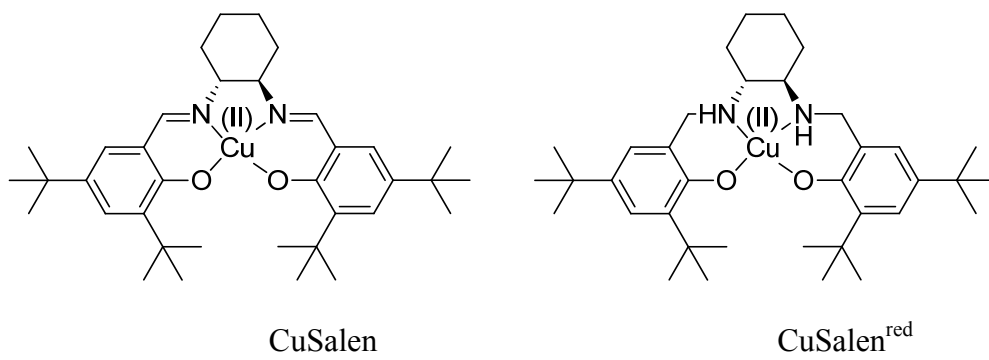
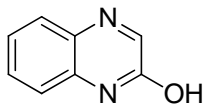


Figure 1.2. CuSalen and tetrahydrosalen CuSalen^{red}

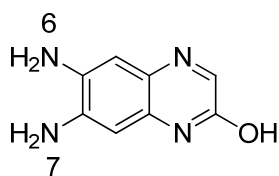
unfavorable axial substrate binding to Cu(III) of [Cu(III)Salen]⁺ species than to Cu(II) of [Cu(II)Salen^{red}]⁺ species.¹⁷⁰

2-Quinoxalinol is a highly conjugated heterocyclic compound. (Figure 1.3) The advantages of substituting the ethylenediamine compound of salen with 2-quinoxalinol include: (1) the conjugation of 2-quinoxalinol will extend to the phenolic moieties through Schiff bases resulting in a more conjugated system. Since subtle changes in ligand structure can have big influence on the metal center,¹⁶⁸ this new system should possess different electronic properties from salen structure and may provide unique features when used as a catalyst. (2) The diamino-2-quinoxalinol intermediate (Figure 1.3) has two chemically different amino groups at the 6- and 7-positions. The 6-amino group is more reactive.¹⁷² This feature allows the preparation of the tridentate Schiff base ligand Salqu-imine (Figure 1.3) and the asymmetric salqu ligand (Figure 1.3), whose phenolic moieties are different.¹⁷² Neither the tridentate Schiff base ligands nor the asymmetric salen-type ligand has been investigated previously as a catalyst support.

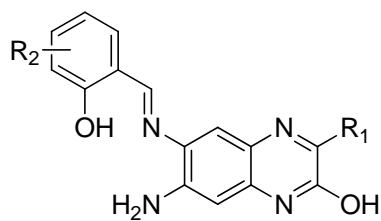
Previously, the benzylic oxidation of a methylene (CH₂) group into a carbonyl using Salqu Cu(II) complex **2** (Figure 1.3) as catalyst has been reported.¹⁷³ The salqu Cu(II) complex exhibited an improved catalytic effect as compared to the salen Cu(II) complex and has a low sensitivity with respect to moisture and air. The rationale for the superiority of salqu ligand was not immediately clear. In this dissertation, the salqu Cu(II) complex **1** (Figure 1.3) has been used to promote the allylic oxidations of Δ^5 -steroids and simple olefin substrates using *tert*-butyl hydroperoxide (TBHP) as the terminal oxidant. Mechanistic studies were also performed to characterize the catalytic cycle of salqu Cu(II) complex **1**, and determine why it is a better catalyst than the salen analog.



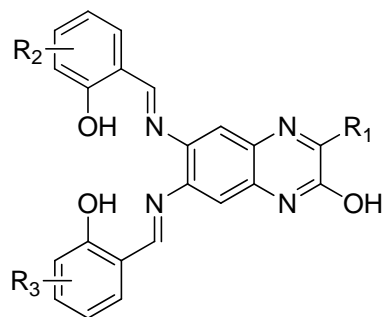
2-quinoxalinol



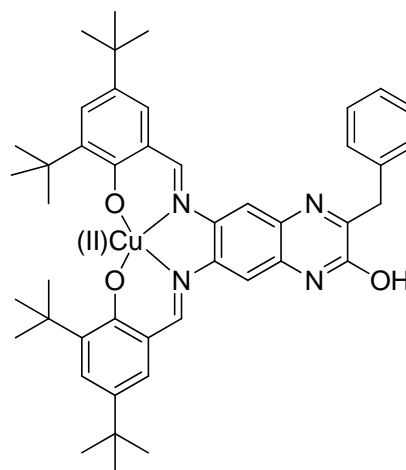
diamino-2-quinoxalinol



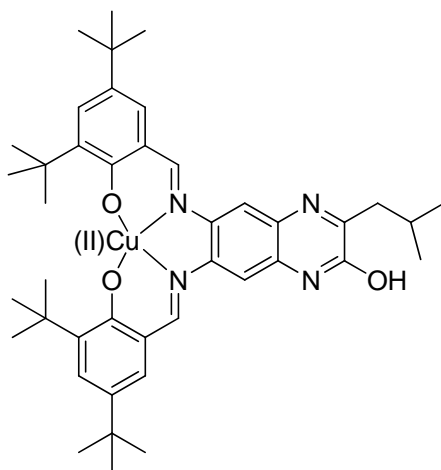
Salqu-imine



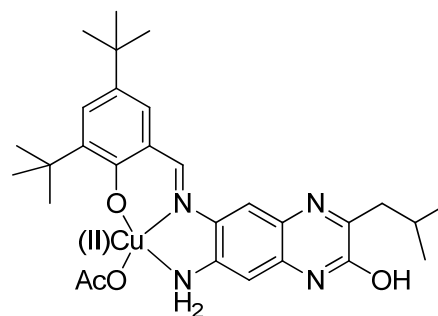
asymmetric salqu



complex 2



complex 1



complex 3

Figure 1.3. Structures of 2-quinoxalinol, diamino-2-quinoxalinol, salqu-imine, asymmetric salqu ligand, complex 2, complex 1, complex 3.

Furthermore, a 2-quinoxalinol based tridentate Schiff base ligand is also used to prepare a Cu(II) complex **3** (Figure 1.3), which also promotes allylic oxidations. In spite of the similar oxidation results, complex **1** and complex **3** exhibit different electronic characteristics. Theoretical calculations also indicate a possible alternative reaction mechanism.

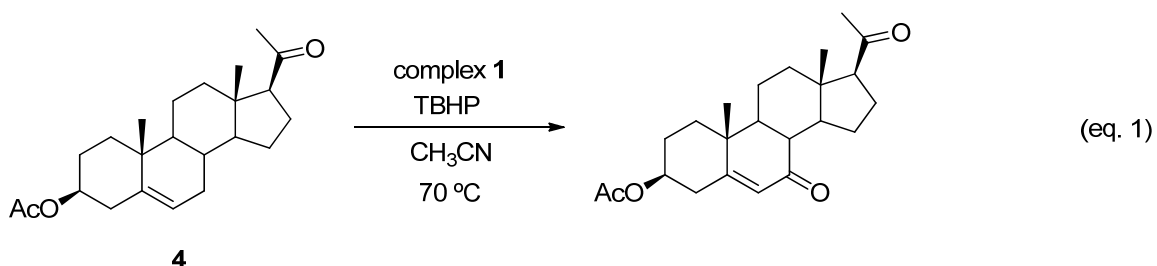
Chapter 2

Salqu Cu(II) Catalyzed Allylic Oxidation of Δ^5 -Steroids

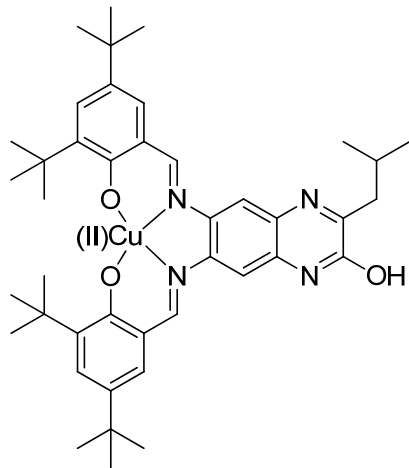
Easy access to the 7-keto- Δ^5 -steroids can be achieved *via* allylic oxidation of Δ^5 -steroids, and the oxidations of Δ^5 -steroids have attracted significant attention because of the biological and physiological properties of the resultant 7-keto- Δ^5 -steroid products.¹⁷⁴⁻¹⁸³ Although a variety of chromium(VI) compounds have been used in the synthetic modifications of Δ^5 -steroids,^{177,184-188} complications in applying these methods remain because of the harsh reaction conditions required and the frequently very difficult work-up and/or purification procedures. In addition, the accumulations of chromic acid or chromium salt wastes that are the side products of these reactions are of great environmental concern.¹⁸⁹ To complete such modifications in a more environmentally friendly yet still efficacious manner, other metal complexes/salts have been employed, such as sodium chlorite,¹⁹⁰ copper iodide,¹⁷⁸ dirhodium caprolactamate,¹⁹¹ ruthenium trichloride,¹⁹² bismuth salt,¹⁹³ cobalt acetate,¹⁹⁴ palladium(II) salts,¹⁹⁵ and manganese(III) acetate;¹⁹⁶ however, numerous limitations remain. All of these methods must strike a balance between good yields and functional group compatibility and they continue to suffer from long reaction time requirements. Oxidations using manganese(III) acetate and dirhodium caprolactamate as catalysts are two more recent representative examples of the current methods.^{191,196} The use of manganese(III) acetate allowed for excellent yields in Δ^5 -steroidal oxidation under ambient temperature when *tert*-butyl hydroperoxide (TBHP)

was used as the oxidant. The reaction times were reduced remarkably when the reaction mixture was heated, but with a significant loss in yield. This method is also not compatible with some sensitive functionalities near allylic sites (e.g. hydroxyl group).¹⁹⁶ The use of dirhodium caprolactamates as the catalyst in such an allylic oxidation showed a wide tolerance for a variety of functional groups, yet it also had only moderate yields.¹⁹¹

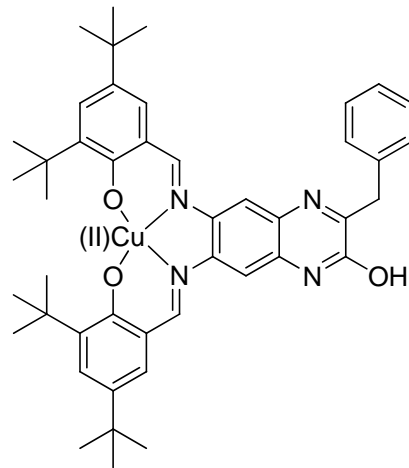
Previously, a catalytic system that consists of salicylic Cu(II) complex **2** (Figure 2.1) as the catalyst and TBHP as the oxidant has been reported.¹⁷³ This system was demonstrated to oxidize benzylic methylenes into carbonyl groups in near quantitative yields with the use of catalyst loading of 1 mol % and 3 equiv of TBHP when different functional groups remained intact. On the basis of this previous success, we sought to modify this system to develop mild conditions that would retain satisfying yields and also be efficacious for allylic oxidations.



The investigation began by using salicylic Cu(II) complex **2** (Figure 2.1) as the catalyst and pregnenolone acetate **4** as the substrate (eq. 1). Two factors were varied to determine the optimal reaction conditions: reaction time and oxidant ratio. The oxidation was performed on a millimole scale using 1 mol % of catalyst complex **2**. CH₃CN/CHCl₃ (50/50) was chosen as the solvent to dissolve the steroids. The solution was heated to 70 °C, and then the TBHP was added. The reaction progress was followed by thin layer



Complex 1



Complex 2

Figure 2.1. Complex 1 and complex 2.

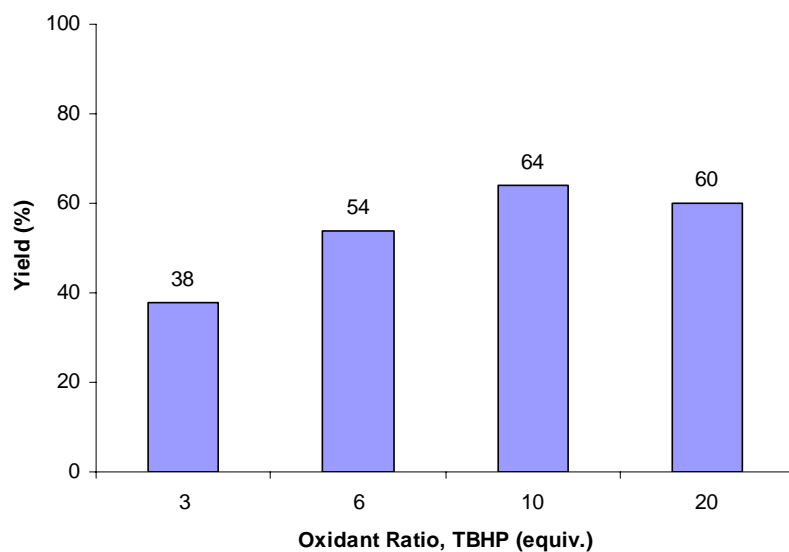
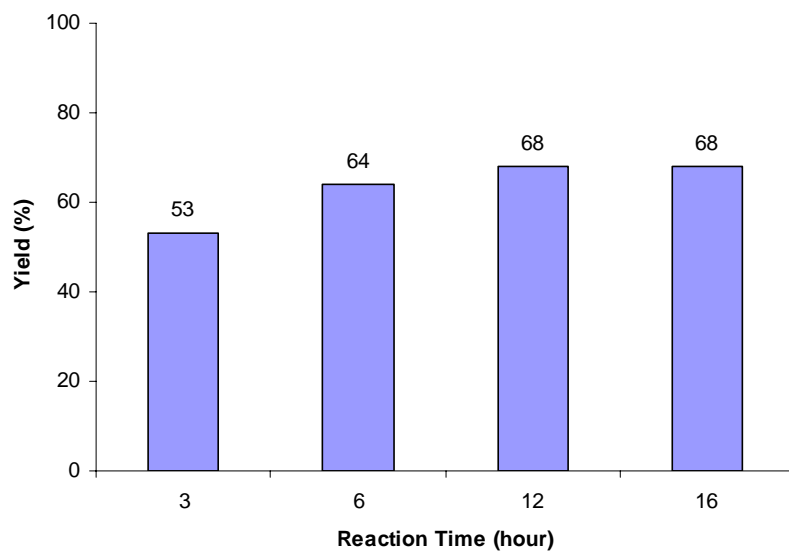


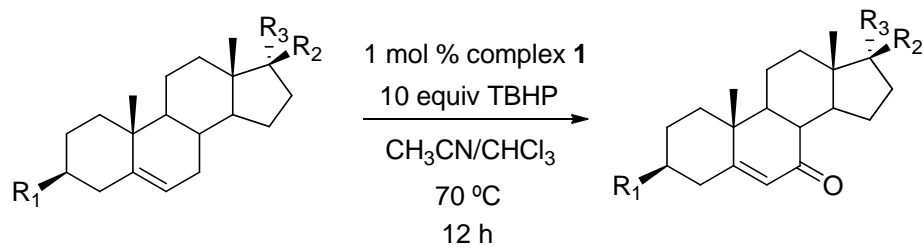
Figure 2.2. Isolated yields with various reaction times and oxidant ratios (equiv. to steroidal substrate).

chromatography (TLC). When the reaction was judged to be complete, the solution was concentrated under reduced pressure, and the residue was purified by flash column chromatography using hexane/ethyl acetate as eluent. Initially, 10 equiv of TBHP was used to determine the optimal reaction time (Figure 2.2). The isolated yields slightly increased when the reaction time was extended from 3 h to 12 h, and did not change when the time was elongated from 12 h to 16 h. Because there is little difference in isolated yields between 6 h and 16 h, the reaction time was set to 6 h to optimize the oxidant ratio (Figure 2.2)

A general trend of increasing isolated yield was observed as the oxidant ratio was increased from 3 equiv to 20 equiv. The highest yield was achieved when 10 equiv of TBHP was used, and the additional amount of oxidant did not result in a higher yield. It is remarkable that the remaining starting material, pregnenolone acetate **3**, was recovered after reaction time of 6 h. When carried out at ambient temperature, the reaction rate was found to be much slower (51% isolated yield for 24 h and 65% isolated yield for 48 h). In the absence of the catalyst complex **2**, only 39% isolated yield was obtained after being heated for 6 h at 70 °C.

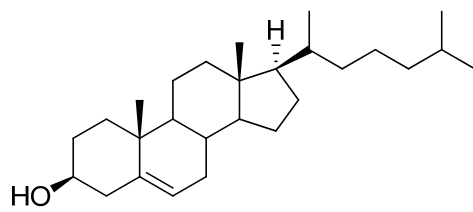
A variety of Δ^5 -steroidal substrates were oxidized using these optimized conditions with 1 mol % of catalyst loading and 10 equiv of oxidant TBHP heated to 70 °C for 12 h (Table 2.1). The even more challenging oxidation of 3-hydroxy- Δ^5 -steroids can also be successfully realized with a small decrease in yields (Table 2.1, entry 5 and 6); however, in all cases, the mass balance was found to be the unreacted steroidal starting materials, and these were readily recovered. Given the fact that the structurally similar salen Cu(II) complexes have been shown to slowly decompose in most organic solvents¹⁶⁹ and the

Table 2.1. Oxidation of steroids using optimized conditions.



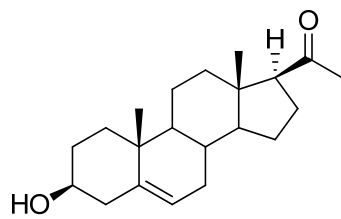
Entry	Substrate	Yield (%)
1		64
2		62
3		55
4		61

5



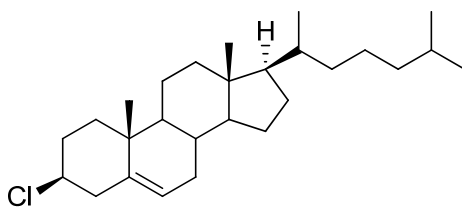
44

6



53

7



49

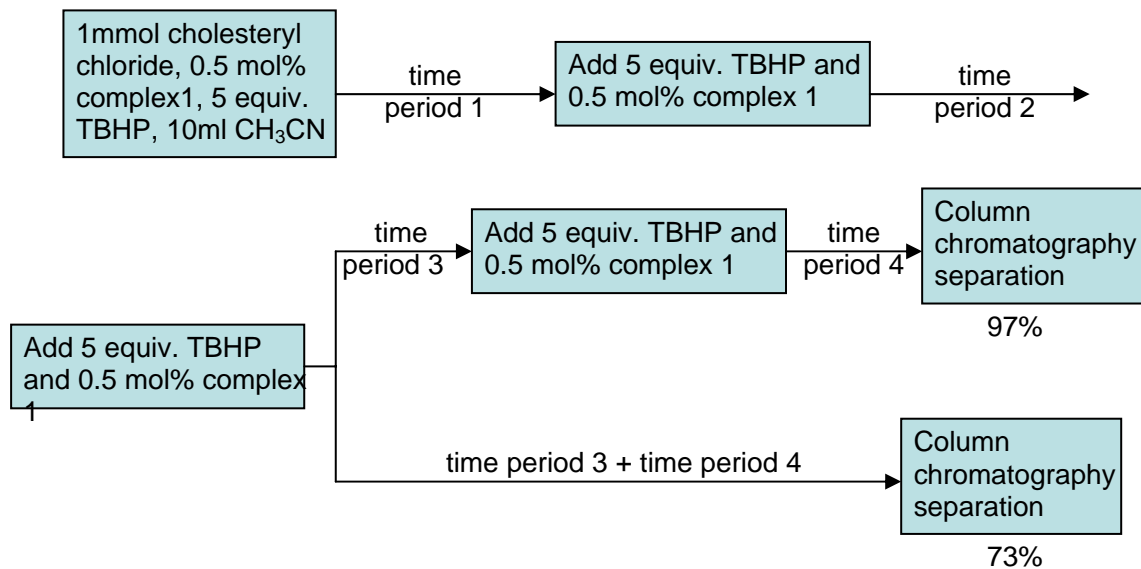
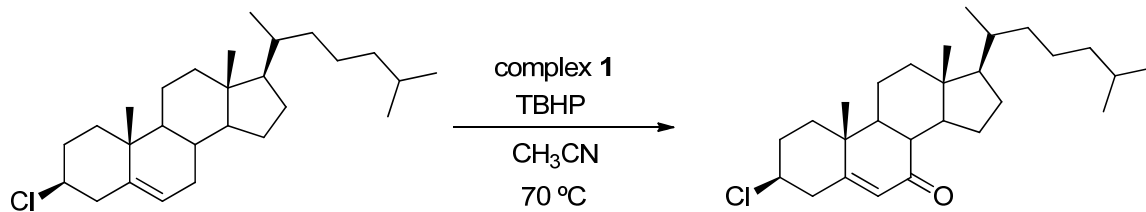
observation that the color of the reaction solution changes from its initial red to yellowish during the course of the reaction, it would appear that the ligand-metal complex **2** was consumed to some extent as the reaction proceeded.

To verify this hypothesis, the oxidation of cholesteryl chloride was carried out in CH₃CN and CHCl₃ independently. Interestingly, the reaction in CH₃CN had an isolated yield of 57%; whereas, the one in CHCl₃ had only 28% isolated yield, despite the fact that complex **2** has much better solubility in CHCl₃ than in CH₃CN. According to the consensus radical mechanism of current allylic oxidation methods using TBHP,^{191,196,197} the reason for this lower yield is likely the stabilizers added to the commercially purchased CHCl₃ that can function as radical scavengers.

The reaction was then repeated, this time using CDCl₃ as solvent. Since the NMR solvent CDCl₃ does not contain stabilizers as commercially available CHCl₃ does, the reaction in CDCl₃ should have a higher yield than that in CHCl₃. Indeed, 48% isolated yield was achieved. Thus, it is clearly shown that the oxidation reaction proceeds better in CH₃CN than in CHCl₃, and the results of reactions in CHCl₃ and CDCl₃ are in accordance with the hypothesis about stabilizers. Although a negative factor was found, the mystery of complex **2** appearing to be consumed over the course of the reaction remained.

It was then decided to change the reaction procedure conditions to increase the catalyst loading and amount of oxidant slightly by adding additional portions of them. Cholesteryl chloride was used for this additional further optimization (Scheme 2.1). Here, the reaction was performed in CH₃CN at 70 °C, and 0.5 mol % of complex **2** and 5 equiv of TBHP were added simultaneously with multiple portions used. For cholesteryl

Scheme 2.1. Further optimization of reaction conditions.

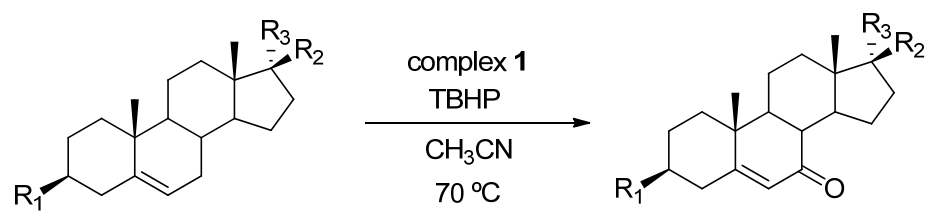


chloride, 3 portions of catalyst and oxidant gave an isolated yield of 73% while the addition of 4 portions resulted in 97% isolated yield. For the reaction using 3 portions, after the addition of the third portion, the reaction was let react for the same length of time as if the fourth portion had been added. The same reaction time consumed in total confirms the necessity of the fourth addition of catalyst and oxidant.

Different Δ^5 -steroidal substrates were tested using these additional optimized reaction conditions (Table 2.2). For each substrate, different numbers of portions were tested to find optimal conditions. Cholesteryl acetate required 3 portions (each addition contains 0.5 mol % of complex **2** and 5 equiv of TBHP) to achieve 99% yield (Table 2.2, entry 1); benzoyl protected pregnenolone required 5 portions to get 77% yield (Table 2.2, entry 2). Simple cholesterol only required 2 portions (Table 2.2, entry 3) while pregnenolone and cholesteryl chloride each required 4 portions (Table 2.2, entry 4 and 5). Generally excellent yields were obtained albeit the unprotected substrates had generally lower yields than the protected ones. The addition of subsequent additional portions of catalyst and oxidant did not increase yields. The benzoyl protected cholesterol is oxidized in significantly lower yield than other protected steroids even though 5 portions were added. This could be due to the insolubility of substrate in CH_3CN .

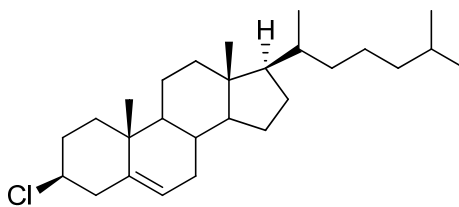
In Δ^5 -steroids, there are two potentially reactive allylic sites. These two sites do not have much difference in reactivity at first glance; however, from our series of reactions, only the 7-keto products were obtained. From the resonance structures, this difference in reactivity becomes clear (Figure 2.3). The species bearing a radical at the 7-position will have two possible resonance structures, one of which is a tertiary radical, and this can significantly lower the energy. Meanwhile, the species bearing a radical at the 4-position

Table 2.2. Oxidation of steroids using further optimized conditions.



Entry	Substrate	Yield (%)
1		97 ^a
2		77 ^b
3		69 ^c
4		88 ^d

5

99^d

^a3 Portions of TBHP and complex **1** were used. ^b5 Portions of TBHP and complex **1** were used. 1 ml CHCl₃ was added to help dissolve the substrate. ^c2 Portions of TBHP and complex **1** were used. ^d4 Portions of TBHP and complex **1** were used.

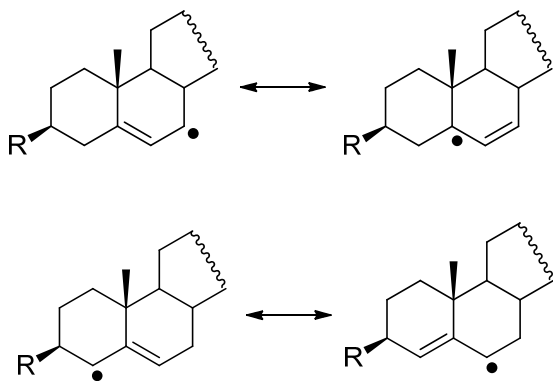


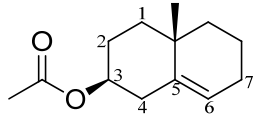
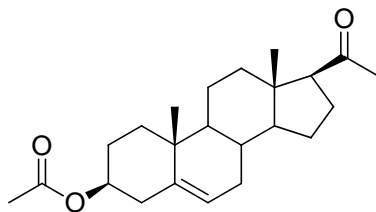
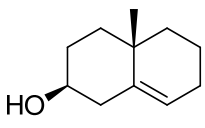
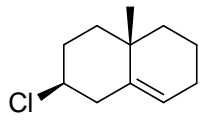
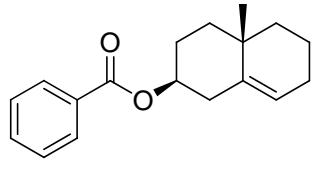
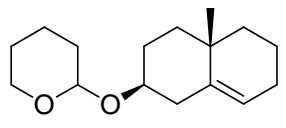
Figure 2.3. Resonance structures of 7-radical species (upper) and 4-radical species (lower).

also has two possible resonance structures, but neither contributes to the lower energy state. Of course, the preference of reactivity is also affected by the configuration of the steroids.

This speculation about the origins of regioselectivity was later supported by theoretical study and computational modeling. Compound **5** was selected as a model to examine the energy differences between the species bearing radicals at two different sites through *ab initio* computational studies at the B3LYP/6-31G(2d,p) level using the Gaussian03 package (Table 2.3). The free energy at 298 K of the 7-position radical is less than that of the 4-position radical by 3.43 kcal/mol. The relative stability becomes more significant (6.21 kcal/mol) when calculations with the more complicated steroid molecule (pregnenolone acetate **4**) were performed with the same level of theory. A series of calculations were carried out for the model compound **5** bearing different functional groups. In each case, compounds with the radical at the 7-position were more stable (lower in energy) than those at the 4-position. It is interesting that the trend of energy difference bearing different functional groups is in agreement with the trend of numbers of portions needed for the corresponding substrates (See Table 2.2, entry 1, 3, and 5).

In summary, a novel system for allylic oxidation of Δ^5 -steroids using TBHP as the oxidant with salqu Cu(II) complex as the catalyst has been demonstrated. A variety of Δ^5 -steroids can be selectively converted to the corresponding enones with excellent yields (up to 99% under optimized conditions) with a significantly reduced reaction compared to other current methods. This system also exhibits the tolerance for a variety of functional groups and low sensitivity to air and water. In addition, the regioselectivity is studied from the substrate point of view *via* theoretical calculation.

Table 2.3. Calculations of free energies of model radicals.

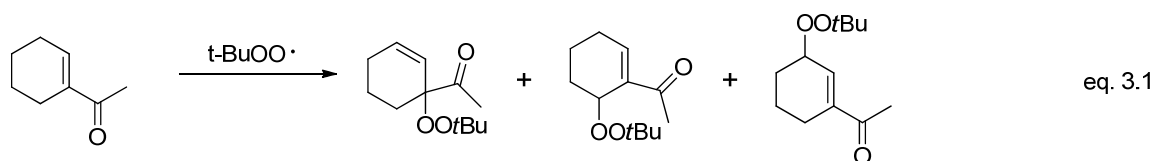
Model molecule	Relative stability of C7 vs V4 radical ^a (kcal/mol)
 5	-3.43
 4	-6.21
	-4.65
	-2.85
	-3.38
	-3.30

^aValue reported as ΔG at 298 K.

Chapter 3

Oxidation of Simple Olefins Using a Salqu Cu(II) Complex

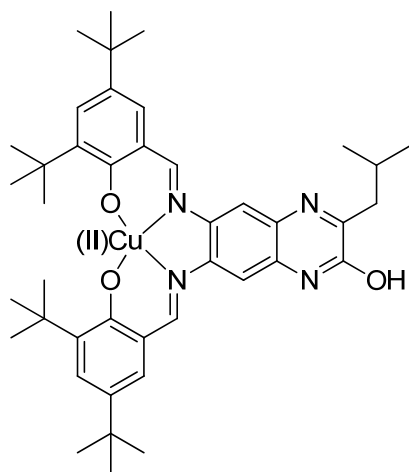
The regioselective activation and subsequent oxidation of the allylic C-H bonds is of great interest. Enone or enedione products from such reactions are commonly used as building blocks in multistep organic synthesis.^{198,199} Direct transformation of alkenes to the corresponding α,β -unsaturated enones or 1,4-enediones are particularly important, because of their wide potential for applications in the synthesis of pharmaceuticals and related natural products.²⁰⁰⁻²⁰⁷ Although non-metal based allylic oxidations have been reported,²⁰⁸⁻²¹⁰ there has been wide interest on the study of highly efficient metal catalyzed allylic oxidations.^{190,191,193,196,197,211-221} Extensive research has been carried out where *tert*-butyl hydroperoxide (TBHP) was used as the oxidant with various metal catalysts, such as chromium compounds,^{211,212} sodium chlorite,¹⁹⁰ copper iodide,²²² dirhodium caprolactamate,^{191,197,216-218} ruthenium trichloride,¹⁹² bismuth salt,¹⁹³ cobalt acetate,^{219,220} palladium(II) salts,²¹³⁻²¹⁵ manganese(III) acetate,¹⁹⁶ and ferric chloride.²²¹ While promising results are reported, numerous limitations remain, e.g., harsh reaction conditions, difficult workup and/or purification procedures, production of harmful waste, low functional group tolerance, and high cost. In addition, there are two major drawbacks of the current methods using TBHP as oxidant: long reaction times and low regioselectivity of the *tert*-butyl peroxy radical, resulting in numerous isomers formed as byproducts (eq. 3.1).¹⁹⁷ The first disadvantage has been addressed to some extent by



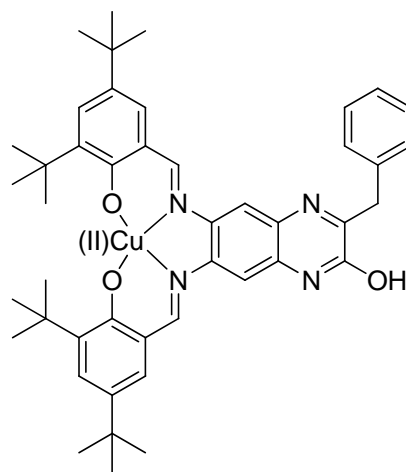
researchers in Doyle group using a dirhodium caprolactamate system, with which the reaction could be completed in 1 hour.²¹⁶ In this system, since *t*BuOO• still formed and acted as an oxidant, the lack of regioselectivity remains a concern.¹⁹⁷ Although the most effective metal catalysts for allylic oxidations are those that are capable of carrying out 1-electron redox processes, such as Cu(I)/Cu(II),^{216,223} little research has been using Cu for catalyzing allylic oxidation, even though Cu is widely used in naturally occurring metalloenzymes to facilitate synthesis.¹⁵⁶ For example, galactose oxidase (GOase), a copper-containing metalloenzyme secreted by the fungus *Fusarium spp.*, is critical in the oxidation of primary alcohols to aldehydes.^{224,225}

Previously, our group reported a catalytic system that consists of Salqu Cu(II) complex **2** (Figure 3.1) as the catalyst and used TBHP as the oxidant for the oxidation of benzylic methylenes into carbonyl groups in quantitative yields.¹⁷³ When our interest shifted from benzylic oxidation to allylic oxidation, several questions arose: (1) will the salqu Cu(II) complex be able to catalyze the allylic oxidation as well, and (2) if so, what is the regioselectivity of the salqu Cu(II)/TBHP system?

In benzylic oxidation, there was only one reactive site where reaction could happen, while in allylic oxidation reaction could occur at multiple sites. The first question is answered by the results of the allylic oxidation of various Δ^5 -steroidal substrates (Chapter 2), while the second one remains unclear. In the oxidation of Δ^5 -steroids, the regioselectivity was studied from the substrate's perspective. The more stable 7-radical and the geometry of steroids made a great contribution to the regioselectivity of the



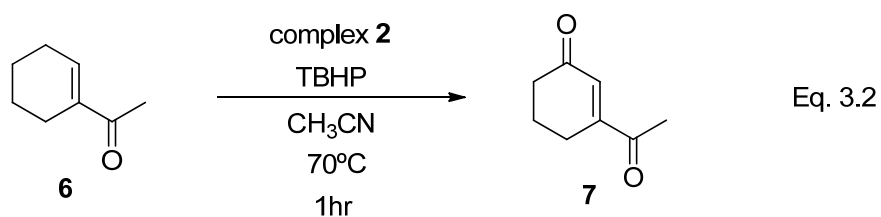
Complex 1



Complex 2

Figure 3.1. Cu(II) salqu complex 1 and complex 2.

reaction; however, these determining factors from thermodynamics and geometry disappear when we turn to the oxidation of simple olefin substrates. Based on our previous success,²²⁶ salqu Cu(II) complex **1** is employed in the allylic oxidation of simple olefins to address the commonly encountered problems as found in other similar catalytic systems, specifically, long reaction time, low selectivity, harsh conditions, low functional group tolerance, and high cost.^{190,191,193,196,197,212-221} In addition, these reactions are probed to better characterize the reactivity of the copper complex and the nature of catalytic mechanism, and thus subsequently gain insight as to how to further exploit this complex as catalyst.



Investigations began by examining the allylic oxidation of 1-acetyl-1-cyclohexene **6** using salqu Cu(II) complex **1** as the catalyst (eq. 3.2). For ease of comparison with other catalytic systems, the oxidation reaction was carried out on a millimole scale using catalyst loading of 0.5 mol %. Acetonitrile (CH₃CN) was first used as solvent for the optimization of TBHP ratio needed. The reaction was monitored by gas chromatography (GC). Within 1 h of reaction, the yield of the corresponding 1,4-enedione product (**7**) increased from 65% to 99% when the TBHP ratio changed from 1 equiv to 3 equiv. Further additions of TBHP did not result in further improvement in yield (Figure 3.2). It is worth noting that the salqu Cu(II) system only requires 3 equiv of TBHP, which is much less than other catalytic methods (5 equiv to 10 equiv). Theoretically, only 1 equiv of TBHP is consumed in the allylic oxidation of olefins to enones; however, excess

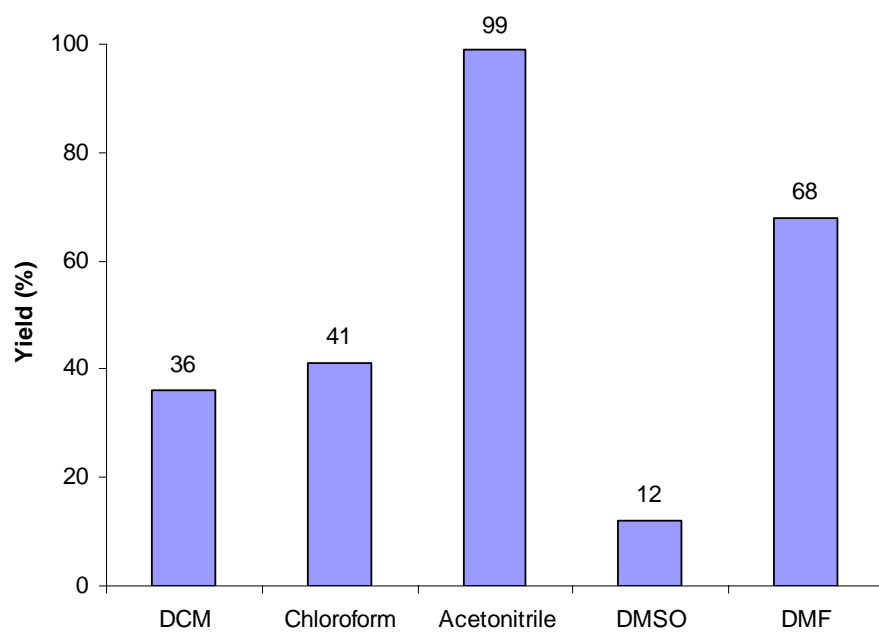
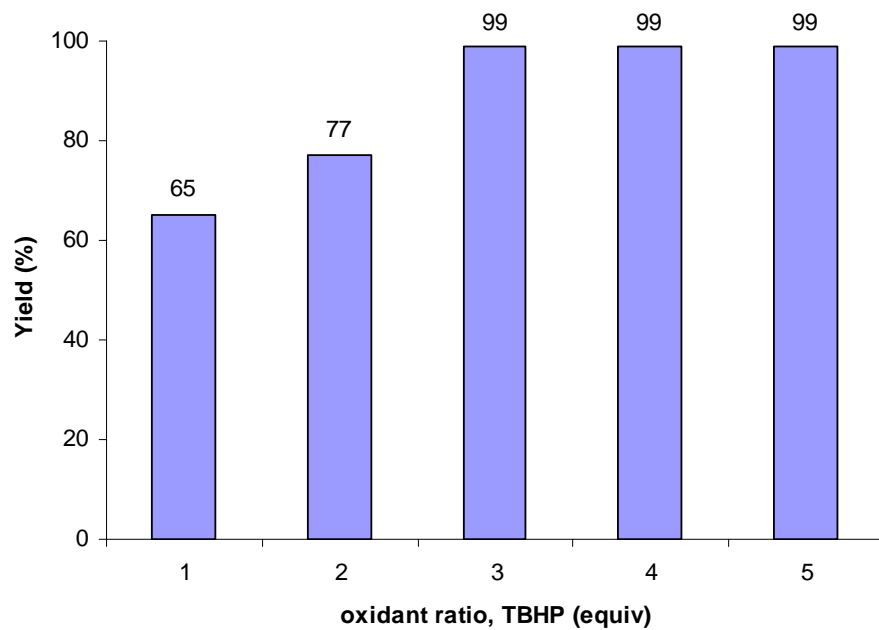


Figure 3.2. Effects of oxidant ratio and solvents on reaction yields.

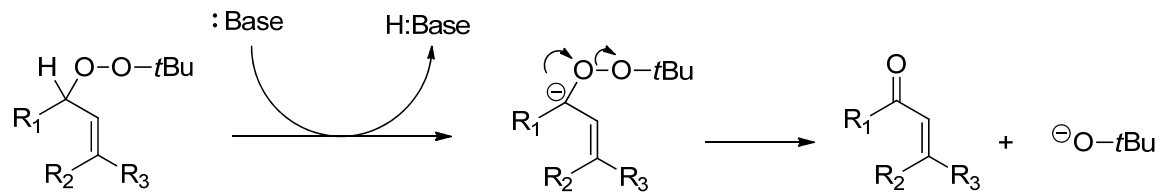
TBHP is required because of decomposition of TBHP during the reaction process. The lower requirement for TBHP in the salqu Cu(II) system is indicative of the better activation of TBHP, and hence a different yet more efficient manner of using it.

Using 3 equiv of TBHP and 0.5 mol % of complex **1**, different solvents were also tested for 1-acetyl-1cyclohexene **6** for 1 h (Figure 3.2). Reaction yields in 1 h are used as the indicators for reaction rates. Reactions proceeded much more slowly in dichloromethane and chloroform than in acetonitrile. This is consistent with our previous observation in the oxidation of Δ^5 -steroids (Chapter 2). The reaction in DMF had a moderate yield, while the yield of the reaction in DMSO was extremely low. In chapter 2, the effects of chloroform and acetonitrile as solvents were discussed. It is believed that the stabilizers often found in commercially available chloroform can function as radical scavengers and consequently lead to the lower yields; however, the results here of reactions in different solvents suggest the possibility of another negative factor.

One noticeable feature that distinguishes acetonitrile from other solvents is oxygen solubility. Oxygen has a greater solubility in acetonitrile (8.1 mM) than in most other commonly used organic solvents, such as DMF (4.5 mM) and DMSO (2.1 mM).²²⁷ To determine whether the oxygen concentration has an influence on the reaction rate, a control experiment was performed in CH₃CN degassed with argon. In this case, only 18% yield was observed after 1 h of reaction as compared to 99% yield in regular acetonitrile. This result indicated the crucial role of dioxygen in this conversion. The surprisingly low yields in DMSO could be ascribed to the ligation of the solvent molecule by the catalyst complex, which prevents the catalyst from functioning normally.²²⁸

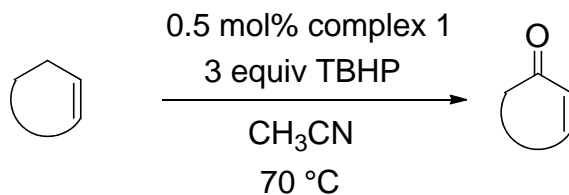
In most metal-catalyzed allylic oxidations using TBHP as the oxidant, the addition of

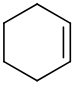
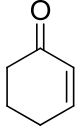
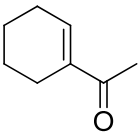
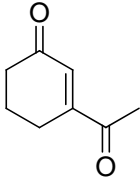
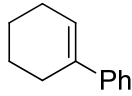
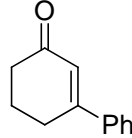
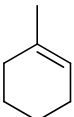
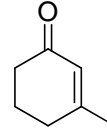
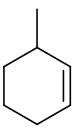
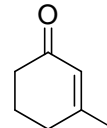
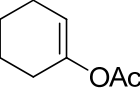
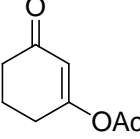
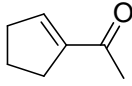
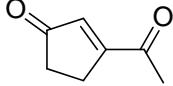
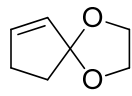
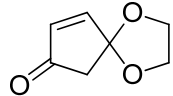
Scheme 3.1. Decomposition of *tert*-Butyl Peroxy Ether under Basic Conditions.

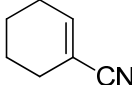
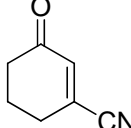
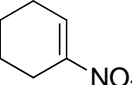
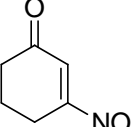


base would accelerate the reaction because of the facile decomposition of the *tert*-butyl peroxy ether intermediates under basic conditions (Scheme 3.1);^{214,216,229} however, the addition of 50 mol % of K₂CO₃ did not bring any change to the reaction rate in our system. This result suggested two possibilities: (1) the decomposition of *tert*-butyl peroxy ether intermediate is not the rate-determining step, or (2) the *tert*-butyl peroxy ether intermediate was not formed. Since the decomposition of *tert*-butyl peroxy ether is known to be slow and can be greatly accelerated by the addition of base,^{214,216,229} the reaction time should decrease with the addition of a base if *tert*-butyl peroxy ether is formed in our system. Thus, it is reasonable to rule out the first scenario. A reaction mechanism bypassing the formation of *tert*-butyl peroxy ether represents a new and an alternative pathway to those reported previously.^{196,213-216} Such a mechanism might consequently lead to improved selectivity because additional isomers can be obtained as side products along with the formation of desired peroxy ether (eq. 3.1).^{197,214,215}

Allylic oxidations of a variety of representative olefins are examined using 0.5 mol % of complex **1** and 3 equiv of TBHP in CH₃CN at 70 °C (Table 3.1). Most of the substrates were converted to the corresponding products with excellent yields within a very short reaction time. The low yield for 1-nitro-1-cyclohexene (Table 3.1, entry 11) could be due to strong binding between the nitro group and the Cu(II) of complex **1** that would poison the catalyst. It could also arise from the strong electron withdrawing capability of the nitro group that could destabilize the radical intermediate. Also worth noting is that 3-methyl-1-cyclohexene and 1-methyl-1-cyclohexene yielded the same oxidation product (Table 3.1, entry 4 and 5). This is further evidence indicative of a radical mechanism.

Table 3.1. Cu(II) Salqu Catalyzed Allylic Oxidation of Olefins.

Entry	Substrate	Product	Time (h)	Yield ^a (%)
1			1	74
2			1	99
3			1	91 88 ^b
4			1	86
5			1	78
6			2	88
7			2	89
8			1	94

9			1	94
10			24	11

^aGC yields with 1,2-dichlorobenzene added as internal standard. ^bIsolated yield obtained from flash column chromatography using hexane/ethyl acetate (4:1) as eluent.

To further explore the nature of this catalytic cycle, additional experiments were performed. It has been documented that TBHP can easily bind to tridentate mononuclear Cu(II) species to form a Cu(II) *tert*-butyl peroxy complex whose crystal structure showed a distorted tetrahedral binding geometry of Cu(II) center.²³⁰ By comparing the resonance Raman spectra of LCu(II)OO*t*Bu and LCu(II)¹⁸O¹⁸O*t*Bu obtained at 77 K with an excitation at 568.2 nm, 5 peaks at 471, 640, 754, 834, and 884 cm⁻¹ assigned to the O-O moiety, while the one at 754 cm⁻¹ was very small.²³¹ Little has been done to demonstrate the binding of TBHP to a tetradentate mononuclear Cu(II) complex. Resonance Raman was also employed to provide evidence about the binding between TBHP and salqu Cu(II) (Figure 3.3). The peaks at 596, 749, 915, and 955 cm⁻¹ are in a similar pattern with reported resonance Raman data associated with the O-O moiety from TBHP upon binding.²³¹ All these bands shifted from 70 to 120 cm⁻¹ to greater wavenumbers as compared to reported data, indicating a higher vibration frequency of the O-O moiety, i.e., a higher energy for the O-O bond.

For the Cu(II) *tert*-butyl peroxy intermediate, the two possible energetically favorable reaction pathways are (1) reductive cleavage of the Cu-O bond forming Cu(I) and *tert*-butyl peroxy radical, or (2) the homolytic cleavage of the O-O bond caused by direct H atom abstraction from the substrate resulting in a Cu(III)-oxo and *tert*-butyl alcohol (Scheme 3.2).²³¹ Given the fact that the addition of 50 mol % of K₂CO₃ to the reaction of 1-acetyl-1-cyclohexene did not bring in change to the reaction rate, indicating that the intermediacy of *tert*-butyl peroxy ether did not form, the reductive cleavage of the Cu-O bond was not likely to occur in the salqu Cu(II) catalytic system. Although it is challenging to prove the formation of Cu(III)-oxo, it is notable that Cu(III) can be

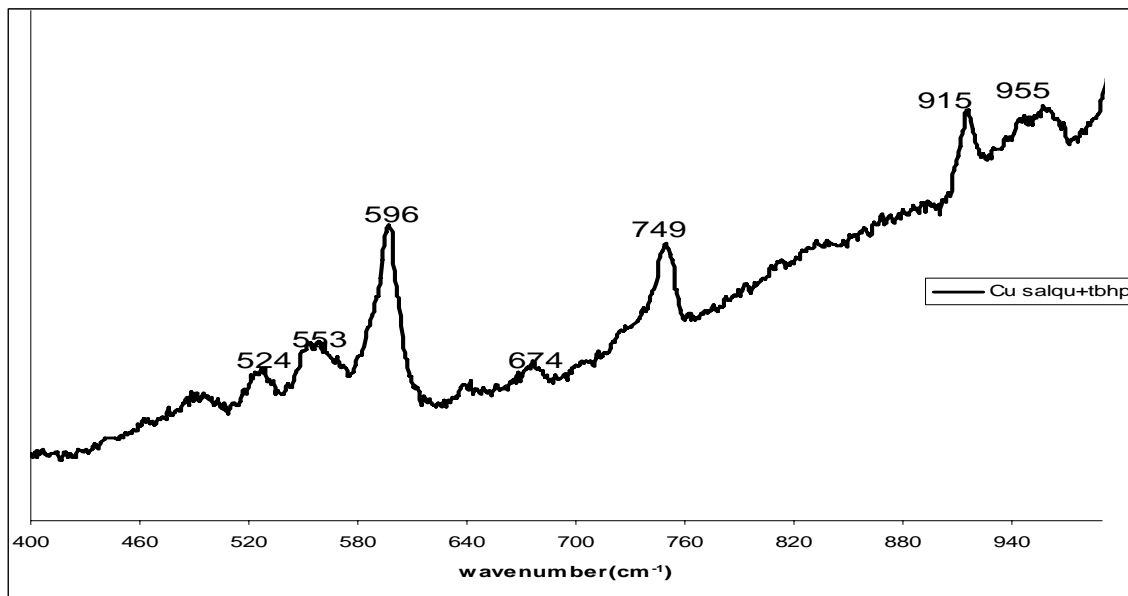
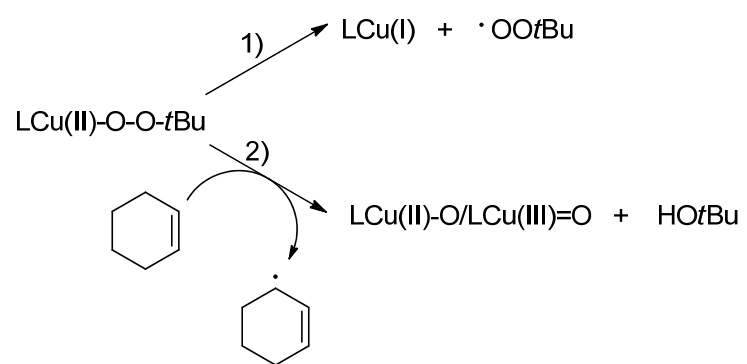


Figure 3.3. Resonance Raman spectroscopy of Cu(II) salqu with TBHP.

Scheme 3.2. Possible Reaction Pathways of LCu(II)OO*t*Bu.



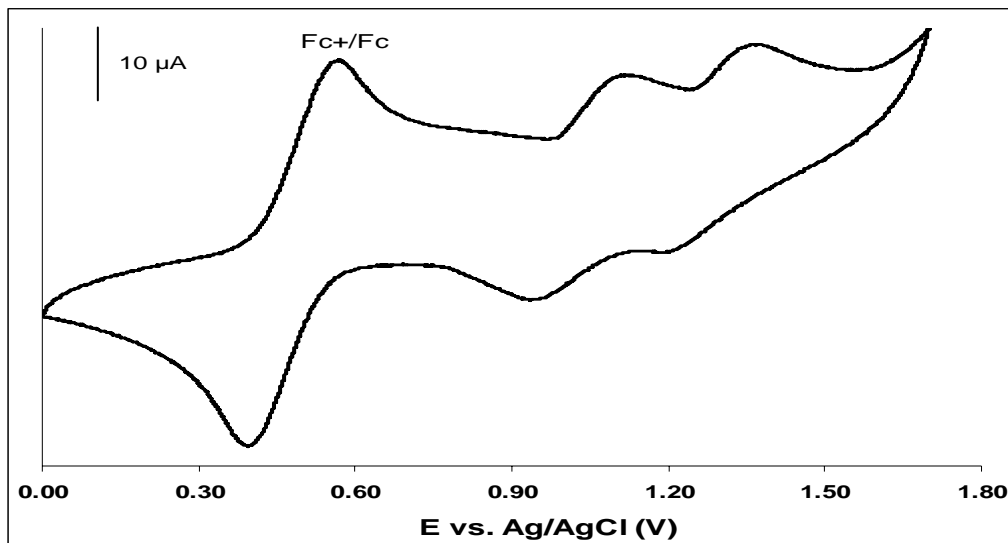


Figure 3.4. Cyclic voltammogram of Cu(II) salqu with supporting electrolyte 0.1 M tetrabutyl ammonium tetrafluoroborate in 5 mL CH₂Cl₂ and 1 mM ferrocene internal standard, reference Ag/AgCl, counter electrode Pt gauze ($A = 0.77 \text{ cm}^2$), and the working electrode was a glassy carbon disk ($d = 0.3 \text{ cm}$, $A = 0.071 \text{ cm}^2$).

stabilized by a non-innocent ligand, such as salen.^{169,170}

Cyclic voltammetry with salqu Cu(II) demonstrated two quasi-reversible oxidations ($E^{\circ\prime} = +547, +802$ mV vs Fc^+/Fc) (Figure 3.4) that could be ascribed to the sequential single electron oxidations of the phenolic moieties.¹⁶⁹ The pattern of quasi-reversible CV peaks of salqu Cu(II) complex suggested the capability of stabilizing Cu(III) by enabling the equilibrium between $[Cu(III)L]^+$ and $[Cu(II)L\cdot]^+$ as seen in previous reports with salen complexes.^{169,170} Calculation at the B3LYP/6-311+G(d,p) level also showed that a salqu ligand could stabilize Cu(III) better than salen by enhancing the spin density dispersion on the heterocyclic quinoxalinol backbone, i.e. the spin density of triplet $[Cu(III)L]^+$ is more delocalized with salqu ligand than salen ligand (Figure 3.5).

In addition, an EPR signal loss during the reaction was observed. From the oxidation reaction of 1-acetyl-1-cyclohexene, 1 mL of solution was taken after 30 min and EPR spectrum was collected from it. Only typical organic radical signal was observed. Such signal loss suggested the transformation of an EPR-active species (LCu(II), d^9) to an EPR-silent species. This could be rationalized in terms of the formation of a LCu(I) d^{10} species, or a low-spin, diamagnetic Cu(III) d^8 species that equilibrates with a ferromagnetically coupled Cu(II)-ligand-radical species as reported previously with salen Cu(II) complex.¹⁷⁰

Based on the study, it is reasonable to believe that TBHP will bind to salqu Cu(II) complex (LCu(II)) at the beginning of the reaction (Scheme 3.3). As mentioned before, the resulting Cu(II) *tert*-butyl peroxy complex **8** is likely to undergo a homolytic cleavage of the O-O bond upon reacting with substrate, yielding *tert*-butyl alcohol, allylic radical

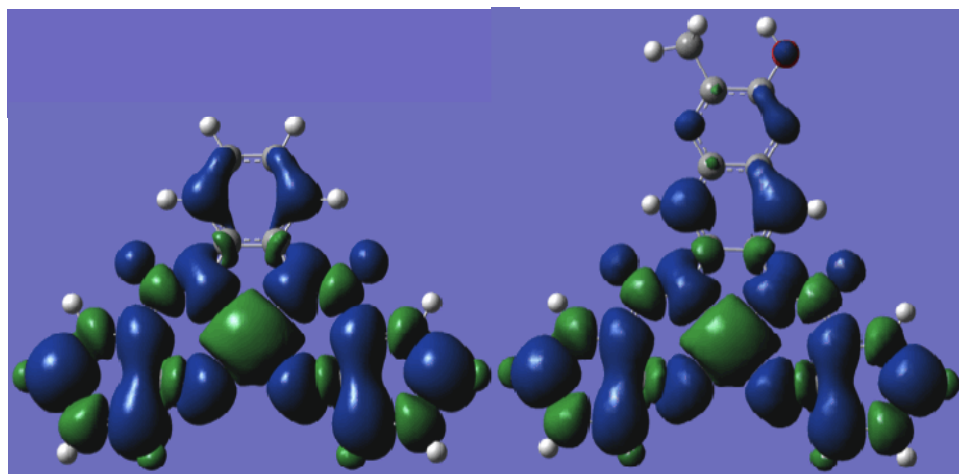
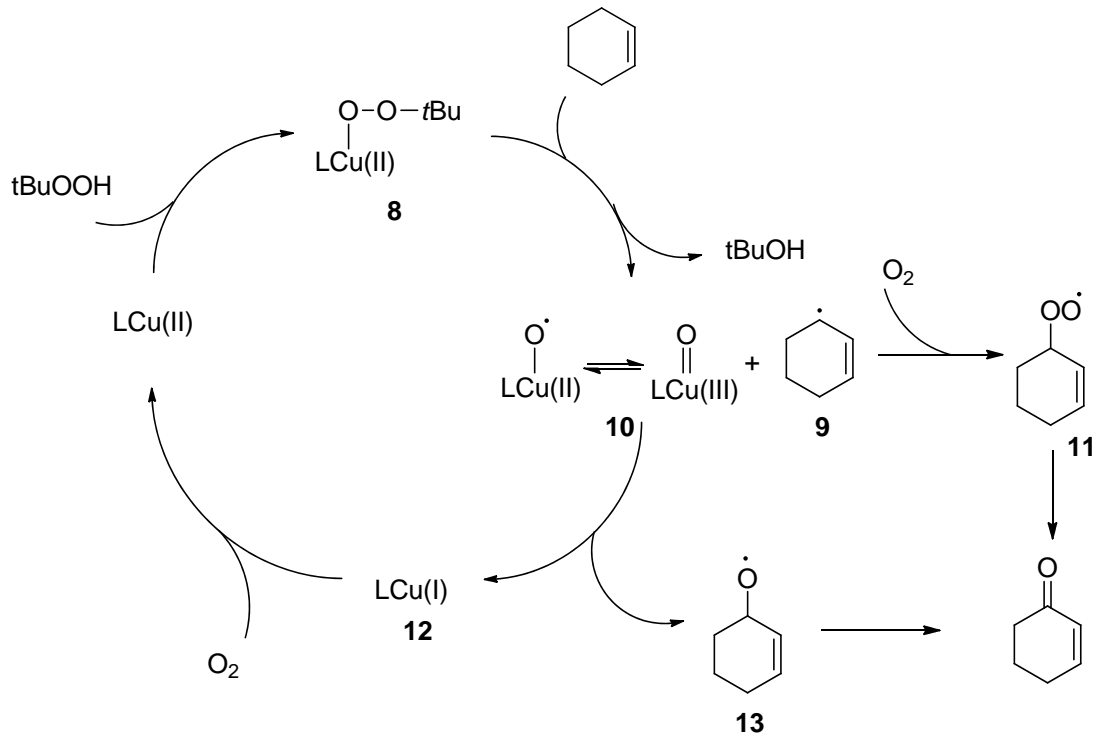


Figure 3.5. Spin density of $[\text{LCu(III)}]^+$ with 0.0004 a.u. isosurface density (L = salen and salqu).

Scheme 3.3. Postulated Catalytic Cycle for Allylic Oxidation Catalyzed by Cu(II) Salqu.



9, and LCu(II)-O•/LCu(III)=O **10**. As proved earlier, dioxygen played a crucial role in this system. One possible way for dioxygen to participate is to react with the allylic radical to form allylic peroxy radical **11** that can be converted to enone product. The active copper complex **10** can also react with the allylic radical **9** resulting in LCu(I) **12** and allylic oxyl radical **13**, the latter can be converted to enone as well. Both LCu(I) and LCu(II)-O•/LCu(III)=O are EPR-silent species. The postulated formation of LCu(I) and LCu(II)-O•/LCu(III)=O is in agreement with the observation in EPR experiment. Copper at oxidation state of +1 favors a tetrahedral geometry, while the rigid salqu ligand only provides a square planar environment. Hence, the oxidation of LCu(I) **12** to LCu(II) will easily occur. This could be another place where a reaction with dioxygen is involved. In addition, the mismatch of Cu(I) and the binding geometry gives an explanation of the earlier observation of salqu Cu(II) catalyst becoming consumed in the steroid oxidation. Further kinetic studies will be performed to better exploit the reaction mechanism.²²⁶

By using this proposed catalytic cycle, the regioselectivity and other experimental results can be well explained. The allylic radical **9** is formed by H atom abstraction when olefin reacted with LCu(II)OO*t*Bu **8**, instead of H atom abstraction by *t*BuOO•. Because of the bulkiness of the reactive Cu(II) peroxy core induced by the two *tert*-butyl groups from the ligand, the H atom abstraction would prefer to take place at the less sterically hindered position. The regioselectivity is thus enhanced. For 3-methyl-1-cyclohexene (Table 3.1, entry 5), the radical formed at the 3-position is thermodynamically more favored, while the radical at the 6-position is sterically more favored. Since the methyl group provides little steric bulkiness, the formation of the energetically favored intermediate overrides the other. Once the radical formed at the 3-position, the enone

product was energetically more favored than the allylic alcohol than can be formed by the oxidation at 3-position. In addition, the reaction at the 1-position of the radical intermediate was sterically favored. Affected by these factors, the oxidation of 3-methyl-1-cyclohexene did not have yield as good as other substrate. In the cyclic voltammetry experiment, although the oxidation potentials of the Cu(II) salqu complex were 100 and 150 mV higher than those of the Cu(II) salen complex (+450, +650 mV vs Fc^+/Fc in CH_2Cl_2 at the same scan rate),¹⁶⁹ indicating the more difficult formation of the $[\text{Cu(II)L}\cdot]^+$, no direct electron transfer from the salqu ligand was required in this system based on the proposed catalytic cycle.

In summary, a highly regioselective allylic oxidation of olefins to enones or 1,4-enediones using salqu Cu(II) complex as the catalyst is demonstrated. Excellent yields (up to 99%) can be achieved in a very short reaction time. Tolerance with a variety of functional groups is exhibited. The behavior of Cu(II) salqu complex as catalyst is studied to explain the regioselectivity, and a different mechanism of using TBHP from current methods is provided.

Chapter 4

2-Quinoxalinol Based Tridentate Schiff Base Ligand in Cu(II) Mediated

Allylic Oxidation

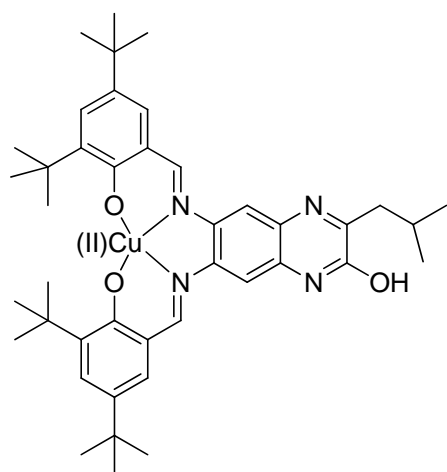
Copper containing enzymes play important roles in oxygen binding, activation, and reduction in biological systems.^{156,158,163,232,233} Numerous modeling studies have been performed to interpret the mechanism of corresponding copper containing proteins, and to extend the understanding of reactive copper species.^{168-171,234-241} Inspired by the modeling studies, many promising results with copper catalysts have been reported.^{168,169,242}

Among these modeling studies, investigations into the utility of copper-peroxide chemistry have been performed mostly with copper/peroxide ratios of 1:1 and 2:1.^{156,243-253} 2:1 Copper/peroxide species have been studied more extensively, since the thermodynamically favored Cu_2O_2 species can be stabilized at low temperatures.^{156,243-245} To date, only a few examples of mononuclear Cu(II)-peroxide species have been reported.^{231,238,254-260} In these examples, the Cu(II) cation is coordinated mainly with N-ligands, while the bound peroxide is stabilized through hydrogen bonding between the pendant ligand and oxygen of peroxide that is bound to copper. Given the extra stability provided by the hydrogen bonding between pendant ligand and peroxide, the mononuclear Cu(II)-peroxide species is stable enough to be examined; however, this increase in stability leads to a loss of reactivity. Very few Cu(II)-peroxide compounds

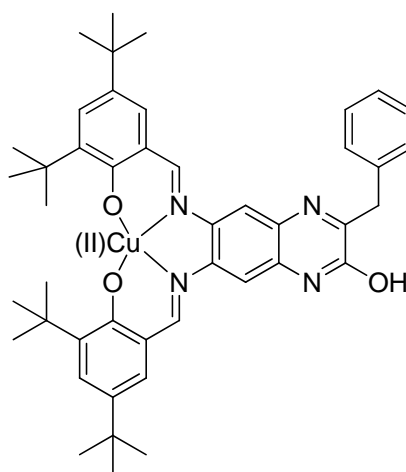
have been reported to exhibit catalytic ability in oxidation reactions.^{230,231}

Previously, we have developed a modified ligand system, abbreviated “salqu”.^{173,226} Salqu is a tetradentate ligand with two Schiff bases and two oxo- units forming a rigid square planar coordinating environment of the type [O, N, N, O]. Salqu Cu(II) complexes (Figure 4.1) have been used as catalysts in benzylic and allylic oxidations of C-H bonds with *tert*-butyl hydroperoxide (TBHP) as terminal oxidant.^{173,226} It is believed that the salqu Cu(II) complex will form a mononuclear Cu(II)-*tert*-butylperoxo complex with the addition of TBHP in solution (chapter 3). Although the peroxide tends to coordinate with two copper cations to form the thermodynamically more favored Cu₂O₂ binuclear species,^{156,243-245} the steric hinderance provided by the two *tert*-butyl groups near Cu site is sufficient to prevent the formation of a multimetallic species. This strategy is particularly useful for stabilizing mononuclear Cu-peroxides from obtaining binuclear or aggregated species.²⁶¹

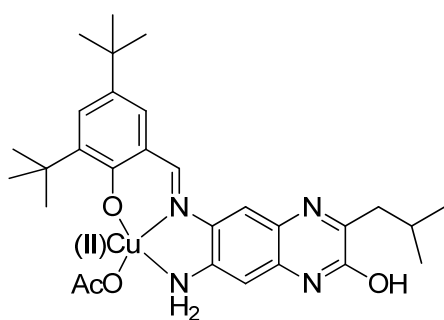
In allylic oxidation, this reaction is believed to have a different mechanism from current oxidation methods using TBHP as oxidant. In this mechanism, an unusual LCu(II)-oxyl (LCu(II)-O•) is believed to form. We propose an equilibrium between LCu(II)-oxyl and LCu(III)-oxo (LCu(III)=O). By using the salqu Cu(II) complex/TBHP system, various olefin substrates can be converted to corresponding enone products with excellent yields and regioselectivity. It is possible that the regioselectivity is also in part the result of steric hinderance from the two *tert*-butyl groups near the copper center; however, there is one complication with this system, namely, the salqu Cu(II) complex catalyst decomposes as the reaction proceeds. The decomposition can be ascribed to the mismatch of the rigid square planar binding environment provided by the salqu ligand



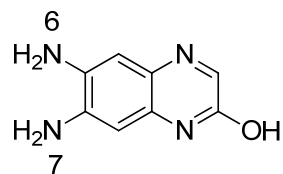
complex 1



complex 2



complex 3

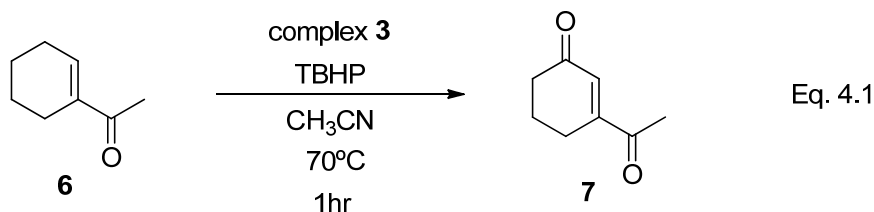


diamino-2-quinoxalinoxy

Figure 4.1. Structures of complex 1 (catalyst for allylic oxidation), complex 2 (catalyst for benzylic oxidation), complex 3, and diamino-2-quinoxalinoxy.

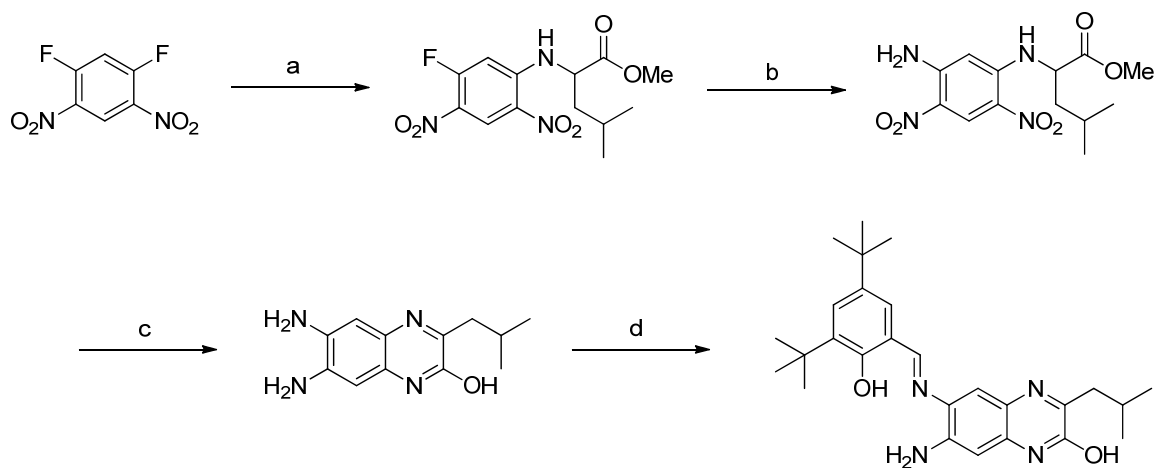
and the Cu(I) cation formed by the reduction of LCu(II)-oxyl intermediate as Cu(I) greatly favors tetrahedral binding geometry.

To address this problem, a tridentate Cu(II) complex **3** (Figure 4.1) is prepared. The different reactivity of the two amino groups of the diamino-2-quinoxalinol synthetic intermediate makes the synthesis possible. The amino group at the 6-position is slightly more reactive than the other amino group at the 7-position because of the hydroxy group on heterocycle, and the formation of the Schiff base at the 6-position also deactivates the 7-position (Figure 4.1).¹⁷² Therefore, the tridentate ligand can be obtained by reacting the diamino-2-quinoxalinol intermediate with 1.1 equiv of 3,5-di-*tert*-butyl-2-hydroxybenzaldehyde (Scheme 4.1). By removing one phenolic moiety from the salqu ligand, the coordination environment of tridentate ligand remains enough flexibility to accommodate the Cu(I) intermediate while still providing enough steric hinderance for good regioselectivity. It is hoped that the Cu(I) complex with the tridentate ligand can persist under the reaction conditions. Meanwhile, given that a subtle change in ligand structure can have a big influence on the properties of the complex,^{168,170} whether the Cu(II) complex will function as a catalyst with the replacement of the tetradentate ligand with a tridentate one becomes a question.

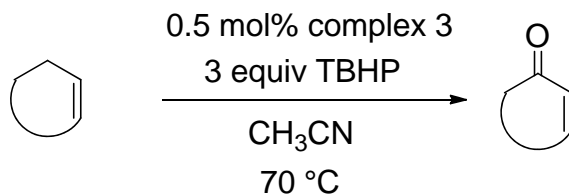


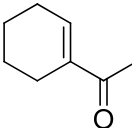
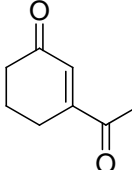
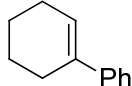
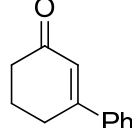
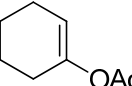
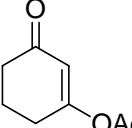
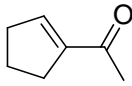
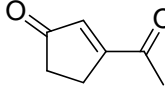
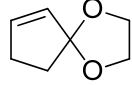
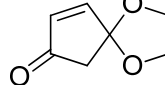
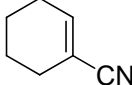
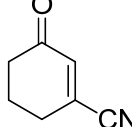
The substrate 1-acetyl-1-cyclohexene **6** was used to test the catalytic capability of the new complex **3** (eq. 4.1). The reaction was performed on a millimole scale for ease of comparison with previous results. As shown before (chapter 3), acetonitrile is the best

Scheme 4.1. Synthesis of 2-Quinoxalinol Based Tridenate Schiff Base Ligand.



(a) L-Leucine methyl ester hydrochloride, DIPEA, THF/EtOH; (b) $\text{NH}_3 \cdot \text{H}_2\text{O}$, THF/EtOH; (c) Pd/C, HCOONH_4 , EtOH, 60°C ; (d) 3,5-di-tert-butyl-2-hydroxybenzaldehyde, EtOH, reflux.

Table 4.1. Tridentate Cu(II) Complex **3** Catalyzed Allylic Oxidation of Olefins.

Entry	Substrate	Product	Time (h)	Yield ^a (%)
1			1	98 ^b
				96
2			1	85
3			2	72
4			3	96
5			1	91
6			3	89

^aIsolated yields unless stated otherwise. ^bGC yields with 1,2-dichlorobenzene added as internal standard.

solvent for this type of reaction under our conditions. All reactions were monitored by gas chromatography (GC). When 0.5 mol % of complex **3** was used as the catalyst and 3 equiv of TBHP was used as the oxidant, 3-acetyl-2-cyclohexenone **7** can be obtained with a yield of 98% in 1 h (Table 4.1, entry 1). The yield was determined by GC with 1 equiv of 1,2-dichlorobenzene added as the internal standard (yield = area of peak for product/area of peak for internal standard). The product yield is similar to that using the salqu Cu(II) complex as the catalyst (99%).

A variety of olefin substrates were also tested using 3 equiv of TBHP and 0.5 mol % of complex **3** as the catalyst (Table 4.1). All the substrates were effectively converted to the corresponding enone products in excellent yields. When comparing to the results with tetradentate Cu(II) complex, there was not much difference in yields between using salqu Cu(II) complex **1** and complex **3** as the catalyst. The tridentate Cu(II) complex **3** seemed to have the same catalytic effect with the tetradentate one.

Surprisingly, no phenolic based redox features were observed in the cyclic voltogram of complex **3**. For complex **1**, two quasi-reversible CV peaks were observed (chapter 3) and can be ascribed to the sequential one-electron oxidations of the two phenolic moieties.¹⁶⁹ Therefore, one CV peak was expected for complex **3** for its phenolic moiety. The lack of this feature suggests that the single electron oxidation of the phenolic moiety of Cu(II) complex **3** is no longer feasible. In another words, the energy gap between the HOMO and the LUMO for the tridentate complex **3** is much greater than that for tetradentate complex **1**.

Electronic spectroscopy data also supports these conclusions. The salqu ligand had an UV-Vis absorption band at 371 nm ($\epsilon = 24\ 100\ \text{M}^{-1}\ \text{cm}^{-1}$), while the salqu Cu(II) complex

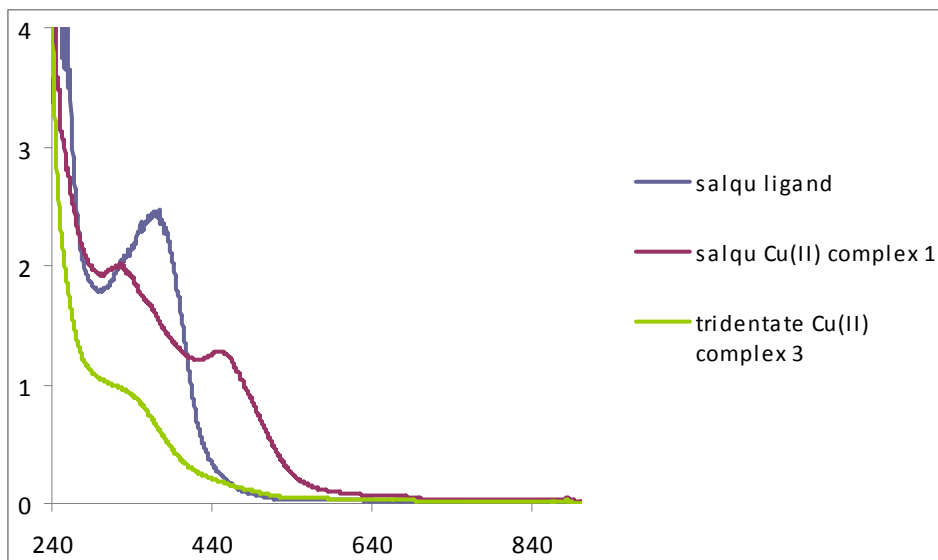


Figure 4.2. UV-vis spectra of salqu ligand, salqu Cu(II) complex 1, and tridentate Cu(II) complex 3.

1 had two UV-Vis absorptions at 327 nm ($\epsilon = 20\,000\text{ M}^{-1}\text{ cm}^{-1}$) and 450 nm ($\epsilon = 13\,000\text{ M}^{-1}\text{ cm}^{-1}$) in CHCl_3 . (Figure 4.2) The absorption of the salqu ligand can be ascribed to the electron excitation from the HOMO to the LUMO. Upon binding of Cu(II), the salqu complex **3** exhibited two absorptions. The one at 450 nm can be ascribed to the electron excitation from the HOMO of complex to the LUMO, while the other intense absorption band at 327 nm is typical of a ligand-to-metal charge transfer (LMCT) transition.¹⁷⁰ The absorptions at 371 nm for the salqu ligand and at 450 nm for salqu Cu(II) complex **1** correspond to the CV peaks for the salqu ligand and complex **1** respectively. As seen in the CV experiment, the salqu ligand exhibited one redox pair within the scan window (Figure 4.3), and its Cu(II) complex **1** exhibited two quasi-reversible peaks (chapter 3).

For the tridentate Cu(II) complex **3**, only one UV-vis absorption was observed at 334 nm ($\epsilon = 9\,000\text{ M}^{-1}\text{ cm}^{-1}$). This band is the result of the LMCT transition. It is around the same wavenumbers as the LMCT band of the tetradentate complex **1**. In addition, this peak is about half of the intensity as compared to the LMCT peak of complex **1**. Since tetradentate complex **1** has two phenolic ligands that can contribute to the LMCT, while tridentate complex **3** only has one phenolic ligand, the ratio of the intensities of complex **1** and complex **3** make sense.

Since the Cu(II) complex **3** has been shown to have different electronic properties compared to the Cu(II) complex **1**, they are not likely to have the same catalytic effect. This conclusion seems contradictory to our experimentally derived results in the allylic oxidations of olefin substrates. To probe these differences, the reaction was repeated using a perdeuterated substrate, cyclohexene- d_{10} . The oxidation of cyclohexene- d_{10} was carried out in acetonitrile using 0.5 mol % of catalyst loading and 3 equiv of TBHP.

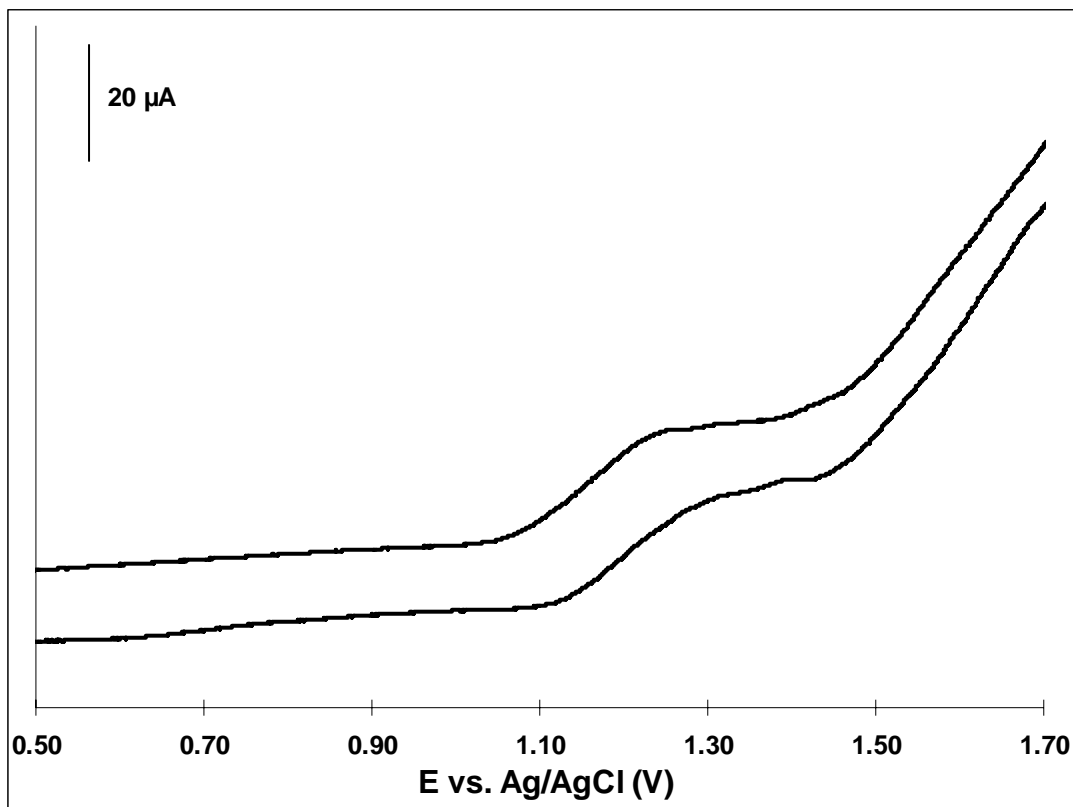
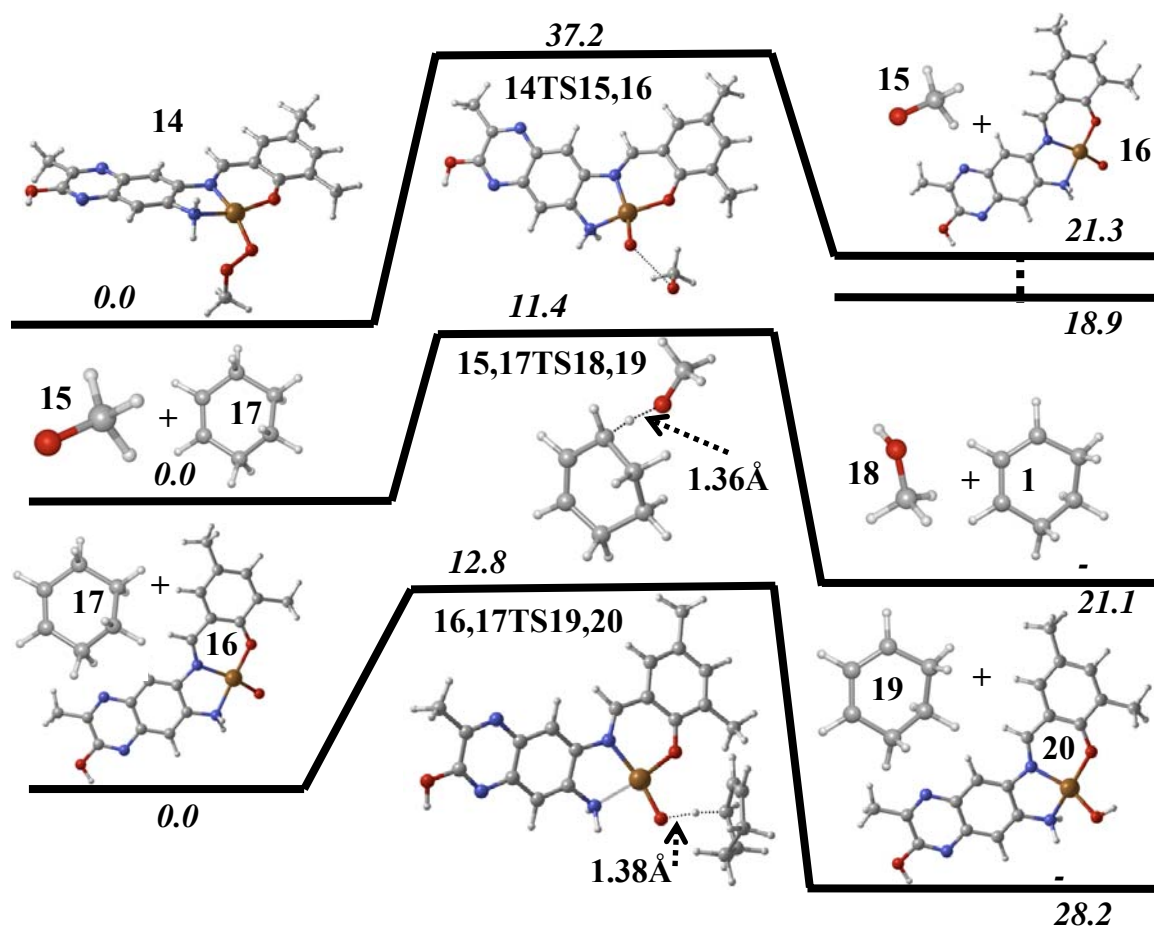


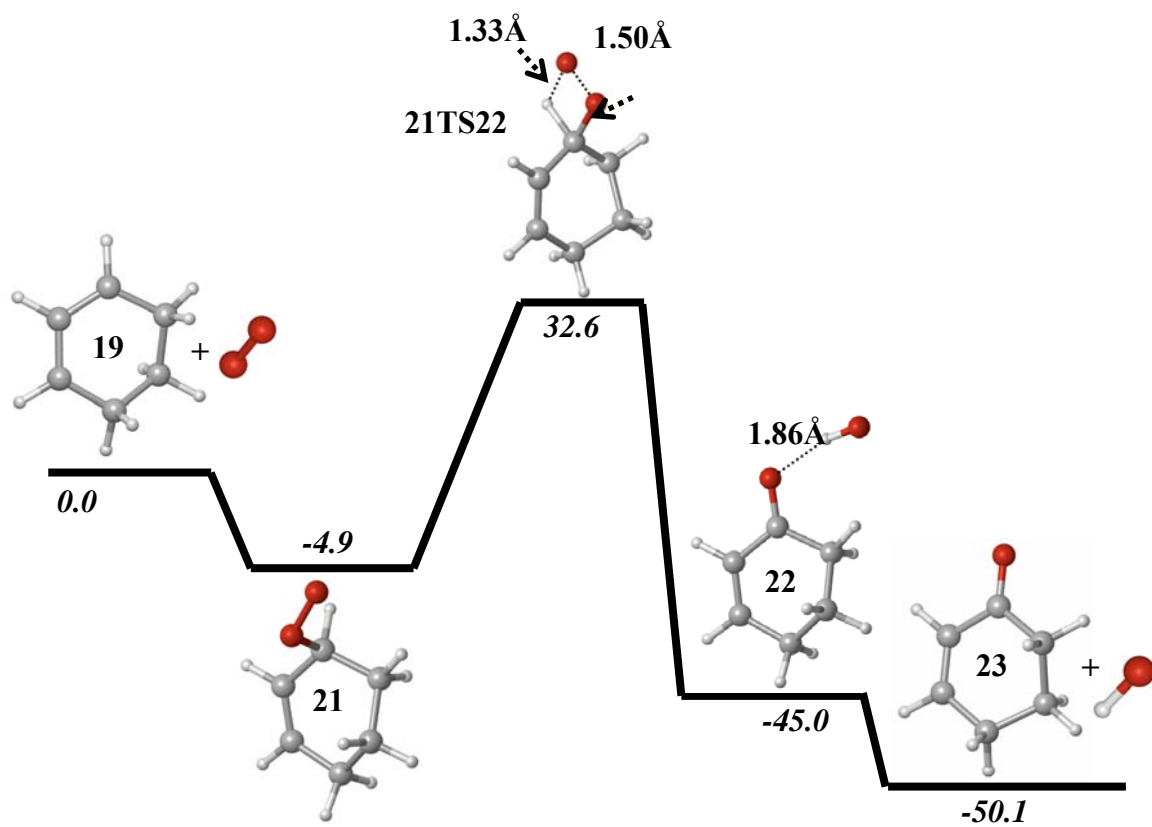
Figure 4.3. Cyclic voltammogram of salqu ligand with supporting electrolyte 0.04 M tetrabutyl ammonium tetrafluoroborate in 5 mL CH_2Cl_2 , reference Ag/AgCl, counter electrode Pt gauze ($A = 0.77 \text{ cm}^2$), and the working electrode was a glassy carbon disk ($d = 0.3 \text{ cm}$, $A = 0.071 \text{ cm}^2$). Scan rate = 100 mV/s.

Under exactly the same reaction conditions, reaction yields at 30 min (GC yields, as 1,2-dichlorobenzene added as the internal standard) were used as the indicator of reaction rates. When using the tetradentate complex **1** as catalyst, the $k_H/k_D = 1.5$; meanwhile, when the complex **3** was used as the catalyst, the reaction had the k_H/k_D value of 3.7. This big change in kinetic isotope effect or KIE value, when the catalyst was change from tetradentate Cu(II) complex **1** to tridentate Cu(II) complex **3** for the same reaction, confirms the difference in their catalytic mechanism.

To further explore these differences, density functional theory (DFT) calculations in acetonitrile media were used to characterize their possible catalytic mechanism, and two possible reaction pathways were provided. All calculations were simplified by replacing the *tert*-butyl groups with methyl groups. In the first pathway (Scheme 4.2), the reaction is initiated by the formation of a Cu(II) peroxy complex **14** that can be obtained from the binding of peroxide to the tridentate Cu(II) complex **3**. The homolytic cleavage of the O-O bond results in the formations of the methoxyl radical **15** and the Cu(II)-oxyl radical **16**. The species **16** is in the triplet state after the cleavage of the O-O bond. A singlet intermediate **16** was formed afterwards through intersystem crossing (ISC). The energy of singlet state is about 2.9 kcal lower in energy than the triplet state intermediate. The triplet state is corresponding to the LCu(II)-oxyl radical species, while the singlet state is corresponding to the LCu(III)=O species. The facile ISC is in agreement with the previously reported research on equilibrium between LCu(II)-O• and LCu(III)=O in solution.¹⁷⁰ The free energy barrier for this step (**14** → **14TS15,16** → **15, 16**) is calculated to be 37.2 kcal. The methoxyl radical **15** can react with the substrate cyclohexene **17** by abstracting the H atom at allylic position, yielding the methanol **18**

Scheme 4.2. Calculated Reaction Pathway 1 for Allylic Oxidation using Complex **3** as the Catalyst.





and cyclohexenyl radical **19**. This step is thermodynamically favored, as the products are 21.1 kcal lower in free energy. The energy barrier for this step (**15, 17** → **15,17TS18,19** → **18, 19**) is 11.4 kcal. The substrate **17** can also react with Cu(II)-oxyl radical **16**. The H atom at the allylic position will be pulled away by the Cu(II)-oxyl species, cyclohexenyl radical **19** will be obtained along with the Cu(II)-OH complex **20**.

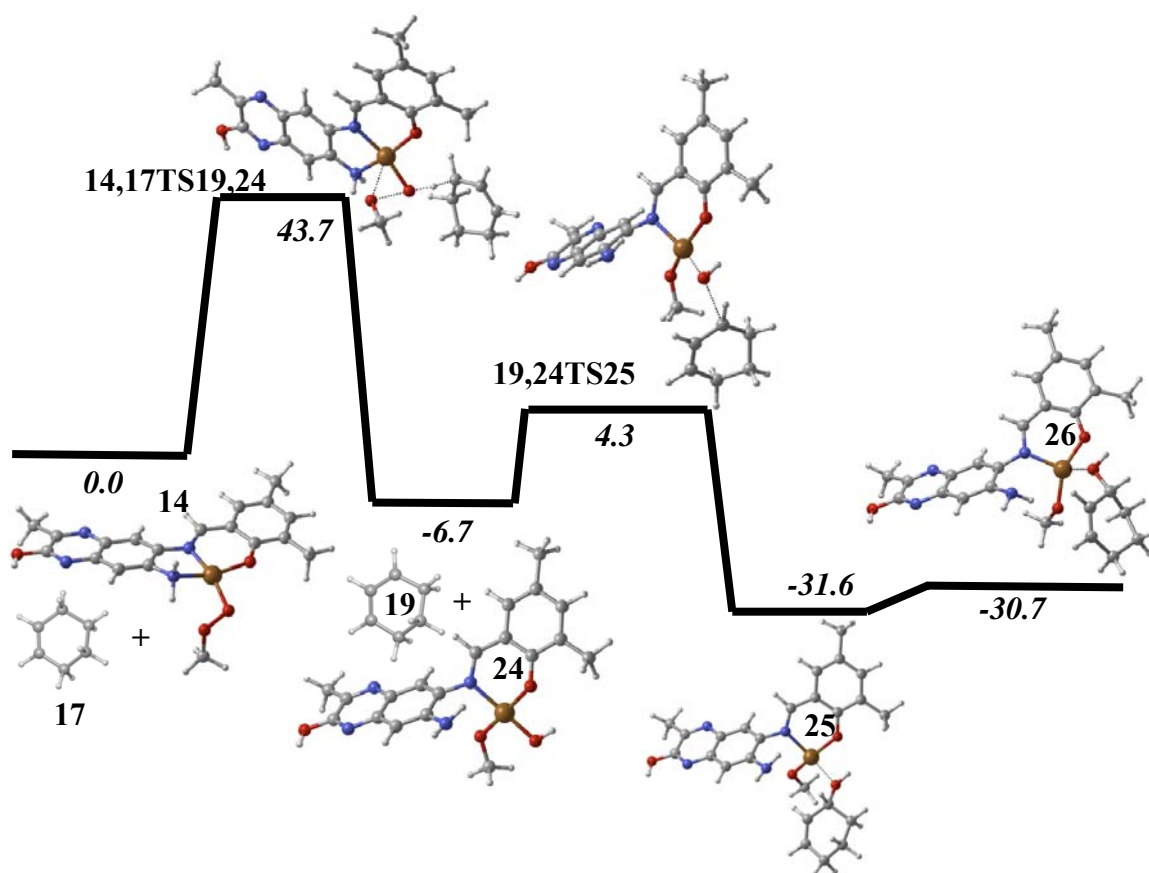
Such Cu(II)-OH complexes have been reported to carry out the ligand exchange with peroxides to form Cu(II)-peroxo species.^{252,261} Under our reaction conditions, Cu(II)-OH **20** can be converted to Cu(II)-peroxo **14** to maintain the catalytic activity. The reaction between dioxygen and the cyclohexenyl radical **19** is spontaneous. The resulting cyclohexenyl peroxy radical will go through a transition state, in which the O-O bond is breaking and O-H bond is forming. The free energy barrier of this step is 37.5 (32.6 + 4.9) kcal. Eventually, the enone product **23** forms along with a hydroxyl radical.

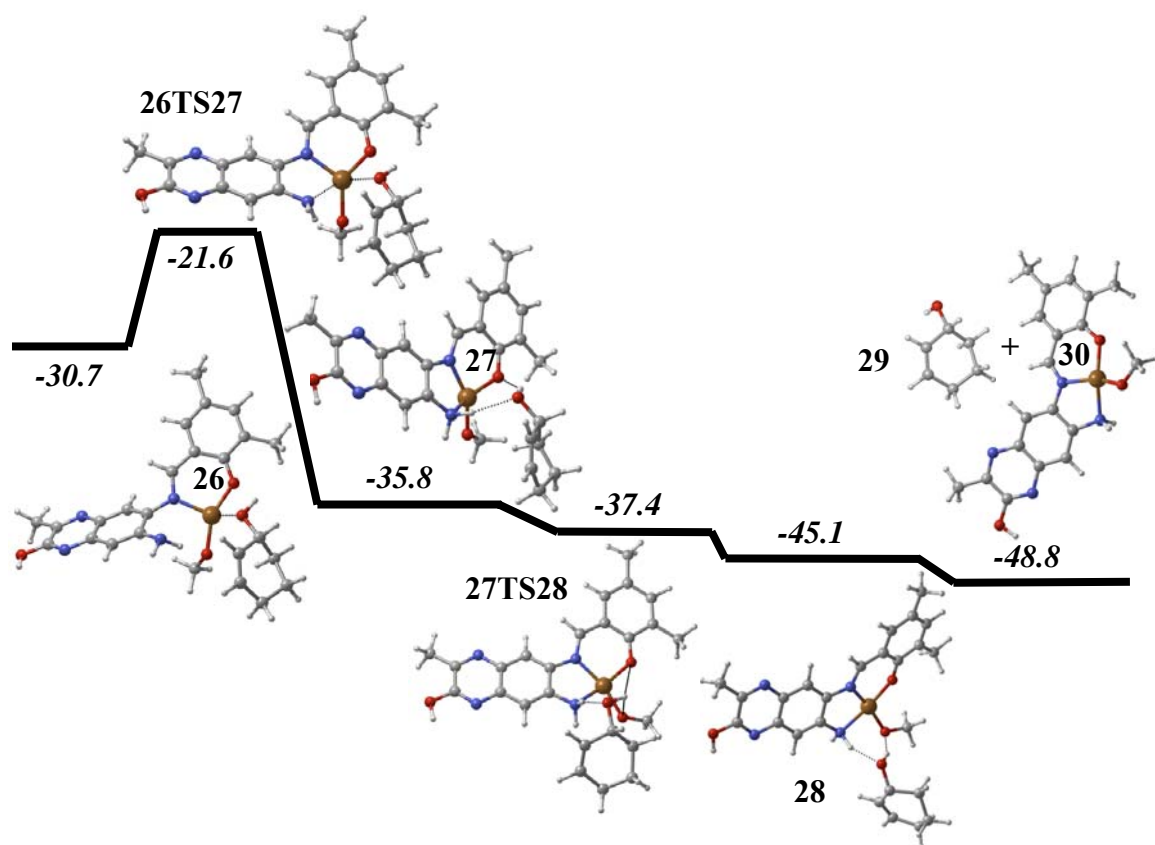
The other possible reaction pathway (Scheme 4.3) involves H atom abstraction from the allylic site by the oxygen connected to the Cu center. The cyclohexenyl radical **19** will be formed as in the first pathway, while a different intermediate **24** was formed in this pathway. The transition state (**14,17TS19,24**) had an energy of 43.7 kcal as compared to the initial reactants. In the transition state, along with the H atom abstraction, the peroxo O-O bond is breaking and the bond between Cu center and the other oxygen of the peroxo is forming. In intermediate **24**, the Cu center was bound to the oxygen and one nitrogen from the ligand, as well as the methoxyl and a hydroxide. The cyclohexenyl radical **19** can further react with the hydroxide of the intermediate **24**, leading to complex **25** with the Cu center bound to an allylic alcohol. The conformational rearrangement of complex **25** resulted in the formation of complex **26** with a slight

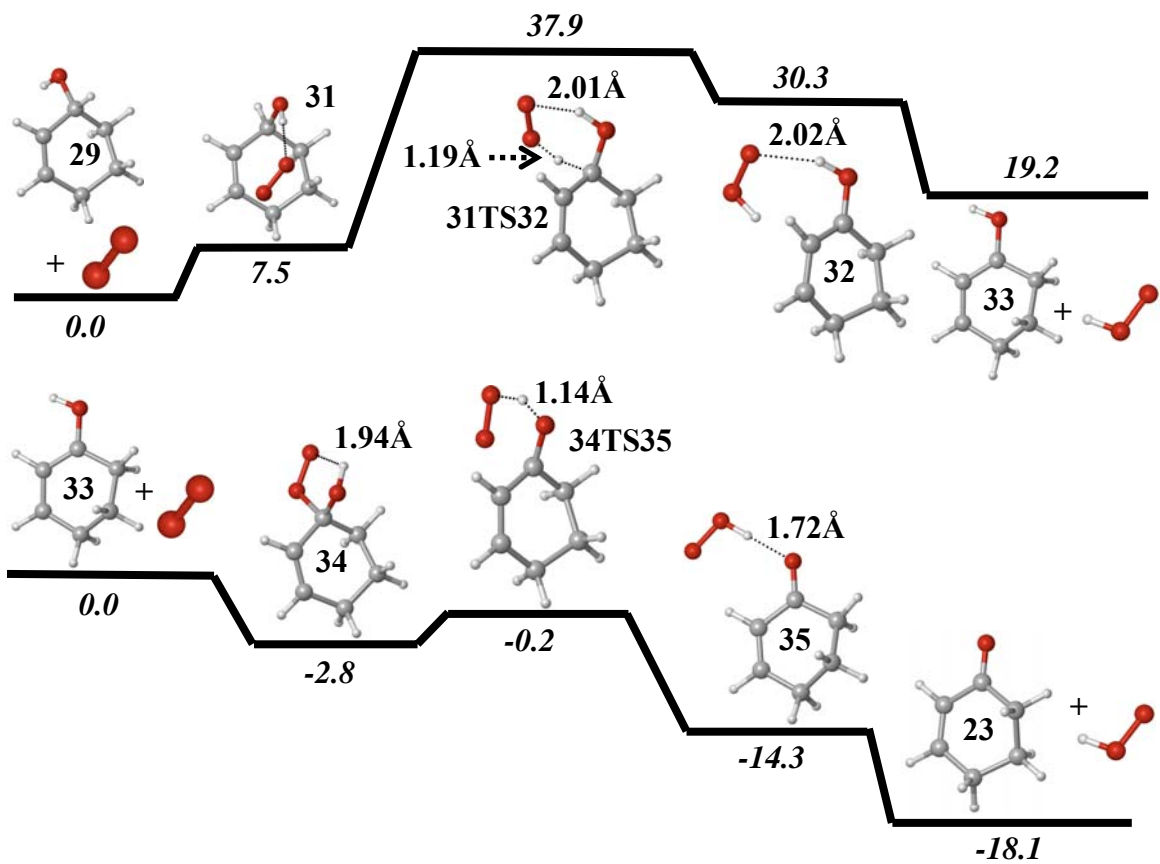
difference in free energy. The unbound nitrogen ligand would come to bind to Cu center again in the transition state (**26TS27**) to allow for the dissociation of the allylic alcohol. In intermediate **27**, the Cu center is bound to the ligand as well as to the methoxyl group, while the allylic alcohol is still in association with the complex through H-bonding. After a series of configurational and conformational changes, the free allylic alcohol **29** and methoxyl group bound to Cu complex **30** are obtained. In a fashion much the same as the Cu(II)-OH species, Cu(II)-OMe can also be converted to Cu(II)-peroxo complex with the presence of TBHP.^{257,261} The catalytic activity of the Cu complex is therefore maintained. These computational results also provided a possible reaction pathway for allylic alcohol **29** to be converted to the enone product **23** (Scheme 4.3). In this calculation, dioxygen is employed to abstract the H atom at the allylic site, resulting in an allylic alcohol **33** bearing a radical at its allylic position. Species **33** will further react with another dioxygen molecule, and is subsequently oxidized to the enone product **23**. The formation of the enone product **23** from the allylic alcohol through calculated pathway has not been supported by experimental evidence.

In the first pathway, the homolytic cleavage of O-O bond in Cu(II) peroxo complex **14** (**14** → **14TS15,16** → **15, 16**) and the intramolecular H atom abstraction (**21** → **21TS22** → **22**) are the two steps that have the greatest energy barriers (37.2 and 37.5 kcal respectively). Therefore, these two steps may be considered as the rate-determining steps. In the second pathway, the rate-determining step is the H atom abstraction by complex **14** (**14, 17** → **14,17TS19,24** → **19, 24**), and has a free energy barrier of 43.7 kcal. A calculated KIE value of 4.0 was obtained based on the second calculated pathway. This value is very close to the experimental result ($k_H/k_D = 3.7$). thus, the second

Scheme 4.3. Calculated Reaction Pathway 2 for Allylic Oxidation using Complex **3** as the Catalyst.







computationally derived pathway seems agree most closely with the experimentally obtained results.

Another difference between these two possible pathways is how TBHP is utilized. In the first pathway, TBHP is used to coordinate with the Cu center to produce the Cu(II)-oxyl radical/Cu(III)-oxo species, and a methoxyl radical. Both this Cu-oxygen species and the methoxyl radical are responsible for the H atom abstraction from the substrate; however, it is the dioxygen molecule that oxidizes the substrate to yield the final enone product. Hence, the oxygen of the enone product is from dioxygen molecule. On the other hand, in the second pathway, the allylic H atom of substrate is still abstracted by Cu(II)-peroxo complex **14**; however, the resulting allylic radical species is oxidized by the hydroxide bound to the Cu center leading to the allylic alcohol compound. Although dioxygen might participate in the oxidation of the allylic alcohol to the enone product, the oxygen atom of the enone product is still from TBHP.

Since these two pathways will lead to the same product with the oxygen atom having different sources, an experiment was designed to elucidate the oxygen source of the product. 1-Phenyl-1-cyclohexene was used as the substrate with 0.5 mol % of complex **3** as the catalyst. The oxidation reaction was performed in acetonitrile degassed with argon under $^{18}\text{O}_2$ atmosphere. Regular TBHP was used as the oxidant. If the oxygen incorporated into the product comes from TBHP, only the ^{16}O product will be obtained; otherwise, ^{18}O containing enone will be in the product. After 1 h of reaction time, the reaction solution was analyzed by GC-MS (Figure 4.4). As a result, both ^{16}O and ^{18}O containing products were observed. The ratio of ^{16}O product to ^{18}O one is about 3:1. This result indicates that both pathways can be happening during the course of the oxidation

reaction. The ratio of ^{16}O product to ^{18}O product shows that the second pathway is more favored than the first, since the first pathway leads to the ^{18}O product while the second one leads to the ^{16}O product.

The ratio of $^{16}\text{O}/^{18}\text{O}$ products are also in accordance with the calculated and experimental KIE value. Based on the second pathway, a $k_{\text{H}}/k_{\text{D}}$ value of 4 was obtained from the calculations. Experimentally, a $k_{\text{H}}/k_{\text{D}}$ value of 3.7 was measured for the reaction using tridentate complex **3** as the catalyst, and a $k_{\text{H}}/k_{\text{D}}$ value of 1.5 was measured for the reaction using tetradentate complex **1** as the catalyst. The oxidation using complex **1** is believed to have the reaction pathway similar to the first one calculated for complex **3** (chapter 3). Therefore, when the reaction using complex **3** goes through the first pathway, a $k_{\text{H}}/k_{\text{D}}$ value close to 1.5 will be expected. Considering the second pathway is more favored concluded from the $^{16}\text{O}/^{18}\text{O}$ products ratio, it is reasonable to expect a $k_{\text{H}}/k_{\text{D}}$ value between 4 and 1.5 for complex **3** with the value closer to 4. The experimental $k_{\text{H}}/k_{\text{D}}$ value of 3.7 for complex **3** perfectly falls into this range.

In conclusion, a tridentate Cu(II) complex has exhibited the same catalytic effect as its structurally related tetradentate Cu(II) complex; however, the tridentate complex possesses very different properties from the tetradentate one. Electronic spectroscopy and cyclic voltammetry have been used to reveal such differences. DFT calculations provide two possible reaction pathways for the tridentate Cu(II) complex in allylic oxidation. Experimental results suggest the existence of two concurrent pathways in these oxidation reactions.

purified

YC_013012_tetra_1 392 (16.626) Cm (385:392-342:354)

TOF MS EI+
7.56e4

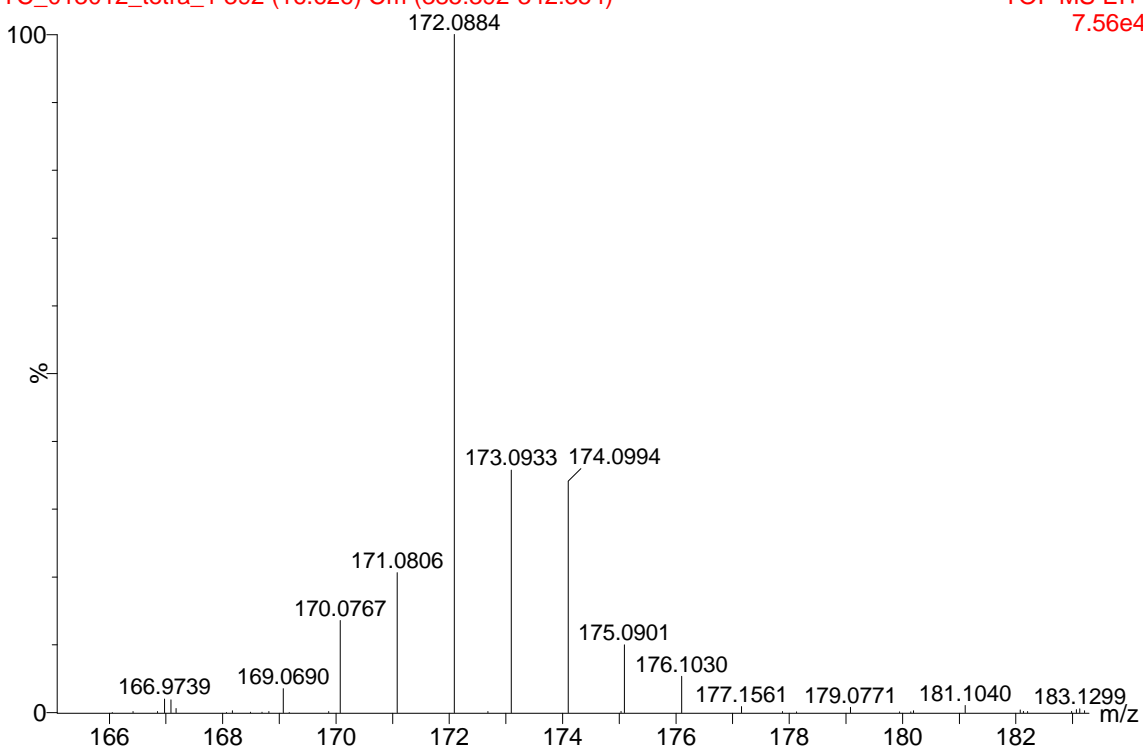


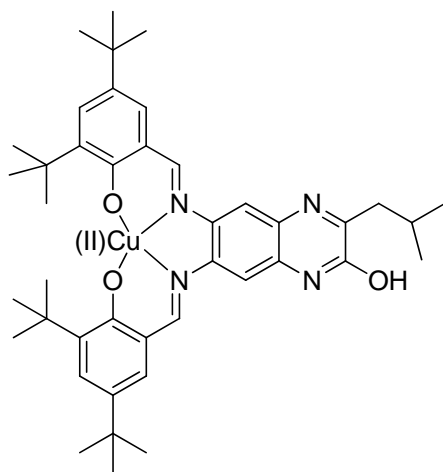
Figure 4.4. MS spectrum of reaction solution using regular TBHP as the oxidant under $^{18}\text{O}_2$ atmosphere.

Chapter 5

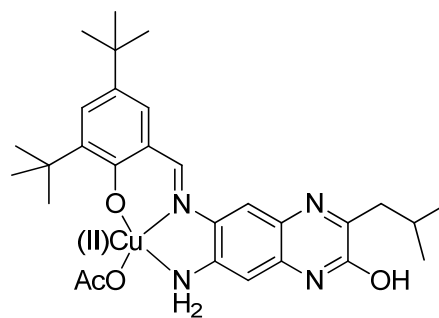
Conclusion and Future Work

In this dissertation, the salen Cu(II) complex **1** (Figure 5.1) is used as catalyst in the allylic oxidation of Δ^5 -steroids into 7-keto- Δ^5 -steroids with *tert*-butyl hydroperoxide (TBHP) as oxidant. After the reaction time and oxidant ratio are optimized using pregnenolone acetate as substrate, a variety of Δ^5 -steroidal substrates are oxidized with moderate yields; meanwhile, unreacted Δ^5 -steroidal starting materials can be recovered after column chromatography. Given the observation that the color of the reaction solution changes from its initial red to yellowish, as well as the reported slow decomposition of salen Cu(II) complex in organic solvent,¹⁶⁹ the Cu(II) complex catalyst is thought to be consumed as the reaction proceeds. The effects of acetonitrile and chloroform as solvents are also examined, and acetonitrile is found to be the better solvent for this oxidation reaction. Therefore, the oxidation reactions are carried out in acetonitrile with 0.5 mol % of complex **1** and 5 equiv of TBHP added simultaneously with multiple portions used. With these further optimized reaction conditions, Δ^5 -steroids can be converted to the 7-keto- Δ^5 -steroidal products in excellent yields (up to 99%). This salen Cu(II)/TBHP catalytic system for Δ^5 -steroids exhibits great tolerance with a various functional groups, and has low sensitivity to air or water, while significantly reduced reaction time is required as compared to other current oxidation methods.

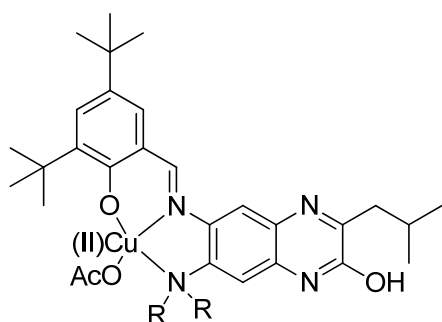
In addition, the regioselectivity of the oxidation is also rationalized from the



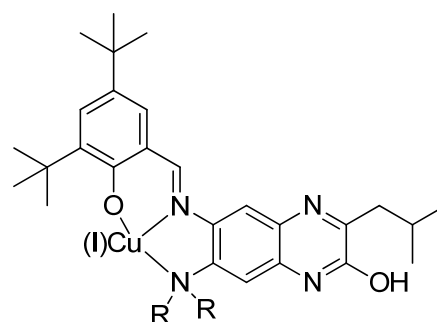
complex 1



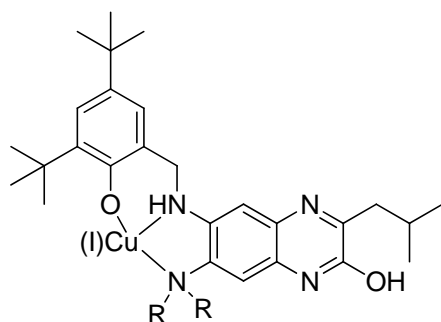
complex 3



complex 36



complex 37



complex 38

Figure 5.1. Structures of complex 1 (catalyst for allylic oxidation), complex 2 (catalyst for benzylic oxidation), complex 3, and diamino-2-quinoxalinol.

substrate's perspective. As predicted by resonance structure theory, the species bearing radical at the 7-position is more stable than the one having unpaired electron at the 4-position, and therefore 7-keto products are obtained. This results is supported by theoretical calculations at the B3LYP/6-31G(2d,p) level.

In addition to Δ^5 -steroids, simple olefin substrates are also oxidized using salqu Cu(II)/TBHP catalytic system. In the oxidations of simple olefins, only 0.5 mol % of complex **1** and 3 equiv of TBHP are needed to complete the oxidation reactions in 1 – 2 hours. Using 1-acetyl-1-cyclohexene as substrate, dichloromethane (DCM), chloroform, acetonitrile, dimethyl sulfoxide (DMSO), and dimethyl formamide (DMF) are tested as solvents. Among these solvents, acetonitrile is found to be the best for the oxidation reaction. The investigation on solvent effects implies the crucial role of dioxygen molecules in the oxidation. The importance of dioxygen is further confirmed by the result of the oxidation reaction in acetonitrile degassed with argon under N_2 atmosphere.

Analytical techniques and theoretical calculations are also employed to investigation this salqu Cu(II)/TBHP catalytic system. Resonance Raman experiment provides evidence for the binding of TBHP to the Cu(II) center of salqu Cu(II) complex. Cyclic voltammetry (CV) experiment of the salqu Cu(II) complex suggests the capability of the salqu ligand in stabilizing Cu(III) cation by achieving the equilibrium between a Cu(II)-ligand-radical species $[Cu(II)L\cdot]^+$ and a Cu(III)-ligand species $[Cu(III)L]^+$. The theoretical calculations at B3LYP/6-311+G(d,p) level show that salqu ligand could stabilize Cu(III) cation better than salen by enhancing the spin density dispersion on the heterocyclic quinoxalinol backbone.

Combining all the results and the conclusion from experimental facts that the *tert*-butylperoxy ether intermediate is not formed in our catalytic system, a reaction mechanism is proposed. In this mechanism, TBHP is utilized in a different fashion from current oxidation method. Upon binding to the salqu Cu(II) complex, the O-O bond of TBHP becomes more reactive. The homolytic cleavage of the O-O bond results in a Cu(II) oxyl radical (Cu(II)-O•) that will participate in the reaction as an oxidant. From this mechanism, the earlier observation of complex **1** consumption in the oxidation of Δ^5 -steroids can be explained, as well as the regioselectivity and some experimental observations in the oxidation of simple olefins.

When tetradentate salqu Cu(II) complex **1** is used as catalyst in the allylic oxidations, the catalyst decomposes to some extent as the reaction proceeds. The decomposition is ascribed to the mismatch of the rigid square planar binding geometry provided by the salqu ligand and the Cu(I) formed from the reduction of Cu(II)-O• species, as Cu(I) greatly favors a tetrahedral binding geometry. Hence, the tridentate Cu(II) complex **3** (Figure 5.1) is prepared to provide more flexible binding environment for the copper cation, yet enough steric hinderance to maintain the regioselectivity for substrate. Although the results of the allylic oxidations of simple olefin substrates using complex **3** is similar to those using complex **1** as catalyst, CV experiment of complex **3** and the UV-Vis spectroscopy suggest different properties of tridentate complex **3** from tetradentate complex **1**.

The density functional theory (DFT) calculations provide two possible reaction pathways. In the kinetic isotope effect (KIE) experiment, a k_H/k_D value of 3.7 is obtained experimentally, while a k_H/k_D value of 4.0 is calculated based on one of the two possible

pathways. Meanwhile, the result of the oxidation reaction under $^{18}\text{O}_2$ atmosphere using regular TBHP indicates the existence of two concurrent pathways in these oxidation reactions.

Based on the experimental results and the theoretical calculations, the allylic oxidation using tridentate Cu(II) complex **3** as catalyst and TBHP as oxidant is believed to undergo two different reaction pathways yielding the same product. The problem of catalyst consumption is solved in this system.

Although some understanding on the properties of 2-quinoxalinol based Schiff base ligand bound Cu(II) complex has been obtained, questions remain. For example, in the second computationally derived reaction pathway (chapter 4), allylic alcohol is obtained and further oxidized by molecular oxygen into enone product. In this step, the complex **3** catalyst is not involved. Such oxidation of allylic alcohol has not been studied experimentally. Hence, investigations of oxidizing allylic alcohol using complex **3** as catalyst with/without molecular oxygen will be of great interest. If the oxidation of allylic alcohols using complex **3** as catalyst led to the enone product, how is the Cu(II) complex **3** functioning will be another question of interest. In addition, if the allylic alcohol was obtained as intermediate as predicted by calculations, will it be possible to stop the reaction at this step experimentally to have the allylic alcohol as the final product, and will this reaction be enantioselective?

Besides continuous investigation on tridentate Cu(II) complex **3**, another tridentate Cu(II) complex **36** (Figure 5.1) is also interesting. In complex **3**, one of the three binding sites provided by the salqu ligand is a NH_2 group. According to the calculation results, the H atom of this NH_2 group can provide extra stability through H-bonding; however,

free H atoms from ligand will introduce uncertainty in catalytic reaction. Thus the replacements of the two H atoms with R groups will provide a simpler model for investigations, and will also provide a comparison to study the effect of H-bonding in the reaction process.

One other work can be performed is to study the tridentate Cu(I) complex **37** and **38** (Figure 5.1). Cu(I) complexes are known to bind and activate molecular oxygen in different fashions;(ref) however, very few Schiff base ligand or salen-type ligand have been utilized in such study. The binding and activation of molecular oxygen with tridentate Cu(I) complexes might be a good point to start with, and might be applied to catalytic oxidations as well.

To sum up, tetradentate Cu(II) complex **1** and tridentate Cu(II) complex **3** have been used as catalysts in allylic oxidation. Excellent results are achieved. A possible reaction mechanism is proposed for oxidation using tetradentate Cu(II) complex **1** based on the experimental results and theoretical calculations. When tridentate Cu(II) complex **3** is used as catalyst, the oxidation reaction is believed to undergo two concurrent reaction pathways yielding the same product. In the follow-up investigations, the studies on allylic alcohol oxidation using complex **3**, catalytic effect of complex **36**, and molecular oxygen binding and activation by complex **37** and **38** will be of great interest.

Chapter 6

Experimental Section

General. All reagents were obtained commercially without further purification. Yields reported are for isolated mass yield after chromatography, unless indicated otherwise. The leucine methyl ester hydrochloride, 1,5-di-fluoro-2,4-di-nitrobenzene (DFDNB), ammonium formate, 3,5-di-*tert*-butyl-2-hydroxybenzaldehyde, ammonium hydroxide (5.0 N), palladium on carbon (wet, 5%), *tert*-butyl hydroperoxide (TBHP, 5.0 - 6.0 M solution in decane) are purchased from Aldrich. $^{18}\text{O}_2$ is purchased from Icon in a 100 mL breakseal (gas at atmos pressure, 98 atom %). ^1H NMR and ^{13}C NMR spectra were recorded on 250 or 400 MHz instruments as solutions in CDCl_3 or DMSO-d_6 ; chemical shift (δ) are reported in ppm relative to Me_4Si . Reaction process was monitored by thin-layer chromatography (TLC) using 0.25mm silica gel precoated plates; spots were detected with UV light and revealed with I_2 . Chromatographic purifications were performed using Fisher (60Å, 70-230 mesh) silica gel. HRMS data were collected with electrospray ionization. IR spectroscopic data was collected using a SHIMADZU Inc. IR, Prestige-21 Fourier Transfer Infrared Spectrophotometer and KBr solid samples. All UV-Vis data was collected using a Cary 50 UV-Vis spectrophotometer with a xenon lamp and an equipment range from 200 to 1000 nm. Atomic absorption spectrum (Varian AA240), its software (AA240FS) and hollow cathode lamp (HLC; Ni 232.0 nm, optimum working range: 0.1 – 20 mg/L; Mn 279.5 nm, optimum working range: 0.02 – 5 mg/L; Cu

324.8 nm, optimum working range: 0.03 – 10 mg/L) are from Varian Inc. Raman spectroscopy was performed using the 785 nm line (6 mW) from an air-cooled argon ion laser (model 163-C42, Spectra-Physics Lasers, Inc.) as the excitation source. Raman spectrum was collected and analyzed using a Renishaw via Raman microscope system. In cyclic voltammetry experiment, the electrochemical circuit was controlled using an Epsilon electrochemistry workstation (Bioanalytical Systems, Inc.). CW EPR spectrum was measured at X-band (9 GHz) frequency on a Bruker EMX spectrometer, fitted with the ER-4119-HS high sensitivity perpendicular-mode cavity. General EPR conditions were: microwave frequency, 9.385 GHz; field modulation frequency, 100 kHz; field modulation amplitude, 0.6 mT. The Oxford Instrument ESR 900 flow cryostat in combination with the ITC4 temperature controller was used for measurements in the 4 K to 300 K range using a helium flow. Measurements at 77 K were performed by fitting the cavity with a liquid nitrogen finger Dewar. All products have been previously described, and ^1H , ^{13}C NMR and IR data are in accordance with literature data.

Synthesis of Diamino-2-quinoxalinol intermediate. To a 150 mL round-bottomed flask charged with a stirring bar, were sequentially added 1,5-difluoro-2,4-dinitrobenzene (DFDNB, 4.0 mmol, 0.8168 g), leucine methyl ester hydrochloride (4.0 mmol, 0.7268 g), tetrahydrofuran (THF, 30 mL), ethanol (30 mL), and di-isopropyl-ethylamine (DIPEA, 8.8 mmol, 1.6 mL). The reaction solution was stirred for 12 h at room temperature. After it was confirmed by thin-layer chromatography (TLC) that the starting material (DFDNB) had been converted, ammonium hydroxide was added as 5.0 N in aqueous solution (12 mmol, 9.6 mL) to the reaction mixture. The reaction solution was stirred at

room temperature for additional 5 h until the reaction was determined to be complete by TLC monitoring. The solvent was then removed under reduced pressure to yield a yellow oily solid.

The yellow solid was then dissolved with ethanol (80 mL). To the solution, HCOONH₄ (80mmol, 4.8 g) and Palladium on carbon (Pd/C, wet, 5%, 1.2 g) were added. The reaction mixture was stirred at 60 °C for 12 h, followed by the filtration of the solution mixture. The filtered solution was concentrated using a rotary evaporator. Precipitation was formed in the concentrated solution, and filtered from the solution. Brown solid (854 mg, 92%) was obtained as the product.

Diamino-2-quinoxalinol. IR (solid): 3352 (br), 3277, 2949, 2868, 2818, 1653, 1512, 1420, 1402, 1271 cm⁻¹. ¹H NMR (250 MHz, DMSO-d₆): δ 12.01 (bs, 1H), 6.81 (s, 1H), 6.36 (s, 1H), 5.39 (bs, 2H), 4.61 (bs, 2H), 2.51 (d, 2H), 2.15 (m, 1H), 0.91 (d, *J* = 6.7 Hz, 6H), ¹³C NMR (62.5 MHz, DMSO-d₆): δ 156.0, 153.7, 140.6, 133.3, 126.5, 126.4, 111.5, 97.2, 41.9, 26.9, 23.1. Formula (M + H): C₁₂H₁₇N₄O. HRMS: found 233.1410 (M + H), calcd. 233.1402 (M + H).

Synthesis of Tetradentate Salqu Ligand. To a 250 mL round-bottomed flask charged with a stirring bar, were sequentially added diamino-2-quinoxalinol (0.6960 g, 3.00 mmol), 3,5-di-*tert*-butyl-2-hydroxybenzaldehyde (1.5454 g, 6.60 mmol), ethanol (120 mL), trifluoroacetic anhydride (0.15 mmol, 20 μL). After the reaction was stirred at refluxing temperature for 6 h, precipitation formed. The reaction mixture was filtered,

and the filtrate was washed with water and ethanol 3 times each to obtain yellow solid as the product (1.2948 g, 65%).

Tetradentate Salqu Ligand. IR (solid): 3426, 2960, 2922, 2879, 1657, 1616, 1584, 1475, 1431, 1389, 1368, 1256, 1206 cm^{-1} . UV-Vis (CHCl_3): 371 nm ($\epsilon = 24\ 100\ \text{M}^{-1}\ \text{cm}^{-1}$). ^1H NMR (400 MHz, CDCl_3): δ 13.23 (s, 1H), 13.14 (s, 1H), 12.04 (bs, 1H), 8.58 (s, 1H), 8.48 (s, 1H), 7.47 (s, 1H), 7.22 (d, 2H), 7.22 (d, 2H), 7.06 (m, 2H), 6.89 (s, 1H), 2.57 (d, $J = 7.1\ \text{Hz}$, 2H), 2.12 (m, 1H), 1.22 (s, 9H), 1.19 (s, 9H), 1.12 (s, 9H), 1.11 (s, 9H), 0.83 (d, $J = 6.6\ \text{Hz}$, 6H). ^{13}C NMR (100 MHz, CDCl_3): δ 166.6, 164.1, 161.4, 158.4, 158.1, 155.6, 144.4, 140.4, 138.7, 136.9, 136.8, 131.3, 128.5, 128.0, 127.0, 126.8, 118.2, 118.0, 117.8, 105.4, 42.0, 34.9, 34.0, 31.3, 29.3, 26.5, 22.6. Formula (M + H): $\text{C}_{42}\text{H}_{57}\text{N}_4\text{O}_3$. HRMS: found 665.4434 (M + H), calcd. 665.4430 (M + H).

Synthesis of Tridentate 2-Quinoxalinol Based Ligand. To a 100 mL round-bottomed flask charged with a stirring bar, were sequentially added diamino-2-quinoxalinol (0.6960 g, 3.00 mmol), 3,5-di-*tert*-butyl-2-hydroxybenzaldehyde (0.7727 g, 3.30 mmol), ethanol (60 mL), trifluoroacetic anhydride (0.075 mmol 10 μL). After the reaction was stirred at refluxing temperature for 6 h, it was confirmed by TLC that the diamino-2-quinoxalinol starting material had been converted. The reaction solution was then concentrated using a rotary evaporator, and the resulting residue was purified by flash column chromatography with hexanes/ethyl acetate (4:1) as the eluent. Yellow solid was obtained as the product (0.7526 g, 56%).

Tridentate 2-Quinoxalinol Based Ligand. ^1H NMR (400 MHz, CDCl_3): δ 13.08 (s, 1H), 11.64 (bs, 1H), 8.74 (s, 1H), 7.52 (s, 1H), 7.49 (d, 1H), 7.25 (d, 1H), 6.56 (s, 1H), 4.52 (bs, 2H), 2.82 (d, $J = 7.2$ Hz, 2H), 2.36 (m, 1H), 1.48 (s, 9H), 1.34 (s, 9H), 1.04 (d, $J = 6.6$ Hz, 6H). ^{13}C NMR (100 MHz, CDCl_3): δ 164.2, 157.8, 156.9, 156.1, 143.3, 141.2, 137.0, 133.8, 131.6, 128.5, 127.1, 118.6, 117.4, 98.2, 92.3, 41.8, 36.7, 35.1, 34.2, 31.6, 31.5, 29.4, 28.4, 27.1, 24.7, 23.4, 22.8. Formula (M + H): $\text{C}_{27}\text{H}_{37}\text{N}_4\text{O}_2$. HRMS: found 449.2932 (M + H), calcd. 449.2917 (M + H).

Synthesis of Salqu Copper(II) Complex 1. In a 100 mL round-bottomed flask charged with a stirring bar, 0.20 mmol of salqu ligand (133 mg) and 0.24 mmol of $\text{Cu}(\text{OAc})_2 \cdot \text{H}_2\text{O}$ (48 mg) were dissolved with 20 mL of dichloromethane and 20 mL of methanol. After 1.2 mmol of triethylamine (0.2 mL) was added, the reaction was stirred for 2 h at refluxing temperature. After solvent was removed, the resulting dark red solid was washed with water and cold ether 3 times each. A product of 127 mg of solid was obtained (87%).

Salqu Copper(II) Complex 1. IR (solid): 3429 (br), 2955, 2909, 2868, 1661, 1556, 1524, 1495, 1462, 1423, 1385, 1202 cm^{-1} . UV-Vis (CHCl_3): 327 ($\epsilon = 20\,000\ \text{M}^{-1}\ \text{cm}^{-1}$), 450 nm ($\epsilon = 13\,000\ \text{M}^{-1}\ \text{cm}^{-1}$). Formula (M + H): $\text{C}_{42}\text{H}_{55}\text{N}_4\text{O}_3\text{Cu}$. HRMS: found 726.3575 (M + H), calcd. 726.3570 (M + H).

Synthesis of Copper(II) Complex 3. In a 100 mL round-bottomed flask charged with a stirring bar, 0.20 mmol of tridentate ligand (89.6 mg) and 0.24 mmol of

Cu(OAc)₂•H₂O (48 mg) were dissolved with 20 mL of dichloromethane and 20 mL of methanol. After 1.2 mmol of triethylamine (0.2 mL) was added, the reaction was stirred for 2 h at refluxing temperature. After solvent was removed, the resulting dark red solid was washed with water and cold ether 3 times each. A product of 93.2 mg of solid was obtained (82%).

Salqu Copper(II) Complex 3. UV-Vis (CHCl₃): 334 nm ($\epsilon = 9\,000\text{ M}^{-1}\text{ cm}^{-1}$). Formula (M + H): C₂₉H₃₉N₄O₄Cu. HRMS: found 571.2351 (M + H), calcd. 571.2346 (M + H).

Representative Procedure for Allylic Oxidation of Δ^5 -Steroids Using Optimized Condition (Table 2.1). To a 50 mL round-bottomed flask charged with a stirring bar, were sequentially added pregnenolone acetate (358 mg, 1 mmol), complex **1** (7.3 mg, 0.01 mmol), CH₃CN (10 mL), CHCl₃ (10 mL), and *t*-BuOOH (2 mL, 10 mmol). After the reaction was stirred at 70 °C for 12 h, solvent was removed under reduced pressure. The residue was purified by flash column chromatography with hexanes/ethyl acetate (5:1) as eluent to yield product as a white solid (239 mg).

3 β -Acetoxypregn-5-ene-7,20-dione (Entry 1, Table 2.1). IR (solid) 1730, 1707, 1672 cm⁻¹. ¹H NMR (400 MHz, CDCl₃): δ 5.72 (d, $J=1.6$ Hz, 1H), 4.75-4.69 (m, 1H), 2.59-1.26 (comp, 18H), 2.12 (s, 3H), 2.05 (s, 3H), 1.22 (s, 3H), 0.64 (s, 3H). ¹³C NMR (100 MHz, CDCl₃): δ 209.7, 201.2, 170.3, 164.3, 126.4, 72.0, 62.2, 49.9, 49.6, 45.2, 44.4, 38.3, 37.7, 37.6, 35.9, 31.6, 27.2, 26.4, 23.5, 21.2, 21.0, 17.2, 13.2.

3 β -Acetoxycholest-5-ene-7-one (Entry 2, Table 2.1). IR (solid) 1728, 1671 cm⁻¹. ¹H NMR (400 MHz, CDCl₃): δ 5.70 (d, J =1.6 Hz, 1H), 4.76-4.67 (m, 1H), 2.58-1.00 (comp. 26H), 2.05 (s, 3H), 1.21 (s, 3H), 0.92 (d, J =6.5 Hz, 3H), 0.87 (d, J =6.6 Hz, 3H), 0.86 (d, J =6.6 Hz, 3H), 0.68 (s, 3H). ¹³C NMR (100 MHz, CDCl₃): δ 201.9, 170.2, 164.0, 126.6, 72.2, 54.7, 49.9, 49.8, 45.4, 43.1, 39.4, 38.6, 38.3, 37.6, 36.2, 36.0, 35.7, 28.5, 28.0, 27.3, 26.3, 23.8, 22.8, 22.6, 21.2, 21.1, 18.8, 17.2, 11.9.

3 β -Benzoyloxy pregn-5-ene-7,20-dione (Entry 3, Table 2.1). IR (solid) 1707, 1672 cm⁻¹. ¹H NMR (400 MHz, CDCl₃): δ 8.04 (d, J =7.2 Hz, 2H), 7.57 (t, 1H), 7.45 (t, 2H), 5.77 (d, J =1.6 Hz, 1H), 5.02-4.94 (m, 1H), 2.78-0.68 (comp. 24H), 2.14 (s, 3H), 1.27 (s, 3H), 0.68 (s, 3H). ¹³C NMR (100 MHz, CDCl₃): δ 209.9, 201.4, 166.0, 164.4, 133.2, 130.4, 130.3, 129.7, 128.5, 126.8, 72.8, 62.4, 50.1, 49.8, 45.4, 44.6, 38.6, 38.0, 37.8, 36.2, 31.8, 27.6, 26.6, 23.8, 21.3, 17.5, 13.4.

3 β -[(Tetrahydropyran-2R,S-yl)oxy]-7-oxo-cholest-5-ene (Entry 4, Table 2.1). IR (solid) 1676, 1630 cm⁻¹. ¹H NMR (400 MHz, CDCl₃): δ 5.68 (d, J =1.0 Hz, 1H), 4.72 (s, 1H), 3.55-3.64 (m, 1H), 3.45-3.49 (m, 2H), 0.93 (s, 3H), 0.90 (d, J =6.6 Hz, 3H), 0.85 (d, J =6.6 Hz, 6H), 0.68 (s, 3H). ¹³C NMR (100 MHz, CDCl₃): δ 202.2, 165.6, 126.0, 97.4, 75.0, 62.9, 54.8, 50.0, 45.4, 43.1, 40.1, 39.5, 38.8, 38.5, 36.5, 36.2, 31.2, 29.4, 28.5, 28.0, 27.7, 26.3, 25.4, 23.8, 22.6, 21.2, 19.9, 19.0, 17.4, 12.0.

3 β -Hydroxycholest-5-ene-7-one (Entry 5, Table 2.1). IR (solid) 1670 cm⁻¹. ¹H NMR (400 MHz, CDCl₃): δ 5.69 (d, J =1.6 Hz, 1H), 3.71-3.64 (m, 1H), 2.54-1.00 (comp. 26H), 1.21 (s, 3H), 0.93 (d, J =6.6 Hz, 3H), 0.88 (d, J =6.6 Hz, 3H), 0.87 (d, J =6.6 Hz, 3H), 0.68 (s, 3H). ¹³C NMR (100 MHz, CDCl₃): δ 202.6, 165.6, 126.0, 70.5, 54.8, 50.0, 49.9, 45.4, 43.1, 41.8, 39.5, 38.7, 38.3, 36.4, 36.2, 35.7, 31.1, 28.6, 28.0, 26.3, 23.8, 22.8, 22.6, 21.2, 18.9, 17.3, 12.0.

3 β -Hydroxypregn-5-ene-7,20-dione (Entry 6, Table 2.1). IR (solid) 1681, 1666 cm⁻¹. ¹H NMR (400 MHz, CDCl₃): δ 5.68 (d, J =1.6 Hz, 1H), 3.67-3.63 (m, 1H), 2.52-1.18 (comp. 19H), 2.10 (s, 3H), 1.18 (s, 3H), 0.63 (s, 3H). ¹³C NMR (100 MHz, CDCl₃): δ 210.0, 201.8, 166.0, 125.8, 70.3, 62.3, 50.0, 49.8, 45.1, 44.4, 41.8, 38.4, 37.7, 36.4, 31.6, 31.0, 26.5, 23.6, 21.1, 17.3, 13.3.

3 β -Chlorocholest-5-ene-7-one (Entry 7, Table 2.1). IR (solid) 1669 cm⁻¹. ¹H NMR (400 MHz, CDCl₃): δ 5.68 (s, 1H), 3.86-3.82 (m, 1H), 2.71 (d, J =8.3 Hz, 2H), 2.43-2.36 (m, 1H), 2.26-2.15 (comp, 2H), 2.04-1.88 (comp, 4H), 1.57-1.05 (comp, 20H), 1.22 (s, 3H), 0.92 (d, J =6.5 Hz, 3H), 0.87 (d, J =6.6 Hz, 3H), 0.86 (d, J =6.6 Hz, 3H), 0.68 (s, 3H). ¹³C NMR (100 MHz, CDCl₃): δ 201.9, 163.9, 126.2, 57.8, 54.8, 49.9, 49.8, 45.4, 43.1, 42.6, 39.5, 38.6, 38.1, 36.2, 35.7, 32.8, 28.5, 28.0, 26.3, 23.8, 22.8, 22.6, 21.1, 18.9, 17.2, 12.0.

Representative Procedure for Allylic Oxidation of Δ^5 -Steroids Using Further Optimized Condition (Table 2.2). To a 50 mL round-bottomed flask charged with a stirring bar, were sequentially added cholesteryl chloride (203 mg, 0.5 mmol), complex **1**

(1.8 mg, 0.0025 mmol), CH₃CN (10 mL), and *t*-BuOOH (0.5 mL, 2.5 mmol). Additional complex **1** (1.8 mg, 0.0025 mmol) and *t*-BuOOH (0.5 mL, 2.5 mmol) were added three times every 2 h. Solvent was then removed under reduced pressure. The residue was purified by flash column chromatography with hexanes/ethyl acetate (15:1) as eluent to yield product as a white solid (201 mg).

3 β -Acetoxycholest-5-ene-7-one (Entry 1, Table 2.2). IR (solid) 1728, 1671 cm⁻¹. ¹H NMR (400 MHz, CDCl₃): δ 5.70 (d, *J*=1.6 Hz, 1H), 4.76-4.67 (m, 1H), 2.58-1.00 (comp. 26H), 2.05 (s, 3H), 1.21 (s, 3H), 0.92 (d, *J*=6.5 Hz, 3H), 0.87 (d, *J*=6.6 Hz, 3H), 0.86 (d, *J*=6.6 Hz, 3H), 0.68 (s, 3H). ¹³C NMR (100 MHz, CDCl₃): δ 201.9, 170.2, 164.0, 126.6, 72.2, 54.7, 49.9, 49.8, 45.4, 43.1, 39.4, 38.6, 38.3, 37.6, 36.2, 36.0, 35.7, 28.5, 28.0, 27.3, 26.3, 23.8, 22.8, 22.6, 21.2, 21.1, 18.8, 17.2, 11.9.

3 β -Benzoyloxypregn-5-ene-7,20-dione (Entry 2, Table 2.2). IR (solid) 1707, 1672 cm⁻¹. ¹H NMR (400 MHz, CDCl₃): δ 8.04 (d, *J*=7.2 Hz, 2H), 7.57 (t, 1H), 7.45 (t, 2H), 5.77 (d, *J*=1.6 Hz, 1H), 5.02-4.94 (m, 1H), 2.78-0.68 (comp. 24H), 2.14 (s, 3H), 1.27 (s, 3H), 0.68 (s, 3H). ¹³C NMR (100 MHz, CDCl₃): δ 209.9, 201.4, 166.0, 164.4, 133.2, 130.4, 130.3, 129.7, 128.5, 126.8, 72.8, 62.4, 50.1, 49.8, 45.4, 44.6, 38.6, 38.0, 37.8, 36.2, 31.8, 27.6, 26.6, 23.8, 21.3, 17.5, 13.4.

3 β -Hydroxycholest-5-ene-7-one (Entry 3, Table 2.2). IR (solid) 1670 cm⁻¹. ¹H NMR (400 MHz, CDCl₃): δ 5.69 (d, *J*=1.6 Hz, 1H), 3.71-3.64 (m, 1H), 2.54-1.00 (comp. 26H), 1.21 (s, 3H), 0.93 (d, *J*=6.6 Hz, 3H), 0.88 (d, *J*=6.6 Hz, 3H), 0.87 (d, *J*=6.6 Hz,

3H), 0.68 (s, 3H). ¹³C NMR (100 MHz, CDCl₃): δ 202.6, 165.6, 126.0, 70.5, 54.8, 50.0, 49.9, 45.4, 43.1, 41.8, 39.5, 38.7, 38.3, 36.4, 36.2, 35.7, 31.1, 28.6, 28.0, 26.3, 23.8, 22.8, 22.6, 21.2, 18.9, 17.3, 12.0.

3β-Hydroxypregn-5-ene-7,20-dione (Entry 4, Table 2.2). IR (solid) 1681, 1666 cm⁻¹. ¹H NMR (400 MHz, CDCl₃): δ 5.68 (d, *J*=1.6 Hz, 1H), 3.67-3.63 (m, 1H), 2.52-1.18 (comp. 19H), 2.10 (s, 3H), 1.18 (s, 3H), 0.63 (s, 3H). ¹³C NMR (100 MHz, CDCl₃): δ 210.0, 201.8, 166.0, 125.8, 70.3, 62.3, 50.0, 49.8, 45.1, 44.4, 41.8, 38.4, 37.7, 36.4, 31.6, 31.0, 26.5, 23.6, 21.1, 17.3, 13.3.

3β-Chlorocholest-5-ene-7one (Entry 5, Table 2.2). IR (solid) 1669 cm⁻¹. ¹H NMR (400 MHz, CDCl₃): δ 5.68 (s, 1H), 3.86-3.82 (m, 1H), 2.71 (d, *J*=8.3 Hz, 2H), 2.43-2.36 (m, 1H), 2.26-2.15 (comp, 2H), 2.04-1.88 (comp, 4H), 1.57-1.05 (comp, 20H), 1.22 (s, 3H), 0.92 (d, *J*=6.5 Hz, 3H), 0.87 (d, *J*=6.6 Hz, 3H), 0.86 (d, *J*=6.6 Hz, 3H), 0.68 (s, 3H). ¹³C NMR (100 MHz, CDCl₃): δ 201.9, 163.9, 126.2, 57.8, 54.8, 49.9, 49.8, 45.4, 43.1, 42.6, 39.5, 38.6, 38.1, 36.2, 35.7, 32.8, 28.5, 28.0, 26.3, 23.8, 22.8, 22.6, 21.1, 18.9, 17.2, 12.0.

Representative Procedure for Allylic Oxidation of Simple Olefins using Complex

1. To a 50 mL round-bottomed flask charged with a stirring bar, were sequentially added complex **1** (2.5 μmol), CH₃CN (10 mL), 1-acetyl-1-cyclohexene (0.5 mmol), and *t*-BuOOH (1.5 mmol). After the reaction was stirred at 70 °C for 1 h, solvent was removed under reduced pressure. The residue was purified by flash column chromatography with hexane/ethyl acetate as eluent to yield product as yellowish oil.

Procedure for Yield Determination by GC. To the reaction flask, 1,2-dichlorobenzene (0.5 mmol) was added after 1 h. 150 μ L of reaction solution was then taken to collect GC data. The yield was determined by the equation Yield = (area of the peak for product)/(area of the peak for internal standard).

2-Cyclohexenone (Entry 1, **Table 3.1**). ^1H NMR: δ 7.03 (m, 1 H), 6.01 (m, 1 H), 2.43, (m, 2 H), 2.37 (m, 2 H), 2.03 (m, 2 H). ^{13}C NMR: δ 199.6, 150.9, 129.8, 38.1, 25.7, 22.8. Formula: $\text{C}_6\text{H}_8\text{O}$. HRMS: found 96.0582, calcd. 96.0575.

3-Acetyl-2-cyclohexenone (Entry 2, **Table 3.1**). ^1H NMR: δ 6.58 (bs, 1 H), 2.50 (m, 2 H), 2.48 (m, 2 H), 2.41 (s, 3 H), 2.00 (m, 2 H). ^{13}C NMR: δ 201.5, 200.1, 154.6, 132.5, 37.9, 26.2, 23.4, 21.9. Formula: $\text{C}_8\text{H}_{10}\text{O}_2$. HRMS: found 138.0687, calcd. 138.0681.

3-Phenyl-2-cyclohexenone (Entry 3, **Table 3.1**). ^1H NMR: δ 7.55-7.53 (m, 2 H), 7.42-7.41 (m, 3H), 6.43 (t, $J = 1.2$ Hz, 1 H), 2.78 (m, 2 H), 2.49 (t, $J = 6.0$ Hz, 2 H), 2.18-2.13 (m, 2 H). ^{13}C NMR: δ 200.0, 159.9, 139.0, 130.0, 128.8, 126.1, 125.5, 37.3, 28.1, 22.8. Formula: $\text{C}_{12}\text{H}_{12}\text{O}$. HRMS: found 172.0881, calcd. 172.0888.

3-Methyl-2-cyclohexenone (Entry 4 and 5, **Table 3.1**). ^1H NMR: δ 5.88 (d, $J = 1.5$ Hz, 1 H), 2.32 (t, $J = 6.3$ Hz, 2 H), 2.31-2.26 (m, 2 H), 2.02-1.98 (m, 2 H), 1.96 (s, 3 H). ^{13}C NMR: δ 199.9, 162.9, 127.0, 37.4, 31.4, 24.9, 23.1. Formula: $\text{C}_7\text{H}_{10}\text{O}$. HRMS: found 110.0728, calcd. 110.0732.

3-Acetoxy-2-cyclohexenone (Entry 6, **Table 3.1**). ^1H NMR: δ 5.92 (s, 1 H), 2.54 (t, J = 6.8 Hz, 2 H), 2.42 (t, J = 6.4 Hz, 2 H), 2.23 (s, 3 H), 2.09 (m, 2 H). ^{13}C NMR: δ 200.0, 170.0, 167.4, 117.5, 36.6, 28.3, 21.2, 21.2. Formula: $\text{C}_8\text{H}_{10}\text{O}_3$. HRMS: found 154.0626, calcd. 154.0630.

3-Acetyl-2-cyclopentenone (Entry 7, **Table 3.1**). ^1H NMR: δ 6.67 (t, J = 2.0 Hz, 1 H), 2.83-2.80 (m, 2 H), 2.56-2.51 (m, 2 H), 2.50 (s, 3 H). ^{13}C NMR: δ 210.6, 197.3, 169.3, 137.0, 35.4, 27.8, 26.3. Formula: $\text{C}_7\text{H}_8\text{O}_2$. HRMS: found 124.0520, calcd. 124.0524.

4-Cyclopentene-1,3-dione Monoethylene Ketal (Entry 8, **Table 3.1**). ^1H NMR: δ 7.20 (d, J = 6.0 Hz, 1 H), 6.19 (d, J = 6.0 Hz, 1 H), 4.03 (m, 4 H), 2.60 (s, 2 H). ^{13}C NMR: δ 204.0, 156.3, 135.4, 111.6, 65.2, 45.2. Formula: $\text{C}_7\text{H}_8\text{O}_3$. HRMS: found 140.0465, calcd. 140.0473.

3-Cyano-2-cyclohexenone (Entry 9, **Table 3.1**). ^1H NMR: δ 6.52 (s, 1 H), 2.57 (dt, J = 6.0 Hz, 2.0 Hz, 2 H), 2.54 (t, J = 6.2 Hz, 2 H), 2.13 (m, 2 H). ^{13}C NMR: δ 196.6, 138.6, 131.1, 117.0, 37.2, 27.6, 22.0. Formula: $\text{C}_7\text{H}_7\text{NO}$. HRMS: found 121.0525, calcd. 121.0528.

3-Nitro-2-cyclohexenone (Entry 10, **Table 3.1**). ^1H NMR: δ 6.91 (m, 1 H), 2.10 (m, 2 H), 2.51 (t, J = 6.4 Hz, 2 H), 2.19-2.15 (m, 2 H). ^{13}C NMR: δ 198.0, 164.0, 125.8, 37.1, 24.4, 21.0. Formula: $\text{C}_6\text{H}_7\text{NO}_3$. HRMS: found 141.0431, calcd. 141.0426.

Procedure for Cyclic Voltammetry Experiment (Chapter 3). Electrochemical measurement was carried out at room temperature using a three electrode set-up in a home built glass cell (20 mL total volume). The supporting electrolyte was 0.1 M tetrabutyl ammonium tetrafluoroborate in 5 mL CH₂Cl₂ with 1 mM ferrocene as internal standard, the reference electrode was home made Ag/AgCl wire, and the counter electrode was Pt gauze (A = 0.77 cm²). The working electrode was a glassy carbon disk (d = 0.3 cm, A = 0.071 cm²). Before electrochemical measurement, the solution was purged with N₂ for 15 min. Cyclic voltammogram of 1 mM Cu(II) salqu was recorded in 5 mL CH₂Cl₂ described above between 0.0 V and 1.7 V using a scan rate of 100 mV/s.

Procedure for Raman Spectroscopy. In a 20 mL vial equipped with a stirring bar, Cu(II) salqucomplex (5 μmol) was dissolved in CH₂Cl₂ (10 mL) followed by the addition of TBHP (20 μmol). After 15 min strring, several drops of the Cu(II) salqu solution was taken and let evaporate on a gold foil. The residue was excited by 785 nm line (6 mW) and Raman spectrum was collected.

Representative Procedure for Allylic Oxidation of Simple Olefins using Complex 3. To a 50 mL round-bottomed flask charged with a stirring bar, were sequentially added complex **3** (2.5 μmol), CH₃CN (10 mL), 1-acetyl-1-cyclohexene (0.5 mmol), and *t*-BuOOH (1.5 mmol). After the reaction was stirred at 70 °C for 1 h, solvent was removed under reduced pressure. The residue was purified by flash column chromatography with hexane/ethyl acetate as eluent to yield product as yellowish oil.

3-Acetyl-2-cyclohexenone (Entry 1, **Table 4.1**). ^1H NMR: δ 6.58 (bs, 1 H), 2.50 (m, 2 H), 2.48 (m, 2 H), 2.41 (s, 3 H), 2.00 (m, 2 H). ^{13}C NMR: δ 201.5, 200.1, 154.6, 132.5, 37.9, 26.2, 23.4, 21.9. Formula: $\text{C}_8\text{H}_{10}\text{O}_2$. HRMS: found 138.0687, calcd. 138.0681.

3-Phenyl-2-cyclohexenone (Entry 2, **Table 4.1**). ^1H NMR: δ 7.55-7.53 (m, 2 H), 7.42-7.41 (m, 3H), 6.43 (t, $J = 1.2$ Hz, 1 H), 2.78 (m, 2 H), 2.49 (t, $J = 6.0$ Hz, 2 H), 2.18-2.13 (m, 2 H). ^{13}C NMR: δ 200.0, 159.9, 139.0, 130.0, 128.8, 126.1, 125.5, 37.3, 28.1, 22.8. Formula: $\text{C}_{12}\text{H}_{12}\text{O}$. HRMS: found 172.0881, calcd. 172.0888.

3-Acetoxy-2-cyclohexenone (Entry 3, **Table 4.1**). ^1H NMR: δ 5.92 (s, 1 H), 2.54 (t, $J = 6.8$ Hz, 2 H), 2.42 (t, $J = 6.4$ Hz, 2 H), 2.23 (s, 3 H), 2.09 (m, 2 H). ^{13}C NMR: δ 200.0, 170.0, 167.4, 117.5, 36.6, 28.3, 21.2, 21.2. Formula: $\text{C}_8\text{H}_{10}\text{O}_3$. HRMS: found 154.0626, calcd. 154.0630.

3-Acetyl-2-cyclopentenone (Entry 4, **Table 4.1**). ^1H NMR: δ 6.67 (t, $J = 2.0$ Hz, 1 H), 2.83-2.80 (m, 2 H), 2.56-2.51 (m, 2 H), 2.50 (s, 3 H). ^{13}C NMR: δ 210.6, 197.3, 169.3, 137.0, 35.4, 27.8, 26.3. Formula: $\text{C}_7\text{H}_8\text{O}_2$. HRMS: found 124.0520, calcd. 124.0524.

4-Cyclopentene-1,3-dione Monoethylene Ketal (Entry 5, **Table 4.1**). ^1H NMR: δ 7.20 (d, $J = 6.0$ Hz, 1 H), 6.19 (d, $J = 6.0$ Hz, 1 H), 4.03 (m, 4 H), 2.60 (s, 2 H). ^{13}C NMR: δ 204.0, 156.3, 135.4, 111.6, 65.2, 45.2. Formula: $\text{C}_7\text{H}_8\text{O}_3$. HRMS: found 140.0465, calcd. 140.0473.

3-Cyano-2-cyclohexenone (Entry 6, **Table 4.1**). ^1H NMR: δ 6.52 (s, 1 H), 2.57 (dt, J = 6.0 Hz, 2.0 Hz, 2 H), 2.54 (t, J = 6.2 Hz, 2 H), 2.13 (m, 2 H). ^{13}C NMR: δ 196.6, 138.6, 131.1, 117.0, 37.2, 27.6, 22.0. Formula: $\text{C}_7\text{H}_7\text{NO}$. HRMS: found 121.0525, calcd. 121.0528.

Procedure for Cyclic Voltammetry Experiment (Chapter 3). Electrochemical measurement was carried out at room temperature using a three electrode set-up in a home built glass cell (20 mL total volume). The supporting electrolyte was 0.04 M tetrabutyl ammonium tetrafluoroborate in 5 mL CH_2Cl_2 , the reference electrode was home made Ag/AgCl wire, and the counter electrode was Pt gauze ($A = 0.77 \text{ cm}^2$). The working electrode was a glassy carbon disk ($d = 0.3 \text{ cm}$, $A = 0.071 \text{ cm}^2$). Before electrochemical measurement, the solution was purged with N_2 for 15 min. Cyclic voltammogram of 1 mM Cu(II) salqu was recorded in 5 mL CH_2Cl_2 described above between 0.0 V and 1.7 V using a scan rate of 100 mV/s.

Theoretical Calculation (Chapter 3)

Procedure of optimization by varying reaction time

Total Energies (hartrees), Zero-point Energies (kcal/mol), Thermal Corrections (kcal/mol), and Entropies (cal/mol·K)

	PG	B3LYP/	ZPE ^c	TC ^d	S ^e
R=AcO, position 4	C ₁	-398.86712	185.95(0)	9.81	121.37
R=AcO, position 7	C ₁	-399.43226	185.79(0)	9.80	121.19
R=OH, position 4	C ₁	-399.43226	219.61(0)	11.57	136.79
R=OH, position 7	C ₁	-398.86713	219.41(0)	11.57	136.80
R=OBz, position 4	C ₁	-398.86712	153.68(0)	7.68	104.21
R=OBz, position 7	C ₁	-399.43226	153.57(0)	7.78	106.12

R=Cl, position 4	C ₁	-399.43226	162.06(0)	7.71	102.90
R=Cl, position 7	C ₁	-398.66959	161.87(0)	7.78	103.88
R=OTHP, position 4	C ₁	-398.86712	241.58(0)	11.12	132.32
R=OTHP, position 7	C ₁	-399.23309	241.37(0)	11.15	132.74

^aPoint group. ^bBased on structures optimized at the B3LYP/6-31G(2d,p) level. ^cZero-point energies and number of imaginary frequencies. ^dThermal corrections to 298K.

^eEntropies.

Cartesian Coordinates of Geometries Optimized at the B3LYP/6-31G(2d,p) Level

R=AcO, position 4

Standard orientation:

Center Number	Atomic Number	Atomic Type	Coordinates (Angstroms)		
			X	Y	Z
1	6	0	-1.211150	0.094849	-0.864531
2	6	0	-0.414243	1.014946	0.070389
3	6	0	1.063892	0.739444	-0.013923
4	6	0	1.529515	-0.708347	0.060621
5	6	0	0.626168	-1.593903	-0.840064
6	6	0	-0.878068	-1.376990	-0.630023
7	6	0	1.987046	1.780364	-0.045307
8	6	0	2.983375	-0.822285	-0.459417
9	6	0	3.941292	0.221586	0.132405
10	6	0	3.356876	1.597862	0.027515
11	1	0	1.601359	2.797179	-0.100272
12	1	0	-0.957292	0.348193	-1.899396
13	1	0	-0.620560	2.061911	-0.176892
14	1	0	0.875294	-2.649033	-0.674726
15	1	0	-1.446775	-1.995353	-1.333657
16	1	0	2.968991	-0.687261	-1.547864
17	1	0	3.358196	-1.835614	-0.271438
18	1	0	4.165250	-0.014583	1.185275
19	1	0	4.907542	0.172230	-0.384697
20	1	0	4.018388	2.458184	0.038888
21	1	0	0.868820	-1.379434	-1.889453
22	1	0	-1.183164	-1.666802	0.377266
23	1	0	-0.776854	0.848488	1.092538
24	6	0	1.453463	-1.201985	1.527814
25	1	0	1.772769	-2.248801	1.594807
26	1	0	2.101063	-0.606519	2.177561
27	1	0	0.439036	-1.134955	1.929829
28	6	0	-3.351373	0.167778	0.290262
29	8	0	-2.638207	0.373032	-0.833797
30	8	0	-2.904703	-0.243377	1.335307
31	6	0	-4.801111	0.527030	0.059438
32	1	0	-4.884081	1.574412	-0.244302
33	1	0	-5.212995	-0.079608	-0.752072
34	1	0	-5.365799	0.358028	0.975458

R=AcO, position 7

Standard orientation:

Center Number	Atomic Number	Atomic Type	Coordinates (Angstroms)		
			X	Y	Z
1	6	0	1.334616	0.316497	-1.139208
2	6	0	0.384823	-0.803862	-0.867207
3	6	0	-0.915172	-0.642420	-0.392623
4	6	0	-1.351847	0.717867	0.164660
5	6	0	-0.585591	1.838392	-0.574577
6	6	0	0.935824	1.656685	-0.515078
7	6	0	-1.817922	-1.695425	-0.443410
8	6	0	-2.869400	0.906392	-0.057388
9	6	0	-3.700496	-0.260438	0.486437
10	6	0	-3.284827	-1.594003	-0.154755
11	1	0	-1.461046	-2.651002	-0.823760
12	1	0	1.394978	0.444755	-2.229573
13	1	0	-0.856776	2.810408	-0.144827
14	1	0	1.441325	2.468184	-1.048745
15	1	0	-3.059077	1.013046	-1.134382
16	1	0	-3.188314	1.846210	0.410526
17	1	0	-3.583005	-0.321503	1.573226
18	1	0	-4.765629	-0.078567	0.307090
19	1	0	-3.827513	-1.730439	-1.105729
20	1	0	-3.608822	-2.437268	0.471132
21	1	0	-0.912600	1.860140	-1.623216
22	1	0	1.276819	1.688732	0.520217
23	1	0	0.693657	-1.783210	-1.226623
24	6	0	-1.021537	0.767414	1.676292
25	1	0	-1.256171	1.757278	2.086407
26	1	0	-1.599257	0.026421	2.234130
27	1	0	0.031430	0.547789	1.860718
28	6	0	3.067617	-0.379708	0.408860
29	8	0	2.726313	-0.038448	-0.847973
30	8	0	2.316179	-0.396173	1.354434
31	6	0	4.533803	-0.742641	0.472649
32	1	0	4.737456	-1.591724	-0.186135
33	1	0	5.143783	0.094361	0.121487
34	1	0	4.799474	-0.995145	1.498449

R=OH, position 4

Standard orientation:

Center Number	Atomic Number	Atomic Type	Coordinates (Angstroms)		
			X	Y	Z

1	6	0	-2.221548	0.391379	-0.395634
2	6	0	-1.186226	1.177341	0.413008
3	6	0	0.228026	0.760602	0.116915
4	6	0	0.550966	-0.727347	0.086948
5	6	0	-0.570358	-1.494152	-0.664902
6	6	0	-1.989634	-1.111363	-0.230405
7	6	0	1.242054	1.703810	-0.022632
8	6	0	1.882980	-0.961856	-0.666516
9	6	0	3.027343	-0.046864	-0.207467
10	6	0	2.580414	1.383445	-0.168276
11	1	0	0.961351	2.755272	0.011954
12	1	0	-2.106475	0.652348	-1.461654
13	1	0	-1.316876	2.250136	0.238576
14	1	0	-0.414496	-2.573109	-0.543569
15	1	0	-2.721888	-1.670351	-0.828457
16	1	0	1.708806	-0.775242	-1.733238
17	1	0	2.174015	-2.015173	-0.573040
18	1	0	3.394156	-0.356653	0.784515
19	1	0	3.886492	-0.163870	-0.879718
20	1	0	3.322880	2.172649	-0.230645
21	1	0	-0.469479	-1.287118	-1.738506
22	1	0	-2.173162	-1.377314	0.817709
23	1	0	-1.427888	1.007066	1.475208
24	6	0	0.668493	-1.260013	1.537662
25	1	0	0.896243	-2.332600	1.534138
26	1	0	1.462940	-0.744513	2.084411
27	1	0	-0.257869	-1.117144	2.100701
28	8	0	-3.503384	0.797914	0.071370
29	1	0	-4.166736	0.302419	-0.421546

R=OH, position 7

Standard orientation:

Center Number	Atomic Number	Atomic Type	Coordinates (Angstroms)		
			X	Y	Z
1	6	0	-2.322406	0.429185	-0.388107
2	6	0	-1.119694	1.255059	-0.060017
3	6	0	0.185689	0.777834	0.016997
4	6	0	0.448727	-0.733804	0.038620
5	6	0	-0.680095	-1.467732	-0.719424
6	6	0	-2.075502	-1.074810	-0.223345
7	6	0	1.258723	1.660843	0.056485
8	6	0	1.804160	-1.027181	-0.643304
9	6	0	2.961515	-0.233204	-0.027894

10	6	0	2.702009	1.281885	-0.084966
11	1	0	1.035820	2.726227	0.071214
12	1	0	-2.569995	0.624638	-1.450662
13	1	0	-0.537330	-2.551434	-0.625726
14	1	0	-2.844952	-1.638364	-0.765522
15	1	0	1.721292	-0.780186	-1.710424
16	1	0	2.013621	-2.102862	-0.586454
17	1	0	3.108845	-0.544841	1.011372
18	1	0	3.896235	-0.468740	-0.548010
19	1	0	3.060573	1.679611	-1.049566
20	1	0	3.309848	1.801907	0.668990
21	1	0	-0.597356	-1.235603	-1.789984
22	1	0	-2.195786	-1.320618	0.836264
23	1	0	-1.289759	2.328417	-0.017554
24	6	0	0.486174	-1.216614	1.508923
25	1	0	0.687720	-2.293615	1.554393
26	1	0	1.260557	-0.701442	2.081734
27	1	0	-0.460410	-1.024493	2.018919
28	8	0	-3.410347	0.890603	0.420691
29	1	0	-4.211953	0.467826	0.091672

R=OBz, position 4

Standard orientation:

Center Number	Atomic Number	Atomic Type	Coordinates (Angstroms)		
			X	Y	Z
1	6	0	-0.245195	0.268001	0.817124
2	6	0	-0.959873	0.794083	-0.435158
3	6	0	-2.456197	0.696566	-0.295916
4	6	0	-3.046663	-0.615227	0.203089
5	6	0	-2.222812	-1.130796	1.414297
6	6	0	-0.705758	-1.140705	1.185416
7	6	0	-3.284718	1.732370	-0.717099
8	6	0	-4.503989	-0.391713	0.675595
9	6	0	-5.368009	0.397611	-0.318333
10	6	0	-4.665408	1.647075	-0.756436
11	1	0	-2.811523	2.649968	-1.063132
12	1	0	-0.472145	0.937958	1.653205
13	1	0	-0.661699	1.831150	-0.622826
14	1	0	-2.563714	-2.138667	1.680057
15	1	0	-0.191711	-1.464704	2.097244
16	1	0	-4.475983	0.169875	1.617392
17	1	0	-4.966274	-1.360753	0.898967
18	1	0	-5.613335	-0.224765	-1.194057

19	1	0	-6.334072	0.639261	0.141857
20	1	0	-5.249222	2.479813	-1.135347
21	1	0	-2.443636	-0.491385	2.279463
22	1	0	-0.429106	-1.837083	0.391759
23	1	0	-0.615284	0.200672	-1.291177
24	6	0	-3.016067	-1.664111	-0.937465
25	1	0	-3.425455	-2.619373	-0.587983
26	1	0	-3.610202	-1.332152	-1.793555
27	1	0	-2.000170	-1.846722	-1.297689
28	6	0	1.891002	-0.303917	-0.196777
29	8	0	1.200342	0.392920	0.724048
30	8	0	1.398901	-1.065068	-1.002751
31	6	0	3.355751	-0.030395	-0.114491
32	6	0	3.906528	0.849346	0.823800
33	6	0	4.192370	-0.690675	-1.020717
34	6	0	5.281295	1.063849	0.852074
35	1	0	3.254923	1.357880	1.523059
36	6	0	5.565246	-0.474382	-0.990100
37	1	0	3.742724	-1.367153	-1.738079
38	6	0	6.111339	0.403454	-0.053311
39	1	0	5.705614	1.746764	1.580809
40	1	0	6.210062	-0.988832	-1.695014
41	1	0	7.183197	0.572837	-0.028888

R=OBz, position 7

Standard orientation:

Center Number	Atomic Number	Atomic Type	Coordinates (Angstroms)		
			X	Y	Z
1	6	0	-0.210410	1.207385	-0.728236
2	6	0	-0.990283	0.010133	-1.162895
3	6	0	-2.264064	-0.314131	-0.700960
4	6	0	-2.828541	0.407291	0.528905
5	6	0	-2.260190	1.843709	0.580575
6	6	0	-0.727512	1.878256	0.547263
7	6	0	-3.029058	-1.266081	-1.360533
8	6	0	-4.369237	0.472463	0.429326
9	6	0	-5.009409	-0.899499	0.192905
10	6	0	-4.473788	-1.556748	-1.089182
11	1	0	-2.582103	-1.772578	-2.214225
12	1	0	-0.241908	1.941631	-1.545996
13	1	0	-2.619023	2.345551	1.487429
14	1	0	-0.364642	2.910524	0.584932
15	1	0	-4.642470	1.144851	-0.395594

16	1	0	-4.771179	0.922745	1.345615
17	1	0	-4.812970	-1.550653	1.050890
18	1	0	-6.098504	-0.800146	0.131710
19	1	0	-5.058648	-1.204270	-1.955878
20	1	0	-4.645385	-2.641968	-1.063737
21	1	0	-2.659490	2.414523	-0.269017
22	1	0	-0.321195	1.360869	1.416885
23	1	0	-0.586225	-0.534195	-2.013686
24	6	0	-2.406744	-0.368547	1.800328
25	1	0	-2.740947	0.162230	2.700124
26	1	0	-2.843823	-1.369823	1.818096
27	1	0	-1.324145	-0.498087	1.846770
28	6	0	1.698990	0.003993	0.158518
29	8	0	1.231399	0.953133	-0.672009
30	8	0	1.012572	-0.657911	0.906907
31	6	0	3.180655	-0.144975	0.056228
32	6	0	3.796937	-1.099203	0.872723
33	6	0	3.956356	0.627720	-0.814869
34	6	0	5.174263	-1.280078	0.819331
35	1	0	3.175118	-1.685697	1.538940
36	6	0	5.335072	0.444827	-0.865667
37	1	0	3.474389	1.364803	-1.444701
38	6	0	5.945091	-0.507790	-0.050075
39	1	0	5.647765	-2.021795	1.454213
40	1	0	5.934251	1.045644	-1.542095
41	1	0	7.020600	-0.648294	-0.091979

R=Cl, position 4

Standard orientation:

Center Number	Atomic Number	Atomic Type	Coordinates (Angstroms)		
			X	Y	Z
1	6	0	1.864613	-0.156466	-0.432057
2	6	0	0.929711	-1.026209	0.410448
3	6	0	-0.516419	-0.722706	0.113531
4	6	0	-0.957440	0.734278	0.089981
5	6	0	0.090795	1.585783	-0.675835
6	6	0	1.547450	1.323114	-0.263869
7	6	0	-1.446131	-1.748309	-0.031623
8	6	0	-2.312309	0.861122	-0.648864
9	6	0	-3.371051	-0.150034	-0.186308
10	6	0	-2.807123	-1.538515	-0.166321
11	1	0	-1.078374	-2.772706	-0.006685
12	1	0	1.805200	-0.443263	-1.484618

13	1	0	1.141292	-2.086090	0.242851
14	1	0	-0.141083	2.649986	-0.547532
15	1	0	2.225165	1.925233	-0.876143
16	1	0	-2.134654	0.697279	-1.718657
17	1	0	-2.689584	1.885374	-0.544119
18	1	0	-3.750136	0.117529	0.813133
19	1	0	-4.244881	-0.098972	-0.847371
20	1	0	-3.481620	-2.386207	-0.231577
21	1	0	-0.008155	1.375266	-1.748638
22	1	0	1.721579	1.610853	0.778915
23	1	0	1.157610	-0.825865	1.468945
24	6	0	-1.099868	1.257223	1.541991
25	1	0	-1.415488	2.307067	1.540274
26	1	0	-1.842269	0.678970	2.098933
27	1	0	-0.158302	1.193474	2.094448
28	17	0	3.609431	-0.490801	0.027141

R=Cl, position 7

Standard orientation:

Center Number	Atomic Number	Atomic Type	Coordinates (Angstroms)		
			X	Y	Z
1	6	0	1.968718	-0.154914	-0.655901
2	6	0	0.857391	-1.098287	-0.412515
3	6	0	-0.460810	-0.729739	-0.144229
4	6	0	-0.811453	0.748456	0.052492
5	6	0	0.154837	1.602795	-0.798591
6	6	0	1.627557	1.326034	-0.470271
7	6	0	-1.458367	-1.694654	-0.109734
8	6	0	-2.263916	1.001589	-0.411776
9	6	0	-3.272854	0.050801	0.240825
10	6	0	-2.929031	-1.417784	-0.053360
11	1	0	-1.161732	-2.734125	-0.237109
12	1	0	2.410551	-0.342006	-1.638068
13	1	0	-0.057793	2.667242	-0.640532
14	1	0	2.286723	1.933480	-1.097159
15	1	0	-2.310594	0.883469	-1.502862
16	1	0	-2.533860	2.043260	-0.198614
17	1	0	-3.290765	0.216099	1.323090
18	1	0	-4.283914	0.273862	-0.115776
19	1	0	-3.364226	-1.712242	-1.023395
20	1	0	-3.411930	-2.080603	0.677946
21	1	0	-0.035153	1.399330	-1.860448
22	1	0	1.835345	1.614059	0.562174

23	1	0	1.085560	-2.152392	-0.544738
24	6	0	-0.665354	1.113460	1.549214
25	1	0	-0.871773	2.178753	1.705960
26	1	0	-1.357520	0.539502	2.169602
27	1	0	0.338979	0.901026	1.922544
28	17	0	3.425988	-0.595015	0.457674

R=PTHP, position 4

Standard orientation:

Center Number	Atomic Number	Atomic Type	Coordinates (Angstroms)		
			X	Y	Z
1	6	0	0.143112	0.705952	-0.989711
2	6	0	-0.422436	-0.642913	-0.515578
3	6	0	-1.916189	-0.590081	-0.336796
4	6	0	-2.509798	0.575074	0.443831
5	6	0	-1.826309	1.899669	0.009003
6	6	0	-0.294712	1.832406	-0.049868
7	6	0	-2.729670	-1.629295	-0.779548
8	6	0	-4.024142	0.695476	0.144260
9	6	0	-4.787438	-0.632672	0.248131
10	6	0	-4.088060	-1.708142	-0.527335
11	1	0	-2.256619	-2.439138	-1.332513
12	1	0	-0.272409	0.916755	-1.982284
13	1	0	-0.141813	-1.430606	-1.220339
14	1	0	-2.142843	2.706985	0.680895
15	1	0	0.111209	2.783479	-0.411256
16	1	0	-4.140177	1.071601	-0.879443
17	1	0	-4.468756	1.445926	0.809214
18	1	0	-4.894262	-0.934193	1.302861
19	1	0	-5.813362	-0.498719	-0.116832
20	1	0	-4.653803	-2.569126	-0.868817
21	1	0	-2.196434	2.166352	-0.989625
22	1	0	0.117450	1.672078	0.953709
23	1	0	0.064604	-0.904405	0.435317
24	6	0	-2.292865	0.345935	1.961145
25	1	0	-2.705854	1.182246	2.537675
26	1	0	-2.781978	-0.573213	2.295599
27	1	0	-1.232369	0.258232	2.213207
28	8	0	1.555012	0.702702	-1.239941
29	6	0	2.425245	0.330479	-0.224326
30	6	0	3.783429	0.971492	-0.498699
31	1	0	2.052984	0.645615	0.768242
32	6	0	3.419265	-1.575881	0.774410

33	6	0	4.834531	0.474037	0.503374
34	1	0	4.066276	0.702460	-1.522772
35	1	0	3.679802	2.060599	-0.459461
36	6	0	4.840905	-1.059135	0.555997
37	1	0	3.372553	-2.666895	0.716928
38	1	0	3.060751	-1.277307	1.775716
39	1	0	5.824594	0.860909	0.240443
40	1	0	4.601572	0.868592	1.502417
41	1	0	5.496429	-1.423072	1.355728
42	1	0	5.220342	-1.464030	-0.390007
43	8	0	2.532850	-1.092143	-0.225602

R=OTHP, position 7

Standard orientation:

Center Number	Atomic Number	Atomic Type	Coordinates (Angstroms)		
			X	Y	Z
1	6	0	0.198489	1.215602	-1.153039
2	6	0	-0.442156	-0.137810	-1.129490
3	6	0	-1.656526	-0.433169	-0.513191
4	6	0	-2.309256	0.583870	0.432768
5	6	0	-1.892066	2.013463	0.020524
6	6	0	-0.373923	2.177293	-0.104680
7	6	0	-2.300949	-1.637035	-0.775325
8	6	0	-3.846642	0.450778	0.344043
9	6	0	-4.334879	-0.977275	0.609389
10	6	0	-3.702658	-1.980256	-0.370124
11	1	0	-1.797410	-2.345990	-1.429986
12	1	0	0.012522	1.649324	-2.148159
13	1	0	-2.289819	2.733401	0.746688
14	1	0	-0.114879	3.204399	-0.380806
15	1	0	-4.168598	0.763592	-0.658410
16	1	0	-4.312301	1.146540	1.053462
17	1	0	-4.094860	-1.262905	1.638899
18	1	0	-5.426543	-1.021103	0.531779
19	1	0	-4.314061	-2.032577	-1.286994
20	1	0	-3.743163	-2.997332	0.044958
21	1	0	-2.361542	2.254148	-0.942982
22	1	0	0.107870	1.987582	0.860019
23	1	0	0.020605	-0.888198	-1.762751
24	6	0	-1.845745	0.303073	1.882654
25	1	0	-2.321880	1.002399	2.580411
26	1	0	-2.096004	-0.713081	2.195812
27	1	0	-0.763054	0.405292	1.987341

28	8	0	1.641583	1.196272	-1.108898
29	6	0	2.248451	0.369659	-0.172610
30	6	0	3.594001	0.975048	0.218018
31	1	0	1.612498	0.241962	0.723556
32	6	0	3.045448	-1.841319	0.114013
33	6	0	4.371025	0.023277	1.139108
34	1	0	4.150053	1.157218	-0.708747
35	1	0	3.425869	1.944435	0.698457
36	6	0	4.444490	-1.379627	0.522349
37	1	0	3.075830	-2.794017	-0.422116
38	1	0	2.417344	-1.981482	1.011483
39	1	0	5.373564	0.417113	1.336512
40	1	0	3.863050	-0.036595	2.111944
41	1	0	4.883344	-2.096367	1.226319
42	1	0	5.082612	-1.362378	-0.369521
43	8	0	2.432958	-0.912372	-0.769055

Theoretical Calculation (Chapter 4)

Point group, Electronic state, total energies (hartrees) with aug-cc-pvtz basis set, zero-point Energies (kcal/mol), thermal corrections (kcal/mol), entropies (cal/mol·K), and solvation free energies (kcal/mol)

	PG ^a	ES ^b	SCF Energy	ZPE ^c (NIF)	TC ^d	S ^e	Solvation Free Energy ^f
1	C ₁	² A	-2896.86773	233.53(0)	17.54	182.47	-26.54
2	C ₂	¹ A	-234.72318	92.26(0)	4.03	72.37	-4.22
1,2TS3,4	C ₁	² A	-3131.54240	321.89(1)	22.13	220.21	-24.50
3	C ₁	¹ A	-2897.51628	239.88(0)	18.21	186.70	-24.04
4	C _s	² A''	-234.08297	83.47(0)	4.04	74.98	-4.40
3,4TS5	C ₁	² A	-3131.59951	323.35(1)	22.68	227.84	-27.76
5	C ₁	² A	-3131.66672	326.69(0)	22.37	221.44	-26.43
6	C ₁	² A	-3131.67303	327.02(0)	22.15	220.45	-21.99
6TS7	C ₁	² A	-3131.65941	326.09(1)	21.96	218.80	-20.86
7	C ₁	² A	-3131.67667	326.78(0)	22.35	222.84	-24.07
7TS8	C ₁	² A	-3131.67855	326.60(1)	21.96	221.07	-24.48
8	C ₁	² A	-3131.68971	327.31(0)	21.99	223.11	-25.31
9	C ₁	¹ A	-309.96884	95.00(0)	4.71	79.31	-7.11
10	C ₁	² A	-2821.69973	230.93(0)	17.07	178.55	-23.16
1TS11,12	C ₁	² A	-2896.79585	230.05(1)	18.22	189.72	-29.47
11	C ₁	³ A	-2781.70645	206.23(0)	15.70	168.16	-28.49

11^f	C ₁	¹ A	-2781.70155	206.20(0)	15.71	166.19	-29.18
12	C ₁	² A	-115.09697	23.10(0)	2.48	56.57	-3.30
2,12TS14,15	C ₁	² A	-349.81611	113.96(1)	6.35	96.94	-6.69
15	C _S	¹ A'	-115.76963	32.30(0)	2.66	56.74	-3.62
14	C _S	² A''	-234.08297	83.47(0)	4.04	74.98	-4.40
2,11TS13,14	C ₁	³ A	-3016.42769	295.57(1)	19.99	206.76	-28.56
2,11TS13,14^f	C ₁	¹ A	-3016.42390	295.99(1)	19.99	205.40	-29.25
13	C ₁	² A	-2782.39162	213.34(0)	15.96	168.97	-25.88
O2	D _{∞h}	³ S _g	-150.37835	2.37(0)	2.08	49.01	-2.40
16	C ₁	² A	-384.48870	89.67(0)	5.23	86.27	-8.69
16TS17	C ₁	² A	-384.42030	85.62(0)	5.18	86.06	-10.08
17	C ₁	² A	-384.53981	87.62(0)	5.93	92.50	-13.55
18	C ₁	¹ A	-308.76956	80.29(0)	4.41	77.73	-8.86
OH	C _{∞v}	² π	-75.76403	5.21(0)	2.07	42.61	-3.79
19	C ₁	³ A	-460.34693	97.71(0)	7.40	111.90	-8.01
19TS20	C ₁	³ A	-460.29642	94.37(1)	6.43	97.49	-9.30
20	C ₁	³ A	-460.31335	96.93(0)	6.97	101.44	-8.24
21	C ₁	² A	-309.33823	86.38(0)	4.73	80.64	-7.08
OOH	C _S	² A''	-150.96573	8.81(0)	2.38	54.71	-6.44
22	C ₁	² A	-459.74373	91.94(0)	5.84	90.66	-9.05
22TS23	C ₁	² A	-459.73324	88.69(1)	5.82	91.7	-9.52
23	C ₁	² A	-459.75382	91.02(0)	6.64	99.65	-11.44

^aPoint group. ^bElectronic state. ^cZero-point energies and number of imaginary frequencies. ^dThermal corrections to 298K. ^eEntropies (cal/mol·K). ^fResult from the open shell singlet state (broken symmetry).

Geometry at B3LYP/6-31G(d) level of calculation 1 C₁
Standard orientation:

Center Number	Atomic Number	Atomic Type	Coordinates (Angstroms)		
			X	Y	Z
1	29	0	1.308570	1.519379	-0.242579
2	6	0	-5.354226	-1.797293	0.355398
3	6	0	-3.217317	-0.987638	0.070552
4	6	0	-3.732774	0.272663	-0.351161
5	6	0	-5.848396	-0.512639	-0.080572
6	1	0	-1.482529	-2.157127	0.503960
7	6	0	-1.823618	-1.193322	0.142790
8	6	0	-2.828965	1.303695	-0.694985
9	6	0	-1.473283	1.082683	-0.620228
10	6	0	-0.941937	-0.181259	-0.209336
11	1	0	-3.226776	2.262624	-1.013697
12	6	0	1.115021	-1.379676	-0.088039
13	6	0	2.522897	-1.527647	-0.030844
14	6	0	3.433515	-0.409958	-0.103528
15	6	0	3.038778	-2.854108	0.077596
16	6	0	4.843475	-0.695013	-0.054887
17	6	0	4.386351	-3.114052	0.127839
18	1	0	2.326785	-3.676924	0.126124
19	6	0	5.270336	-2.000245	0.059219
20	1	0	6.342514	-2.190898	0.097404
21	1	0	0.540423	-2.310369	-0.088978
22	7	0	0.463622	-0.240446	-0.155666
23	8	0	3.070108	0.824307	-0.228019
24	6	0	5.801227	0.463707	-0.131291
25	1	0	5.615954	1.181372	0.676150
26	1	0	6.839131	0.121664	-0.067803
27	1	0	5.672216	1.021051	-1.066590
28	6	0	4.935411	-4.514742	0.252202
29	1	0	5.527533	-4.637149	1.168657
30	1	0	4.130560	-5.256618	0.276457
31	1	0	5.594718	-4.766557	-0.588734
32	7	0	-4.061886	-2.009060	0.423541
33	7	0	-5.080448	0.487082	-0.420164
34	8	0	-7.189932	-0.360269	-0.130516
35	1	0	-7.351524	0.551428	-0.436795
36	6	0	-6.311376	-2.891157	0.731621
37	1	0	-5.749579	-3.777001	1.033936
38	1	0	-6.964466	-2.574980	1.553730
39	1	0	-6.967481	-3.144538	-0.109649
40	7	0	-0.491826	2.093060	-0.949991

41	1	0	-0.617578	2.995005	-0.470924
42	1	0	-0.458821	2.279546	-1.953086
43	8	0	1.853022	3.237646	0.203639
44	8	0	0.710606	4.136844	0.367987
45	6	0	0.677157	4.478569	1.737636
46	1	0	0.494635	3.597621	2.371423
47	1	0	1.620877	4.946357	2.042216
48	1	0	-0.145457	5.195407	1.852327

2 C₂

Standard orientation:

Center Number	Atomic Number	Atomic Type	Coordinates (Angstroms)		
			X	Y	Z
1	6	0	-0.005187	1.503056	0.047817
2	6	0	-0.371449	0.671579	-1.192338
3	6	0	0.371449	-0.671579	-1.192338
4	6	0	0.005187	-1.503056	0.047817
5	6	0	-0.005187	-0.668485	1.306185
6	6	0	0.005187	0.668485	1.306185
7	1	0	0.983277	1.970244	-0.089870
8	1	0	-1.454055	0.482516	-1.192849
9	1	0	0.149634	-1.236805	-2.105944
10	1	0	0.708859	-2.339186	0.163919
11	1	0	-0.019119	-1.204621	2.254763
12	1	0	0.019119	1.204621	2.254763
13	1	0	1.454055	-0.482516	-1.192849
14	1	0	-0.149634	1.236805	-2.105944
15	1	0	-0.708859	2.339186	0.163919
16	1	0	-0.983277	-1.970244	-0.089870

1,2TS3,4 C₁

Standard orientation:

Center Number	Atomic Number	Atomic Type	Coordinates (Angstroms)		
			X	Y	Z
1	29	0	0.911597	-0.383565	0.188246
2	6	0	-6.610100	0.080816	-0.367472
3	6	0	-4.318461	0.112883	-0.146239
4	6	0	-4.286133	-1.310518	-0.080067
5	6	0	-6.549116	-1.358596	-0.290505
6	1	0	-3.197158	1.924495	-0.177954

7	6	0	-3.117264	0.848167	-0.076450
8	6	0	-3.041289	-1.960359	0.067383
9	6	0	-1.878284	-1.226374	0.150075
10	6	0	-1.897247	0.203872	0.075732
11	1	0	-3.022969	-3.044886	0.122975
12	6	0	-0.499076	2.126003	0.174992
13	6	0	0.711566	2.858323	0.053156
14	6	0	1.974715	2.237925	-0.254636
15	6	0	0.632804	4.275056	0.187944
16	6	0	3.107378	3.101344	-0.448321
17	6	0	1.727075	5.090945	0.022152
18	1	0	-0.335615	4.712957	0.425976
19	6	0	2.960910	4.465398	-0.303203
20	1	0	3.838167	5.096587	-0.443320
21	1	0	-1.395085	2.731704	0.332433
22	7	0	-0.630138	0.822820	0.098082
23	8	0	2.146093	0.959770	-0.380527
24	6	0	4.431690	2.471263	-0.787915
25	1	0	5.211543	3.230293	-0.906408
26	1	0	4.743681	1.769104	-0.005195
27	1	0	4.367142	1.891731	-1.717172
28	6	0	1.646822	6.591320	0.170584
29	1	0	0.627226	6.913020	0.406660
30	1	0	2.302635	6.954361	0.972885
31	1	0	1.953197	7.106796	-0.749104
32	7	0	-5.504763	0.783610	-0.296311
33	7	0	-5.441522	-2.036790	-0.156132
34	8	0	-7.723321	-2.025153	-0.366923
35	1	0	-7.502841	-2.972667	-0.298862
36	6	0	-7.930288	0.778286	-0.529954
37	1	0	-7.767980	1.857206	-0.569588
38	1	0	-8.436609	0.451956	-1.446248
39	1	0	-8.604519	0.541602	0.301829
40	7	0	-0.583655	-1.828566	0.274005
41	1	0	-0.495401	-2.686674	-0.265086
42	1	0	-0.293915	-2.029537	1.250091
43	8	0	2.199750	-1.687562	0.618585
44	8	0	1.032867	-1.295697	2.229161
45	6	0	1.933297	-1.382482	3.280013
46	1	0	2.357646	-2.395067	3.389902
47	1	0	2.769991	-0.673002	3.180582
48	1	0	1.406624	-1.141162	4.222707
49	6	0	5.722487	-4.010833	-0.364336
50	6	0	4.212430	-4.302391	-0.364364
51	6	0	3.481951	-3.456051	-1.416465
52	6	0	3.733341	-1.982758	-1.177726

53	6	0	5.105478	-1.619264	-0.833425
54	6	0	6.022564	-2.539627	-0.463685
55	1	0	6.191025	-4.422597	0.540263
56	1	0	4.034417	-5.370401	-0.536042
57	1	0	3.848860	-3.713521	-2.424299
58	1	0	3.225246	-1.291498	-1.850091
59	1	0	5.373062	-0.566072	-0.865871
60	1	0	7.040331	-2.220087	-0.244576
61	1	0	3.125696	-1.635757	-0.017496
62	1	0	2.408055	-3.663765	-1.403710
63	1	0	3.792103	-4.054676	0.617503
64	1	0	6.213074	-4.529514	-1.205386

3 C₁

Standard orientation:

Center Number	Atomic Number	Atomic Type	Coordinates (Angstroms)		
			X	Y	Z
1	29	0	1.372345	-1.621649	-0.381425
2	6	0	-5.271570	1.446290	-0.742210
3	6	0	-3.149919	0.751758	-0.190531
4	6	0	-3.659655	-0.076295	0.853994
5	6	0	-5.764490	0.606332	0.318451
6	1	0	-1.377463	1.377501	-1.242777
7	6	0	-1.756040	0.780700	-0.419229
8	6	0	-2.772868	-0.831761	1.646026
9	6	0	-1.405220	-0.795160	1.416619
10	6	0	-0.900903	0.034709	0.361095
11	1	0	-3.186274	-1.443320	2.442937
12	6	0	1.158114	1.161640	0.177340
13	6	0	2.574355	1.311234	0.068040
14	6	0	3.432161	0.177947	0.177066
15	6	0	3.122202	2.615578	-0.022944
16	6	0	4.840653	0.396345	0.212172
17	6	0	4.485953	2.828528	-0.024022
18	1	0	2.439760	3.460240	-0.098217
19	6	0	5.320333	1.691678	0.099995
20	1	0	6.399300	1.840642	0.109840
21	1	0	0.577418	2.071941	0.344968
22	7	0	0.505571	0.032886	0.145032
23	8	0	2.987128	-1.051670	0.320227
24	6	0	5.759240	-0.788180	0.357552
25	1	0	5.613314	-1.505151	-0.459301
26	1	0	6.807529	-0.474640	0.357108

27	1	0	5.561566	-1.332867	1.288440
28	6	0	5.083969	4.209598	-0.148302
29	1	0	5.675728	4.311545	-1.067091
30	1	0	4.305709	4.979059	-0.169885
31	1	0	5.753634	4.435948	0.690861
32	7	0	-3.979387	1.502522	-0.973372
33	7	0	-5.006439	-0.125433	1.091380
34	8	0	-7.103348	0.588063	0.513526
35	1	0	-7.257786	-0.026345	1.254994
36	6	0	-6.218979	2.255411	-1.581869
37	1	0	-5.651281	2.822687	-2.322433
38	1	0	-6.940727	1.609547	-2.096350
39	1	0	-6.803022	2.948028	-0.963781
40	7	0	-0.513362	-1.555539	2.157297
41	1	0	-0.880920	-1.966939	3.004914
42	1	0	0.419712	-1.181270	2.269591
43	8	0	2.151341	-3.152432	-0.837448
44	8	0	-0.166717	-2.110415	-1.128071
45	6	0	-0.367613	-3.406616	-1.619243
46	1	0	0.347558	-3.684821	-2.403093
47	1	0	-0.336790	-4.170879	-0.830352
48	1	0	-1.379111	-3.401017	-2.056160
49	1	0	3.063876	-3.029892	-0.521134

4 C_s

Standard orientation:

Center Number	Atomic Number	Atomic Type	Coordinates (Angstroms)		
			X	Y	Z
1	6	0	-0.108186	-0.694320	1.274119
2	6	0	0.502718	-1.305691	0.000000
3	6	0	-0.108186	-0.694320	-1.274119
4	6	0	-0.108186	0.809006	-1.218098
5	6	0	-0.098409	1.478107	0.000000
6	6	0	-0.108186	0.809006	1.218098
7	1	0	-1.141713	-1.062139	1.400211
8	1	0	1.582547	-1.108573	0.000000
9	1	0	0.437306	-1.045154	-2.160460
10	1	0	-0.098916	2.567160	0.000000
11	1	0	-0.139485	1.370009	2.148664
12	1	0	-1.141713	-1.062139	-1.400211
13	1	0	0.374759	-2.394745	0.000000
14	1	0	0.437306	-1.045154	2.160460
15	1	0	-0.139485	1.370009	-2.148664

3,4TS5 C₁

Standard orientation:

Center Number	Atomic Number	Atomic Type	Coordinates (Angstroms)		
			X	Y	Z
1	29	0	1.225231	-0.060533	-0.151628
2	6	0	-6.054488	-0.239692	-1.001256
3	6	0	-3.891905	0.089474	-0.290856
4	6	0	-4.088894	-0.792708	0.813585
5	6	0	-6.232310	-1.122942	0.119777
6	1	0	-2.473578	1.341724	-1.319087
7	6	0	-2.627873	0.699649	-0.457803
8	6	0	-3.033720	-1.030179	1.715169
9	6	0	-1.794788	-0.429043	1.540583
10	6	0	-1.600733	0.457507	0.427829
11	1	0	-3.212231	-1.697256	2.553871
12	6	0	-0.280856	2.375471	0.232346
13	6	0	0.874590	3.195140	0.070889
14	6	0	2.186961	2.642047	-0.030114
15	6	0	0.695519	4.604805	0.070483
16	6	0	3.294589	3.544692	-0.111189
17	6	0	1.759931	5.474802	-0.025850
18	1	0	-0.318063	4.994568	0.148941
19	6	0	3.056058	4.906824	-0.113759
20	1	0	3.911051	5.578166	-0.187421
21	1	0	-1.227148	2.906750	0.366950
22	7	0	-0.323428	1.068814	0.270032
23	8	0	2.435095	1.360855	-0.044475
24	6	0	4.684765	2.973829	-0.206167
25	1	0	4.791501	2.336169	-1.092086
26	1	0	5.434243	3.769517	-0.260520
27	1	0	4.913718	2.341541	0.660418
28	6	0	1.577611	6.973866	-0.036453
29	1	0	1.951966	7.420100	-0.966912
30	1	0	0.521481	7.245999	0.058700
31	1	0	2.119934	7.453454	0.788627
32	7	0	-4.892122	0.347643	-1.182464
33	7	0	-5.303304	-1.396225	0.997704
34	8	0	-7.449888	-1.699778	0.261591
35	1	0	-7.387425	-2.258324	1.058486
36	6	0	-7.180763	0.017822	-1.962322
37	1	0	-6.844079	0.712930	-2.734453
38	1	0	-7.517751	-0.912379	-2.435748

39	1	0	-8.052136	0.441632	-1.448346
40	7	0	-0.743303	-0.670270	2.406101
41	1	0	-0.981343	-1.065669	3.305079
42	1	0	-0.015882	0.029528	2.445855
43	8	0	2.652597	-1.191599	-0.025968
44	8	0	0.108261	-1.324399	-0.765621
45	6	0	0.485461	-2.654897	-0.932094
46	1	0	1.197459	-2.802917	-1.760448
47	1	0	0.926418	-3.095196	-0.024626
48	1	0	-0.431093	-3.222583	-1.164924
49	1	0	3.392039	-0.558927	0.004652
50	6	0	3.362635	-5.446702	-0.681419
51	6	0	4.659905	-4.819434	-1.220204
52	6	0	4.710143	-3.306386	-0.943253
53	6	0	4.384876	-2.991716	0.487589
54	6	0	3.628614	-3.876299	1.265384
55	6	0	3.100430	-5.034753	0.739147
56	1	0	2.510846	-5.135190	-1.309073
57	1	0	5.514902	-5.302782	-0.729255
58	1	0	5.693974	-2.899902	-1.211557
59	1	0	3.422043	-3.617244	2.301162
60	1	0	2.471564	-5.671538	1.357065
61	1	0	3.976995	-2.782500	-1.573763
62	1	0	4.757309	-5.010324	-2.295097
63	1	0	3.403801	-6.541161	-0.758616
64	1	0	4.829809	-2.120164	0.955265

5 C₁

Standard orientation:

Center Number	Atomic Number	Atomic Type	Coordinates (Angstroms)		
			X	Y	Z
1	29	0	1.196157	0.303290	0.695463
2	6	0	-5.972414	-1.024257	0.544217
3	6	0	-3.732954	-0.814990	0.062076
4	6	0	-3.991009	0.306849	-0.780551
5	6	0	-6.209717	0.106452	-0.312791
6	1	0	-2.206717	-2.072384	0.914965
7	6	0	-2.399412	-1.252260	0.231042
8	6	0	-2.922030	0.941025	-1.445994
9	6	0	-1.619968	0.501632	-1.274075
10	6	0	-1.361166	-0.613812	-0.411728
11	1	0	-3.146576	1.777741	-2.101765
12	6	0	0.344811	-2.221764	-0.426019

13	6	0	1.654664	-2.784548	-0.283208
14	6	0	2.803541	-2.003655	0.061288
15	6	0	1.799657	-4.171521	-0.548931
16	6	0	4.071940	-2.659765	0.110492
17	6	0	3.022408	-4.807922	-0.487243
18	1	0	0.908204	-4.740410	-0.808637
19	6	0	4.147692	-4.016408	-0.153963
20	1	0	5.123725	-4.498028	-0.102709
21	1	0	-0.432623	-2.911540	-0.771323
22	7	0	-0.004303	-0.981661	-0.216961
23	8	0	2.747751	-0.720368	0.311432
24	6	0	5.290291	-1.846576	0.461570
25	1	0	5.176639	-1.362998	1.439332
26	1	0	6.187947	-2.472169	0.487698
27	1	0	5.455957	-1.041624	-0.266064
28	6	0	3.175296	-6.285426	-0.760877
29	1	0	3.565820	-6.820903	0.114246
30	1	0	2.215712	-6.741444	-1.025223
31	1	0	3.871754	-6.474503	-1.588002
32	7	0	-4.744370	-1.461289	0.712956
33	7	0	-5.272589	0.752122	-0.955457
34	8	0	-7.494070	0.513561	-0.452895
35	1	0	-7.465693	1.280819	-1.054034
36	6	0	-7.112181	-1.708107	1.245323
37	1	0	-6.725073	-2.542932	1.833399
38	1	0	-7.641534	-1.013621	1.908990
39	1	0	-7.852391	-2.081921	0.527555
40	7	0	-0.538040	1.120578	-1.904592
41	1	0	-0.799691	1.755906	-2.648893
42	1	0	0.195969	0.485232	-2.193620
43	8	0	2.605009	1.825004	0.595148
44	8	0	-0.122073	1.134400	1.641680
45	6	0	0.256041	1.743621	2.842854
46	1	0	0.759561	1.054551	3.548770
47	1	0	0.927259	2.610586	2.701371
48	1	0	-0.642548	2.117662	3.361477
49	1	0	3.352688	1.261581	0.317786
50	6	0	2.287459	5.917242	-0.422316
51	6	0	3.438105	5.126697	-1.068308
52	6	0	3.702711	3.819789	-0.307154
53	6	0	2.457585	2.934769	-0.336489
54	6	0	1.216003	3.689953	0.050069
55	6	0	1.147994	5.023910	0.003869
56	1	0	2.657079	6.467951	0.457139
57	1	0	3.178668	4.891507	-2.110038
58	1	0	4.561640	3.285765	-0.735474

59	1	0	0.374581	3.078447	0.369861
60	1	0	0.222283	5.515503	0.300170
61	1	0	3.940329	4.035841	0.742148
62	1	0	4.348785	5.735677	-1.103322
63	1	0	1.921644	6.687232	-1.115521
64	1	0	2.328152	2.502481	-1.342152

6 C₁

Standard orientation:

Center Number	Atomic Number	Atomic Type	Coordinates (Angstroms)		
			X	Y	Z
1	29	0	-1.459952	-0.216569	0.410934
2	6	0	6.188136	0.173955	0.553340
3	6	0	3.918545	0.053840	0.208401
4	6	0	4.066090	-1.145118	-0.547343
5	6	0	6.315134	-1.034231	-0.219658
6	1	0	2.530648	1.500951	0.963668
7	6	0	2.623949	0.587915	0.384447
8	6	0	2.919113	-1.792490	-1.040715
9	6	0	1.639567	-1.285208	-0.837208
10	6	0	1.502984	-0.018790	-0.158521
11	1	0	3.050532	-2.732004	-1.570708
12	6	0	0.241712	1.918255	-0.348137
13	6	0	-0.819142	2.873363	-0.247355
14	6	0	-2.148181	2.548166	0.163441
15	6	0	-0.499628	4.218760	-0.578244
16	6	0	-3.110341	3.600409	0.250115
17	6	0	-1.427592	5.235826	-0.500387
18	1	0	0.517836	4.441876	-0.894703
19	6	0	-2.734040	4.891256	-0.076092
20	1	0	-3.481528	5.680658	-0.004159
21	1	0	1.188016	2.333818	-0.702682
22	7	0	0.233904	0.634887	-0.074362
23	8	0	-2.521386	1.328825	0.452887
24	6	0	-4.509962	3.263003	0.692435
25	1	0	-4.508461	2.763952	1.668640
26	1	0	-5.128714	4.162926	0.763254
27	1	0	-4.995317	2.571621	-0.008925
28	6	0	-1.084716	6.665383	-0.846824
29	1	0	-1.240446	7.337308	0.007070
30	1	0	-0.038436	6.758984	-1.154965
31	1	0	-1.707310	7.042759	-1.668348
32	7	0	4.996620	0.692084	0.752133

33	7	0	5.310281	-1.678128	-0.751841
34	8	0	7.566462	-1.520054	-0.396720
35	1	0	7.465103	-2.327247	-0.934528
36	6	0	7.401991	0.844781	1.131620
37	1	0	7.094086	1.737046	1.680876
38	1	0	7.941784	0.171349	1.808365
39	1	0	8.109623	1.130649	0.343862
40	7	0	0.513755	-1.943360	-1.319001
41	1	0	0.747980	-2.834206	-1.745402
42	1	0	-0.199358	-2.076716	-0.585431
43	8	0	-3.175197	-0.903722	-0.643289
44	8	0	-1.045757	-1.887085	1.039254
45	6	0	-0.177822	-2.062734	2.128506
46	1	0	0.771528	-1.511822	2.017651
47	1	0	-0.631460	-1.742449	3.082560
48	1	0	0.081395	-3.128395	2.234707
49	1	0	-3.737897	-0.131864	-0.454787
50	6	0	-3.861335	-5.015603	0.072653
51	6	0	-4.886848	-4.036024	0.666869
52	6	0	-4.313772	-2.613079	0.727535
53	6	0	-3.967931	-2.120487	-0.679260
54	6	0	-3.196955	-3.146259	-1.464433
55	6	0	-3.156851	-4.439391	-1.130379
56	1	0	-3.107692	-5.276268	0.831833
57	1	0	-5.795189	-4.042441	0.047473
58	1	0	-5.025283	-1.924838	1.202626
59	1	0	-2.674835	-2.775889	-2.344384
60	1	0	-2.581775	-5.130325	-1.745847
61	1	0	-3.386871	-2.600577	1.311522
62	1	0	-5.189410	-4.364606	1.667981
63	1	0	-4.349434	-5.961781	-0.198443
64	1	0	-4.888025	-1.867046	-1.230230

6TS7 C₁

Standard orientation:

Center Number	Atomic Number	Atomic Type	Coordinates (Angstroms)		
			X	Y	Z
1	29	0	-1.259523	-0.289071	0.505518
2	6	0	6.257391	0.641997	0.103382
3	6	0	3.964213	0.453155	0.101669
4	6	0	4.054528	-0.922591	-0.257659
5	6	0	6.321866	-0.750004	-0.268527
6	1	0	2.669652	2.091665	0.550791

7	6	0	2.694955	1.044357	0.270342
8	6	0	2.869535	-1.679065	-0.375602
9	6	0	1.629234	-1.100694	-0.180288
10	6	0	1.534254	0.309340	0.079249
11	1	0	2.953061	-2.740026	-0.592807
12	6	0	0.073630	2.142561	-0.188067
13	6	0	-1.144561	2.885696	-0.192770
14	6	0	-2.427582	2.300146	0.063306
15	6	0	-1.053145	4.273465	-0.493247
16	6	0	-3.577040	3.152438	0.020357
17	6	0	-2.159963	5.092815	-0.530204
18	1	0	-0.067134	4.691001	-0.690895
19	6	0	-3.418054	4.495616	-0.264758
20	1	0	-4.306266	5.126252	-0.288412
21	1	0	0.959046	2.710089	-0.484218
22	7	0	0.234889	0.878525	0.111413
23	8	0	-2.603519	1.033640	0.316616
24	6	0	-4.929379	2.547142	0.290149
25	1	0	-4.950689	2.042094	1.262930
26	1	0	-5.712829	3.311225	0.276323
27	1	0	-5.183157	1.785990	-0.459168
28	6	0	-2.060859	6.568118	-0.837047
29	1	0	-2.655308	6.838752	-1.719298
30	1	0	-2.429170	7.180560	-0.003724
31	1	0	-1.025126	6.864374	-1.032268
32	7	0	5.089332	1.213304	0.280891
33	7	0	5.275040	-1.510947	-0.442901
34	8	0	7.554153	-1.279916	-0.442031
35	1	0	7.414991	-2.214099	-0.685002
36	6	0	7.516173	1.440350	0.288419
37	1	0	7.258162	2.463556	0.568816
38	1	0	8.151065	0.999217	1.066140
39	1	0	8.112300	1.454604	-0.631929
40	7	0	0.417430	-1.835202	-0.258118
41	1	0	0.473312	-2.627370	-0.892697
42	1	0	0.079911	-2.161848	0.663411
43	8	0	-2.727628	-1.232716	-0.995067
44	8	0	-1.254009	-1.624654	1.833540
45	6	0	-1.279698	-1.405345	3.213563
46	1	0	-2.204873	-0.897337	3.540012
47	1	0	-1.226030	-2.358957	3.766697
48	1	0	-0.435707	-0.783275	3.566734
49	1	0	-3.399798	-0.566557	-0.765870
50	6	0	-2.905051	-5.385425	-0.301572
51	6	0	-4.152513	-4.580196	0.098078
52	6	0	-3.827242	-3.084463	0.213853

53	6	0	-3.338972	-2.533600	-1.130577
54	6	0	-2.320187	-3.438423	-1.773082
55	6	0	-2.126917	-4.708965	-1.403750
56	1	0	-2.248003	-5.519465	0.571846
57	1	0	-4.935682	-4.731674	-0.658690
58	1	0	-4.709594	-2.521548	0.546903
59	1	0	-1.747502	-2.997910	-2.587372
60	1	0	-1.375910	-5.306761	-1.920182
61	1	0	-3.033424	-2.914473	0.951540
62	1	0	-4.556734	-4.954511	1.045864
63	1	0	-3.188098	-6.399099	-0.617083
64	1	0	-4.190816	-2.422544	-1.823162

7 C₁

Standard orientation:

Center Number	Atomic Number	Atomic Type	Coordinates (Angstroms)		
			X	Y	Z
1	29	0	-0.952784	-0.275556	1.000622
2	6	0	6.314003	0.869727	-0.181655
3	6	0	4.023452	0.673185	-0.056668
4	6	0	4.133554	-0.739824	0.096157
5	6	0	6.396577	-0.562877	-0.032433
6	1	0	2.717651	2.366798	-0.115900
7	6	0	2.751066	1.284731	-0.049268
8	6	0	2.958266	-1.513030	0.236135
9	6	0	1.726060	-0.900561	0.231261
10	6	0	1.604764	0.519122	0.087019
11	1	0	3.051899	-2.589626	0.342597
12	6	0	-0.056575	2.182951	-0.279037
13	6	0	-1.368028	2.741517	-0.254571
14	6	0	-2.531995	1.999012	0.148068
15	6	0	-1.508119	4.086708	-0.698512
16	6	0	-3.799808	2.665561	0.092280
17	6	0	-2.727693	4.724248	-0.739449
18	1	0	-0.610069	4.620621	-1.005887
19	6	0	-3.864120	3.978557	-0.333204
20	1	0	-4.838747	4.465002	-0.360214
21	1	0	0.714349	2.808997	-0.737928
22	7	0	0.283753	1.006211	0.179024
23	8	0	-2.509528	0.751203	0.529183
24	6	0	-5.027358	1.897670	0.506149
25	1	0	-5.185848	1.024081	-0.138485
26	1	0	-4.924726	1.509180	1.525722

27	1	0	-5.921231	2.527535	0.457677
28	6	0	-2.874432	6.156364	-1.194905
29	1	0	-3.289698	6.792205	-0.402161
30	1	0	-1.908878	6.581301	-1.487852
31	1	0	-3.549152	6.239569	-2.056807
32	7	0	5.140311	1.455911	-0.189888
33	7	0	5.358888	-1.344137	0.103194
34	8	0	7.633559	-1.107180	-0.034730
35	1	0	7.509441	-2.068018	0.077170
36	6	0	7.561655	1.692785	-0.325985
37	1	0	7.291941	2.746068	-0.424638
38	1	0	8.218748	1.564685	0.542458
39	1	0	8.138955	1.380478	-1.204440
40	7	0	0.488734	-1.607859	0.402085
41	1	0	0.562698	-2.426307	1.002107
42	1	0	0.041997	-1.877375	-0.480201
43	8	0	-1.892952	-1.334865	-1.456267
44	8	0	-1.570121	-1.438572	2.265571
45	6	0	-2.743607	-1.201169	2.983526
46	1	0	-2.782758	-1.869184	3.861288
47	1	0	-2.826600	-0.167490	3.364447
48	1	0	-3.656887	-1.397947	2.391752
49	6	0	-2.841125	-5.341066	-0.607535
50	6	0	-3.987326	-4.330970	-0.436402
51	6	0	-3.446977	-2.897745	-0.344082
52	6	0	-2.696595	-2.517662	-1.626748
53	6	0	-1.760609	-3.612861	-2.070925
54	6	0	-1.816878	-4.866403	-1.609137
55	1	0	-2.345152	-5.515343	0.360348
56	1	0	-4.669675	-4.412257	-1.294469
57	1	0	-4.264813	-2.186115	-0.171901
58	1	0	-2.434389	-0.646863	-1.021206
59	1	0	-1.016839	-3.325810	-2.813476
60	1	0	-1.097334	-5.601198	-1.969890
61	1	0	-2.758396	-2.799913	0.505118
62	1	0	-4.575328	-4.572726	0.456421
63	1	0	-3.234332	-6.319267	-0.916933
64	1	0	-3.424454	-2.323355	-2.434193

7TS8 C₁

Standard orientation:

Center Number	Atomic Number	Atomic Type	Coordinates (Angstroms)		
			X	Y	Z

1	29	0	-1.291632	0.477067	-0.660176
2	6	0	5.354223	-2.923294	-0.097908
3	6	0	3.228035	-2.039023	-0.096320
4	6	0	3.758392	-0.715644	-0.112261
5	6	0	5.863932	-1.573682	-0.106625
6	1	0	1.475920	-3.263301	-0.133399
7	6	0	1.830979	-2.239131	-0.100463
8	6	0	2.868378	0.382295	-0.128152
9	6	0	1.509006	0.167382	-0.127105
10	6	0	0.965921	-1.155589	-0.102364
11	1	0	3.276215	1.388520	-0.140744
12	6	0	-1.091625	-2.294446	0.222991
13	6	0	-2.500707	-2.465018	0.224465
14	6	0	-3.415257	-1.409499	-0.126283
15	6	0	-3.005814	-3.737418	0.621947
16	6	0	-4.821887	-1.701369	-0.067445
17	6	0	-4.352616	-4.008520	0.671705
18	1	0	-2.288106	-4.512683	0.886701
19	6	0	-5.242023	-2.957865	0.316522
20	1	0	-6.313143	-3.155313	0.351176
21	1	0	-0.512807	-3.150454	0.581230
22	7	0	-0.443194	-1.214645	-0.144526
23	8	0	-3.052391	-0.215608	-0.474728
24	6	0	-5.790992	-0.608755	-0.432554
25	1	0	-5.665987	0.264895	0.218411
26	1	0	-5.619392	-0.253697	-1.455527
27	1	0	-6.825717	-0.957071	-0.352790
28	6	0	-4.890862	-5.357767	1.083154
29	1	0	-5.483675	-5.818614	0.282127
30	1	0	-4.079990	-6.049316	1.334241
31	1	0	-5.546082	-5.281658	1.960787
32	7	0	4.058710	-3.129489	-0.094187
33	7	0	5.109142	-0.508238	-0.115860
34	8	0	7.208051	-1.427864	-0.106799
35	1	0	7.377945	-0.467612	-0.115249
36	6	0	6.296904	-4.092301	-0.093831
37	1	0	5.722982	-5.021004	-0.088772
38	1	0	6.950531	-4.072581	-0.974063
39	1	0	6.953097	-4.064487	0.784296
40	7	0	0.538820	1.226883	-0.174135
41	1	0	0.783330	1.961883	-0.836472
42	1	0	0.376234	1.701278	0.729296
43	8	0	-0.491481	2.860688	1.979803
44	8	0	-1.669949	2.130079	-1.367478
45	6	0	-2.894479	2.453880	-1.958879
46	1	0	-2.927799	2.195431	-3.033896

47	1	0	-3.748983	1.950840	-1.479917
48	1	0	-3.074302	3.542045	-1.888652
49	6	0	0.931582	5.979945	-0.460482
50	6	0	-0.494308	6.155881	0.086032
51	6	0	-1.060877	4.821290	0.589085
52	6	0	-0.199407	4.258641	1.725333
53	6	0	1.273545	4.353073	1.419378
54	6	0	1.776313	5.112723	0.440353
55	1	0	0.897262	5.531294	-1.465589
56	1	0	-0.475604	6.882271	0.910742
57	1	0	-2.091783	4.955594	0.944944
58	1	0	-1.424089	2.715694	1.748534
59	1	0	1.929345	3.761853	2.057272
60	1	0	2.853542	5.125338	0.275327
61	1	0	-1.097464	4.080603	-0.222175
62	1	0	-1.148008	6.574343	-0.687504
63	1	0	1.415158	6.957681	-0.590779
64	1	0	-0.407619	4.808622	2.658322

8 C₁

Standard orientation:

Center Number	Atomic Number	Atomic Type	Coordinates (Angstroms)		
			X	Y	Z
1	29	0	1.072897	0.247366	-0.887574
2	6	0	-6.349160	-0.101442	0.327157
3	6	0	-4.071652	0.152846	0.103011
4	6	0	-3.940903	-1.208217	-0.299538
5	6	0	-6.186976	-1.477509	-0.077534
6	1	0	-3.092110	2.017702	0.443386
7	6	0	-2.931398	0.979804	0.174400
8	6	0	-2.659010	-1.708984	-0.618457
9	6	0	-1.556868	-0.888705	-0.534073
10	6	0	-1.673656	0.476322	-0.127033
11	1	0	-2.565919	-2.746328	-0.926162
12	6	0	-0.377252	2.393136	0.412500
13	6	0	0.743329	3.259858	0.354689
14	6	0	1.943732	2.931028	-0.368018
15	6	0	0.639863	4.515412	1.022667
16	6	0	2.988375	3.916712	-0.411229
17	6	0	1.650331	5.446482	0.989765
18	1	0	-0.278335	4.731984	1.566757
19	6	0	2.820596	5.113686	0.253521
20	1	0	3.628829	5.843390	0.213552

21	1	0	-1.238339	2.774640	0.967310
22	7	0	-0.465318	1.202392	-0.135017
23	8	0	2.134858	1.808831	-0.988104
24	6	0	4.240861	3.593040	-1.180920
25	1	0	4.729320	2.696462	-0.781482
26	1	0	4.013321	3.374007	-2.230900
27	1	0	4.952122	4.424304	-1.143984
28	6	0	1.546312	6.777402	1.694891
29	1	0	1.640857	7.615837	0.992512
30	1	0	0.584588	6.881570	2.207694
31	1	0	2.337669	6.899986	2.445936
32	7	0	-5.299865	0.681176	0.407834
33	7	0	-5.038478	-2.018174	-0.382640
34	8	0	-7.306798	-2.231718	-0.138946
35	1	0	-7.022771	-3.119925	-0.424512
36	6	0	-7.711417	0.438467	0.655249
37	1	0	-7.627362	1.490666	0.933966
38	1	0	-8.388969	0.341028	-0.201366
39	1	0	-8.167126	-0.121955	1.480304
40	7	0	-0.224537	-1.326442	-0.862863
41	1	0	-0.200202	-1.868852	-1.725654
42	1	0	0.208614	-1.923714	-0.130562
43	8	0	1.682205	-2.421476	0.849628
44	8	0	2.427746	-0.989821	-1.220178
45	6	0	3.754244	-0.616650	-1.488369
46	1	0	4.363236	-1.522278	-1.643132
47	1	0	3.837227	-0.004315	-2.399078
48	1	0	4.212659	-0.038996	-0.668415
49	6	0	4.660812	-5.445719	0.568020
50	6	0	4.395903	-4.828955	1.951906
51	6	0	3.656958	-3.490026	1.826537
52	6	0	2.290018	-3.677448	1.152731
53	6	0	2.406711	-4.552561	-0.076082
54	6	0	3.462522	-5.328593	-0.341583
55	1	0	5.523104	-4.951110	0.092933
56	1	0	3.785694	-5.524431	2.545451
57	1	0	3.519631	-3.014481	2.804331
58	1	0	2.184079	-1.962082	0.105352
59	1	0	1.564244	-4.517624	-0.766149
60	1	0	3.480124	-5.913573	-1.260935
61	1	0	4.250178	-2.797630	1.212936
62	1	0	5.338936	-4.697910	2.496171
63	1	0	4.949135	-6.501369	0.669339
64	1	0	1.603204	-4.154121	1.868388

9 C₁

Standard orientation:

Center Number	Atomic Number	Atomic Type	Coordinates (Angstroms)		
			X	Y	Z
1	8	0	2.365379	-0.010639	-0.199102
2	6	0	-1.885342	0.157494	-0.238553
3	6	0	-1.232820	-1.144287	0.256769
4	6	0	0.230619	-1.232857	-0.195451
5	6	0	1.055590	-0.071611	0.376176
6	6	0	0.329647	1.244950	0.219844
7	6	0	-0.971657	1.347445	-0.071963
8	1	0	-2.163660	0.060846	-1.300435
9	1	0	-1.272912	-1.172512	1.354585
10	1	0	0.685679	-2.185879	0.096556
11	1	0	2.249039	0.216698	-1.136266
12	1	0	0.941871	2.136301	0.350968
13	1	0	-1.417435	2.334236	-0.195620
14	1	0	0.275730	-1.180626	-1.294074
15	1	0	-1.799104	-2.013008	-0.099526
16	1	0	-2.829281	0.338353	0.293945
17	1	0	1.250817	-0.256102	1.441747

10 C₁

Standard orientation:

Center Number	Atomic Number	Atomic Type	Coordinates (Angstroms)		
			X	Y	Z
1	29	0	1.289297	-1.688267	-0.036604
2	6	0	-5.430383	1.537636	0.345196
3	6	0	-3.281986	0.750586	0.084950
4	6	0	-3.778674	-0.536910	-0.271944
5	6	0	-5.905497	0.225791	-0.025994
6	1	0	-1.562424	1.964373	0.458132
7	6	0	-1.891340	0.981265	0.140014
8	6	0	-2.859786	-1.568397	-0.572078
9	6	0	-1.507551	-1.322756	-0.515736
10	6	0	-0.995192	-0.032273	-0.167928
11	1	0	-3.244604	-2.547536	-0.841722
12	6	0	1.036965	1.206463	-0.145724
13	6	0	2.442611	1.388070	-0.090163
14	6	0	3.377100	0.289801	-0.042037
15	6	0	2.928269	2.729392	-0.109199

16	6	0	4.779325	0.611007	-0.011405
17	6	0	4.269565	3.024838	-0.073882
18	1	0	2.197881	3.536429	-0.148530
19	6	0	5.177582	1.930701	-0.024628
20	1	0	6.245075	2.147883	0.002614
21	1	0	0.444214	2.121176	-0.238729
22	7	0	0.408800	0.054161	-0.114404
23	8	0	3.041454	-0.960038	-0.040271
24	6	0	5.764330	-0.526301	0.036408
25	1	0	5.597421	-1.155795	0.918326
26	1	0	5.649670	-1.184796	-0.832751
27	1	0	6.793864	-0.155257	0.060625
28	6	0	4.785462	4.443526	-0.085273
29	1	0	5.441131	4.628678	-0.946184
30	1	0	3.963312	5.164973	-0.133560
31	1	0	5.371697	4.667979	0.815485
32	7	0	-4.141371	1.773630	0.394441
33	7	0	-5.122906	-0.776370	-0.322341
34	8	0	-7.244562	0.049160	-0.060286
35	1	0	-7.392402	-0.879081	-0.320317
36	6	0	-6.403499	2.632129	0.675868
37	1	0	-5.854838	3.539954	0.933833
38	1	0	-7.067803	2.835828	-0.172468
39	1	0	-7.047238	2.343652	1.515339
40	7	0	-0.507283	-2.329360	-0.796526
41	1	0	-0.434443	-2.528253	-1.794618
42	1	0	-0.665667	-3.216753	-0.317509
43	8	0	1.542315	-3.391896	0.559874
44	6	0	2.766136	-3.895551	1.001632
45	1	0	2.595763	-4.707555	1.730330
46	1	0	3.372019	-4.325128	0.181810
47	1	0	3.392817	-3.137361	1.500235

1TS11,12 C₁

Standard orientation:

Center Number	Atomic Number	Atomic Type	Coordinates (Angstroms)		
			X	Y	Z
1	29	0	-1.200810	-1.427701	-0.464240
2	6	0	5.676640	1.384269	-0.087090
3	6	0	3.475380	0.707619	-0.008230
4	6	0	3.879910	-0.649401	0.151290
5	6	0	6.059230	0.000339	0.083860
6	1	0	1.838260	2.072099	-0.231870

7	6	0	2.103720	1.034349	-0.063120
8	6	0	2.892810	-1.655521	0.262830
9	6	0	1.561820	-1.313151	0.212590
10	6	0	1.143820	0.041279	0.054700
11	1	0	3.204140	-2.687871	0.389410
12	6	0	-0.814910	1.382179	0.184010
13	6	0	-2.206680	1.666449	0.093000
14	6	0	-3.193020	0.665129	-0.209400
15	6	0	-2.610690	3.011089	0.334860
16	6	0	-4.565820	1.079929	-0.266680
17	6	0	-3.930090	3.401799	0.277530
18	1	0	-1.838950	3.743009	0.566020
19	6	0	-4.890840	2.402469	-0.029160
20	1	0	-5.939750	2.692289	-0.078990
21	1	0	-0.177910	2.219449	0.477510
22	7	0	-0.253140	0.220589	-0.040470
23	8	0	-2.921450	-0.591531	-0.418970
24	6	0	-5.617430	0.049219	-0.585600
25	1	0	-5.611580	-0.766971	0.147010
26	1	0	-6.615550	0.497549	-0.594200
27	1	0	-5.438870	-0.413111	-1.564350
28	6	0	-4.361500	4.827679	0.526040
29	1	0	-5.062560	4.895429	1.367800
30	1	0	-3.503130	5.467459	0.753920
31	1	0	-4.872560	5.252089	-0.347690
32	7	0	4.406590	1.708389	-0.131020
33	7	0	5.205320	-0.981661	0.196230
34	8	0	7.381090	-0.258671	0.123960
35	1	0	7.485840	-1.222051	0.240920
36	6	0	6.726480	2.449249	-0.214350
37	1	0	6.248930	3.423009	-0.339720
38	1	0	7.368490	2.473249	0.674110
39	1	0	7.380150	2.253509	-1.072490
40	7	0	0.493840	-2.286671	0.308830
41	1	0	0.277130	-2.491141	1.287650
42	1	0	0.761140	-3.174101	-0.116110
43	8	0	-1.734550	-2.939511	-1.297900
44	8	0	-3.647950	-4.325681	0.414820
45	6	0	-3.369190	-3.562651	1.521600
46	1	0	-2.425940	-3.829261	2.026170
47	1	0	-3.401750	-2.485041	1.297560
48	1	0	-4.195200	-3.751541	2.237910

11 C₁

Standard orientation:

Center Number	Atomic Number	Atomic Type	Coordinates (Angstroms)		
			X	Y	Z
1	29	0	-1.320290	-1.921576	0.171316
2	8	0	-1.603361	-3.557840	0.807821
3	6	0	5.248143	1.614351	0.245887
4	6	0	3.132555	0.725049	0.055011
5	6	0	3.680410	-0.560416	-0.225633
6	6	0	5.775134	0.302234	-0.047024
7	1	0	1.365993	1.886730	0.372559
8	6	0	1.733868	0.900963	0.110215
9	6	0	2.803396	-1.644733	-0.456523
10	6	0	1.443283	-1.448928	-0.403661
11	6	0	0.877588	-0.165704	-0.124234
12	1	0	3.227806	-2.620744	-0.673694
13	6	0	-1.208093	0.977872	-0.142246
14	6	0	-2.617835	1.098804	-0.082081
15	6	0	-3.499960	-0.040037	0.014662
16	6	0	-3.166126	2.414858	-0.155129
17	6	0	-4.916744	0.216451	0.038366
18	6	0	-4.519058	2.647497	-0.124836
19	1	0	-2.474532	3.252900	-0.231179
20	6	0	-5.375211	1.514074	-0.026505
21	1	0	-6.451493	1.682711	-0.002616
22	1	0	-0.657996	1.911072	-0.293537
23	7	0	-0.526280	-0.142328	-0.053655
24	8	0	-3.108144	-1.270266	0.058514
25	6	0	-5.845736	-0.963836	0.135702
26	1	0	-6.891660	-0.641540	0.155880
27	1	0	-5.705555	-1.646774	-0.710471
28	1	0	-5.641125	-1.552825	1.037278
29	6	0	-5.102265	4.038242	-0.191350
30	1	0	-5.764850	4.158174	-1.058542
31	1	0	-5.699937	4.268939	0.700247
32	1	0	-4.315610	4.795935	-0.267926
33	7	0	3.950766	1.799767	0.292234
34	7	0	5.032705	-0.747805	-0.273237
35	8	0	7.119761	0.179053	-0.082230
36	1	0	7.305259	-0.756631	-0.285213
37	6	0	6.177142	2.766346	0.498608
38	1	0	6.837697	2.557439	1.348461
39	1	0	6.826772	2.943334	-0.366891
40	1	0	5.593177	3.665390	0.704480
41	7	0	0.488259	-2.518145	-0.616629
42	1	0	0.800642	-3.401065	-0.214626

43 1 0 0.326675 -2.683874 -1.611561

11 C₁ open shell singlet (broken symmetry)
Standard orientation:

Center Number	Atomic Number	Atomic Type	Coordinates (Angstroms)		
			X	Y	Z
1	29	0	-1.321057	-1.925220	0.158739
2	8	0	-1.631368	-3.583944	0.753504
3	6	0	5.240713	1.617626	0.257645
4	6	0	3.128814	0.721872	0.056977
5	6	0	3.681699	-0.561266	-0.224215
6	6	0	5.772969	0.307794	-0.036159
7	1	0	1.357674	1.876826	0.373081
8	6	0	1.729335	0.893254	0.107977
9	6	0	2.808971	-1.647972	-0.459967
10	6	0	1.448017	-1.456453	-0.412032
11	6	0	0.877796	-0.175771	-0.132327
12	1	0	3.236874	-2.622449	-0.676996
13	6	0	-1.205923	0.968255	-0.161498
14	6	0	-2.613356	1.099064	-0.092908
15	6	0	-3.498375	-0.033712	0.034772
16	6	0	-3.156598	2.416252	-0.183188
17	6	0	-4.913799	0.228081	0.073478
18	6	0	-4.508132	2.654354	-0.140734
19	1	0	-2.462671	3.249866	-0.282587
20	6	0	-5.367474	1.526256	-0.010178
21	1	0	-6.442634	1.700070	0.024190
22	1	0	-0.650474	1.895769	-0.325366
23	7	0	-0.527492	-0.154405	-0.065583
24	8	0	-3.107980	-1.263231	0.095879
25	6	0	-5.845672	-0.946455	0.205264
26	1	0	-6.889951	-0.619594	0.234195
27	1	0	-5.720002	-1.645288	-0.630141
28	1	0	-5.630625	-1.519810	1.114445
29	6	0	-5.087294	4.045744	-0.226168
30	1	0	-5.759950	4.151784	-1.087375
31	1	0	-5.673233	4.295192	0.668142
32	1	0	-4.298995	4.798929	-0.326497
33	7	0	3.942568	1.798705	0.299661
34	7	0	5.034773	-0.744165	-0.267229
35	8	0	7.118048	0.189010	-0.066518
36	1	0	7.307411	-0.745654	-0.270678
37	6	0	6.165041	2.772000	0.516490

38	1	0	6.823234	2.563191	1.368197
39	1	0	6.817185	2.953177	-0.346250
40	1	0	5.577427	3.668652	0.722420
41	7	0	0.494786	-2.525294	-0.627039
42	1	0	0.802550	-3.408254	-0.221424
43	1	0	0.334404	-2.693140	-1.621747

12 C₁

Standard orientation:

Center Number	Atomic Number	Atomic Type	Coordinates (Angstroms)		
			X	Y	Z
1	6	0	0.575017	0.000209	-0.012882
2	1	0	0.871214	-0.007846	1.057348
3	1	0	1.014774	0.911965	-0.451469
4	1	0	1.014129	-0.906015	-0.463614
5	8	0	-0.793778	0.000080	-0.008121

2,12TS14,15 C₁

Standard orientation:

Center Number	Atomic Number	Atomic Type	Coordinates (Angstroms)		
			X	Y	Z
1	8	0	2.104349	0.208368	-0.862662
2	6	0	-2.280219	-0.461156	-0.514978
3	6	0	-1.059778	-1.360241	-0.256985
4	6	0	-0.285572	-0.903092	0.987135
5	6	0	0.177715	0.540857	0.817116
6	6	0	-0.841081	1.447955	0.258377
7	6	0	-1.960426	1.001252	-0.346562
8	1	0	-2.676659	-0.638350	-1.524372
9	1	0	-1.375744	-2.405228	-0.155017
10	1	0	-0.928061	-0.974497	1.878480
11	1	0	0.683422	0.949925	1.700256
12	1	0	-0.659479	2.519008	0.328927
13	1	0	-2.688411	1.718778	-0.722735
14	1	0	1.085417	0.499679	-0.005018
15	1	0	0.574534	-1.559230	1.165950
16	1	0	-0.380718	-1.308985	-1.117199
17	1	0	-3.102183	-0.727470	0.170342

18	6	0	3.233046	-0.114798	-0.113271
19	1	0	4.030132	-0.350442	-0.838041
20	1	0	3.599754	0.714866	0.515157
21	1	0	3.101101	-1.009661	0.519589

14 C_s

Standard orientation:

Center Number	Atomic Number	Atomic Type	Coordinates (Angstroms)		
			X	Y	Z
1	6	0	-0.108186	-0.694320	1.274119
2	6	0	0.502718	-1.305691	0.000000
3	6	0	-0.108186	-0.694320	-1.274119
4	6	0	-0.108186	0.809006	-1.218098
5	6	0	-0.098409	1.478107	0.000000
6	6	0	-0.108186	0.809006	1.218098
7	1	0	-1.141713	-1.062139	1.400211
8	1	0	1.582547	-1.108573	0.000000
9	1	0	0.437306	-1.045154	-2.160460
10	1	0	-0.098916	2.567160	0.000000
11	1	0	-0.139485	1.370009	2.148664
12	1	0	-1.141713	-1.062139	-1.400211
13	1	0	0.374759	-2.394745	0.000000
14	1	0	0.437306	-1.045154	2.160460
15	1	0	-0.139485	1.370009	-2.148664

15 C_s

Standard orientation:

Center Number	Atomic Number	Atomic Type	Coordinates (Angstroms)		
			X	Y	Z
1	8	0	0.046868	-0.757690	0.000000
2	6	0	0.046868	0.660853	0.000000
3	1	0	-0.437012	1.086274	0.893285
4	1	0	1.094153	0.974885	0.000000
5	1	0	-0.437012	1.086274	-0.893285
6	1	0	-0.876287	-1.051030	0.000000

2,11TS13,14 C₁

Standard orientation:

Center Number	Atomic Number	Atomic Type	Coordinates (Angstroms)		
			X	Y	Z
1	29	0	0.910958	-0.591486	-0.956359
2	6	0	-6.210046	0.452720	0.966887
3	6	0	-4.008634	0.405867	0.292871
4	6	0	-4.260475	-0.746515	-0.507316
5	6	0	-6.437934	-0.710570	0.142926
6	1	0	-2.555302	1.801377	1.011957
7	6	0	-2.709965	0.954481	0.352498
8	6	0	-3.196763	-1.319319	-1.241767
9	6	0	-1.939512	-0.765871	-1.173684
10	6	0	-1.672862	0.391967	-0.377060
11	1	0	-3.396749	-2.196025	-1.850871
12	6	0	0.018419	2.023662	-0.019514
13	6	0	1.341415	2.533141	0.011408
14	6	0	2.489128	1.763615	-0.404554
15	6	0	1.509916	3.883665	0.439036
16	6	0	3.770633	2.419146	-0.377575
17	6	0	2.740247	4.493696	0.475410
18	1	0	0.623122	4.436319	0.746435
19	6	0	3.860608	3.725839	0.052473
20	1	0	4.842784	4.197632	0.065770
21	1	0	-0.769972	2.731521	0.253330
22	7	0	-0.328835	0.807040	-0.368729
23	8	0	2.441726	0.538559	-0.818009
24	6	0	4.977144	1.641447	-0.831658
25	1	0	5.878883	2.261267	-0.800674
26	1	0	5.142034	0.758161	-0.203264
27	1	0	4.842884	1.267898	-1.853516
28	6	0	2.923255	5.919453	0.936609
29	1	0	1.965696	6.375075	1.209156
30	1	0	3.580803	5.979762	1.813800
31	1	0	3.377316	6.542448	0.154928
32	7	0	-5.012337	0.983683	1.027023
33	7	0	-5.510477	-1.294526	-0.566846
34	8	0	-7.694284	-1.206957	0.122250
35	1	0	-7.673921	-1.981611	-0.469852
36	6	0	-7.335742	1.057126	1.755410
37	1	0	-6.966860	1.921705	2.310527
38	1	0	-8.153850	1.368998	1.095245
39	1	0	-7.759303	0.327528	2.455846
40	7	0	-0.798864	-1.307543	-1.880312
41	1	0	-0.784961	-1.019239	-2.859550
42	1	0	-0.766106	-2.326167	-1.860363

43	8	0	1.607482	-2.246005	-1.082388
44	6	0	3.792487	-4.236119	2.318617
45	6	0	3.408616	-4.694725	0.901889
46	6	0	4.213090	-3.936822	-0.163420
47	6	0	3.958226	-2.435408	-0.049501
48	6	0	3.965168	-1.929494	1.343951
49	6	0	3.894871	-2.734319	2.419174
50	1	0	3.059621	-4.607621	3.049145
51	1	0	3.553007	-5.778028	0.803106
52	1	0	5.287662	-4.140414	-0.031578
53	1	0	4.591052	-1.838711	-0.715798
54	1	0	4.010632	-0.850487	1.482925
55	1	0	3.919665	-2.301376	3.418914
56	1	0	2.860612	-2.260177	-0.503257
57	1	0	3.942156	-4.283921	-1.167160
58	1	0	2.343919	-4.490605	0.731361
59	1	0	4.753856	-4.687523	2.616413

2,11TS13,14 C₁ open shell singlet (broken symmetry)

Standard orientation:

Center Number	Atomic Number	Atomic Type	Coordinates (Angstroms)		
			X	Y	Z
1	29	0	0.952545	-0.602388	-1.069722
2	6	0	-6.098583	0.681946	0.957713
3	6	0	-3.903905	0.553993	0.272276
4	6	0	-4.208263	-0.571203	-0.547954
5	6	0	-6.379404	-0.455115	0.113301
6	1	0	-2.392466	1.875418	1.007991
7	6	0	-2.583345	1.046615	0.335320
8	6	0	-3.172431	-1.175066	-1.296913
9	6	0	-1.892883	-0.676280	-1.224107
10	6	0	-1.573144	0.455090	-0.409561
11	1	0	-3.410855	-2.031929	-1.920235
12	6	0	0.187468	2.004056	-0.009851
13	6	0	1.529087	2.457542	0.028302
14	6	0	2.640168	1.656853	-0.427824
15	6	0	1.759204	3.780767	0.510682
16	6	0	3.950615	2.252094	-0.379058
17	6	0	3.015573	4.332925	0.564570
18	1	0	0.899429	4.358743	0.846903
19	6	0	4.099944	3.533880	0.104618
20	1	0	5.102196	3.960585	0.133904
21	1	0	-0.568593	2.730155	0.302587

22	7	0	-0.213309	0.817080	-0.405257
23	8	0	2.535652	0.455430	-0.892687
24	6	0	5.117846	1.438035	-0.870175
25	1	0	6.050679	2.006761	-0.802225
26	1	0	5.230360	0.514034	-0.290656
27	1	0	4.970804	1.127205	-1.911118
28	6	0	3.264498	5.728636	1.083129
29	1	0	2.329975	6.213866	1.383124
30	1	0	3.930498	5.723064	1.955982
31	1	0	3.739947	6.363443	0.323978
32	7	0	-4.879202	1.160222	1.021992
33	7	0	-5.480624	-1.064542	-0.611672
34	8	0	-7.655823	-0.896784	0.089739
35	1	0	-7.671527	-1.660279	-0.516834
36	6	0	-7.194376	1.318741	1.762591
37	1	0	-6.786896	2.156190	2.332097
38	1	0	-8.000891	1.677486	1.112052
39	1	0	-7.646022	0.594642	2.451076
40	7	0	-0.780354	-1.252743	-1.950914
41	1	0	-0.786784	-0.983091	-2.935528
42	1	0	-0.763353	-2.271850	-1.912702
43	8	0	1.608547	-2.268001	-1.304048
44	6	0	2.944658	-4.204851	2.490054
45	6	0	2.686321	-4.734297	1.069528
46	6	0	3.766850	-4.249559	0.093135
47	6	0	3.781032	-2.722346	0.041633
48	6	0	3.697355	-2.082574	1.380958
49	6	0	3.325388	-2.744714	2.489766
50	1	0	2.055551	-4.355922	3.119057
51	1	0	2.629858	-5.830187	1.079054
52	1	0	4.752804	-4.618583	0.416885
53	1	0	4.610398	-2.324453	-0.555479
54	1	0	3.935185	-1.021884	1.443747
55	1	0	3.299312	-2.222439	3.445966
56	1	0	2.825702	-2.406230	-0.579507
57	1	0	3.586128	-4.653063	-0.909703
58	1	0	1.719021	-4.359095	0.711965
59	1	0	3.745101	-4.789613	2.973673

13 C₁

Standard orientation:

Center Number	Atomic Number	Atomic Type	Coordinates (Angstroms)		
			X	Y	Z

1	29	0	1.323196	-1.899009	0.097644
2	6	0	-5.260015	1.617971	0.259015
3	6	0	-3.145268	0.728596	0.059037
4	6	0	-3.693938	-0.558395	-0.213413
5	6	0	-5.788049	0.304727	-0.025626
6	1	0	-1.378319	1.893409	0.358417
7	6	0	-1.746419	0.905617	0.104002
8	6	0	-2.817758	-1.643728	-0.442639
9	6	0	-1.456771	-1.449523	-0.398933
10	6	0	-0.891791	-0.161654	-0.133206
11	1	0	-3.241874	-2.621955	-0.649372
12	6	0	1.188845	0.992279	-0.163253
13	6	0	2.599195	1.124302	-0.093147
14	6	0	3.490674	-0.002034	0.044942
15	6	0	3.135424	2.443258	-0.185300
16	6	0	4.902963	0.270596	0.090639
17	6	0	4.485682	2.692062	-0.137432
18	1	0	2.436864	3.272102	-0.292232
19	6	0	5.350716	1.571286	0.002889
20	1	0	6.424796	1.751092	0.041298
21	1	0	0.634133	1.922304	-0.317178
22	7	0	0.514337	-0.130888	-0.076574
23	8	0	3.107046	-1.235334	0.114818
24	6	0	5.844087	-0.895675	0.233014
25	1	0	6.886187	-0.561251	0.252674
26	1	0	5.640345	-1.457769	1.152241
27	1	0	5.720180	-1.606095	-0.592933
28	6	0	5.054231	4.087663	-0.227503
29	1	0	4.260312	4.833630	-0.337243
30	1	0	5.632438	4.347746	0.668853
31	1	0	5.731197	4.194534	-1.085244
32	7	0	-3.962435	1.804049	0.296955
33	7	0	-5.046736	-0.745875	-0.252171
34	8	0	-7.133191	0.180535	-0.052444
35	1	0	-7.318312	-0.756190	-0.250916
36	6	0	-6.187895	2.770766	0.512914
37	1	0	-5.602854	3.670715	0.711829
38	1	0	-6.842747	2.944470	-0.349324
39	1	0	-6.843317	2.565143	1.367547
40	7	0	-0.498438	-2.511532	-0.610789
41	1	0	-0.411534	-2.759910	-1.596725
42	1	0	-0.713274	-3.367801	-0.099671
43	8	0	1.608307	-3.592867	0.686823
44	1	0	2.525233	-3.710550	0.974767

O₂ D_{∞h}

Standard orientation:

Center Number	Atomic Number	Atomic Type	Coordinates (Angstroms)		
			X	Y	Z
1	8	0	0.000000	0.000000	0.607259
2	8	0	0.000000	0.000000	-0.607259

16 C₁

Standard orientation:

Center Number	Atomic Number	Atomic Type	Coordinates (Angstroms)		
			X	Y	Z
1	6	0	2.140517	-0.314116	-0.254179
2	6	0	0.992166	-1.331498	-0.325953
3	6	0	-0.070601	-1.026902	0.736016
4	6	0	-0.647926	0.376111	0.557720
5	6	0	0.383914	1.414861	0.231135
6	6	0	1.636735	1.099433	-0.116573
7	1	0	2.801072	-0.542392	0.597974
8	1	0	0.526697	-1.282577	-1.318287
9	1	0	-0.895344	-1.746487	0.705721
10	1	0	0.072857	2.455205	0.292647
11	1	0	2.350853	1.899925	-0.306588
12	1	0	0.372298	-1.084995	1.739843
13	1	0	1.376542	-2.350110	-0.201609
14	1	0	2.776946	-0.390151	-1.145762
15	1	0	-1.252076	0.663660	1.423760
16	8	0	-1.611260	0.378942	-0.581688
17	8	0	-2.731074	-0.245119	-0.262899

16TS17 C₁

Standard orientation:

Center Number	Atomic Number	Atomic Type	Coordinates (Angstroms)		
			X	Y	Z
1	6	0	-2.244386	0.050862	-0.171634
2	6	0	-1.464553	-1.170557	0.340516
3	6	0	-0.069606	-1.236614	-0.306232
4	6	0	0.695335	0.066375	-0.075620
5	6	0	-0.083655	1.306035	0.041654

6	6	0	-1.427153	1.311838	-0.055833
7	1	0	-2.542772	-0.104660	-1.221288
8	1	0	-1.356896	-1.095966	1.430030
9	1	0	0.527092	-2.060534	0.094885
10	1	0	0.479534	2.221353	0.203382
11	1	0	-1.960122	2.259747	-0.005907
12	1	0	-0.189290	-1.411174	-1.383818
13	1	0	-2.016681	-2.094029	0.131729
14	1	0	-3.181268	0.168360	0.387559
15	1	0	1.557743	0.180923	-1.051310
16	8	0	1.812160	-0.005643	0.770804
17	8	0	2.718686	0.001687	-0.423599

17 C₁

Standard orientation:

Center Number	Atomic Number	Atomic Type	Coordinates (Angstroms)		
			X	Y	Z
1	6	0	2.247656	-0.711840	0.082087
2	6	0	0.963480	-1.461333	-0.301059
3	6	0	-0.268101	-0.828754	0.361154
4	6	0	-0.368485	0.660874	0.073614
5	6	0	0.897294	1.399725	-0.079605
6	6	0	2.090207	0.778482	-0.051229
7	1	0	2.529314	-0.942418	1.122949
8	1	0	0.843600	-1.426792	-1.391763
9	1	0	-1.205530	-1.305873	0.060923
10	1	0	0.811884	2.476713	-0.196404
11	1	0	3.000716	1.372375	-0.123441
12	1	0	-0.195743	-0.934190	1.455650
13	1	0	1.040725	-2.518488	-0.024556
14	1	0	3.092812	-1.049280	-0.531217
15	1	0	-2.955606	0.155291	-0.039924
16	8	0	-1.448750	1.247870	0.011389
17	8	0	-3.593060	-0.604152	-0.116638

18 C₁

Standard orientation:

Center Number	Atomic Number	Atomic Type	Coordinates (Angstroms)		
			X	Y	Z
1	6	0	-1.819134	0.093660	0.131885

2	6	0	-1.075866	-1.163638	-0.342485
3	6	0	0.328718	-1.243373	0.271427
4	6	0	1.143295	0.022378	0.017904
5	6	0	0.380531	1.289621	-0.051952
6	6	0	-0.960786	1.326041	0.025528
7	1	0	-2.743244	0.236084	-0.443072
8	1	0	-1.652489	-2.063132	-0.098050
9	1	0	0.974024	2.195331	-0.147430
10	1	0	-1.471135	2.288807	0.014823
11	1	0	-0.988027	-1.130393	-1.436480
12	1	0	-2.140484	-0.025425	1.179885
13	1	0	0.898714	-2.099017	-0.103304
14	1	0	0.251538	-1.365250	1.363325
15	8	0	2.361320	0.001858	-0.080443

OH C_{∞v}

Standard orientation:

Center Number	Atomic Number	Atomic Type	Coordinates (Angstroms)		
			X	Y	Z
1	8	0	0.000000	0.000000	0.109192
2	1	0	0.000000	0.000000	-0.873537

19 C₁

Standard orientation:

Center Number	Atomic Number	Atomic Type	Coordinates (Angstroms)		
			X	Y	Z
1	6	0	-0.234792	1.048359	-0.125309
2	6	0	-1.466709	1.548379	0.017308
3	6	0	-2.713047	0.699627	0.029619
4	6	0	-2.391705	-0.789378	0.226386
5	6	0	-1.212913	-1.211854	-0.658452
6	6	0	0.051898	-0.426042	-0.302203
7	1	0	-1.598966	2.625079	0.123877
8	1	0	0.791189	-0.548333	-1.111703
9	1	0	-2.119513	-0.967713	1.273412
10	1	0	-3.276379	-1.400317	0.011419
11	1	0	-1.452519	-1.032449	-1.715616
12	1	0	-0.999942	-2.280852	-0.547474
13	1	0	0.626935	1.717053	-0.113344
14	8	0	0.584114	-1.010648	0.900774

15	1	0	1.218696	-0.382300	1.278914
16	1	0	-3.390969	1.053865	0.818263
17	1	0	-3.259701	0.850739	-0.915758
18	8	0	3.652136	0.040962	-0.663644
19	8	0	3.421848	0.363521	0.484609

19TS20 C₁

Standard orientation:

Center Number	Atomic Number	Atomic Type	Coordinates (Angstroms)		
			X	Y	Z
1	6	0	0.228488	0.900438	-0.784107
2	6	0	1.405248	1.443879	-0.393723
3	6	0	2.400229	0.671285	0.431062
4	6	0	2.222239	-0.841121	0.218652
5	6	0	0.765553	-1.277101	0.452483
6	6	0	-0.229034	-0.394905	-0.294182
7	1	0	1.662213	2.452695	-0.709068
8	1	0	-1.177835	0.088669	0.666194
9	1	0	2.508609	-1.085015	-0.812134
10	1	0	2.889397	-1.403453	0.881664
11	1	0	0.549946	-1.253902	1.530255
12	1	0	0.606774	-2.310376	0.126947
13	1	0	-0.454625	1.460215	-1.421227
14	8	0	-1.118202	-1.121291	-1.068708
15	1	0	-1.913322	-0.566130	-1.215621
16	1	0	3.420818	0.975478	0.166991
17	1	0	2.281217	0.919503	1.498694
18	8	0	-2.219883	0.429370	1.125525
19	8	0	-3.053105	0.405354	0.131457

20 C₁

Standard orientation:

Center Number	Atomic Number	Atomic Type	Coordinates (Angstroms)		
			X	Y	Z
1	6	0	0.003171	-0.516203	-0.768518
2	6	0	-0.992962	-1.471576	-0.540416
3	6	0	-2.204386	-1.120395	0.279209
4	6	0	-2.521266	0.384770	0.179875
5	6	0	-1.289576	1.251070	0.496639
6	6	0	-0.078785	0.775769	-0.251695

7	1	0	-0.897130	-2.465531	-0.966096
8	1	0	1.612524	-0.917887	0.589250
9	1	0	-2.855770	0.605746	-0.841528
10	1	0	-3.345858	0.648201	0.851812
11	1	0	-1.081283	1.241993	1.578721
12	1	0	-1.473012	2.301685	0.237531
13	1	0	0.850484	-0.766794	-1.408409
14	8	0	0.903241	1.705887	-0.378565
15	1	0	1.736175	1.255854	-0.625931
16	1	0	-3.070889	-1.709101	-0.047490
17	1	0	-2.045593	-1.389213	1.338573
18	8	0	2.589108	-0.958370	0.784014
19	8	0	3.141799	-0.075713	-0.040075

21 C₁

Standard orientation:

Center Number	Atomic Number	Atomic Type	Coordinates (Angstroms)		
			X	Y	Z
1	6	0	-0.354804	1.249470	-0.078779
2	6	0	1.032223	1.346736	-0.002864
3	6	0	1.872971	0.114703	0.196102
4	6	0	1.161008	-1.143217	-0.336802
5	6	0	-0.277827	-1.259411	0.199026
6	6	0	-1.014823	0.034171	0.025346
7	1	0	1.512354	2.318819	-0.060227
8	1	0	1.123973	-1.088949	-1.432252
9	1	0	1.730093	-2.043815	-0.078463
10	1	0	-0.264941	-1.542251	1.264403
11	1	0	-0.822150	-2.058497	-0.320190
12	1	0	-0.946673	2.156574	-0.213814
13	8	0	-2.377137	-0.098308	-0.006728
14	1	0	-2.774801	0.784245	-0.087570
15	1	0	2.846776	0.228801	-0.298417
16	1	0	2.099971	-0.023169	1.268178

OOH C_s

Standard orientation:

Center Number	Atomic Number	Atomic Type	Coordinates (Angstroms)		
			X	Y	Z
1	8	0	0.055873	0.720103	0.000000

2	8	0	0.055873	-0.611635	0.000000
3	1	0	-0.893969	-0.867745	0.000000

22 C₁

Standard orientation:

Center Number	Atomic Number	Atomic Type	Coordinates (Angstroms)		
			X	Y	Z
1	6	0	-0.362405	1.329448	0.113969
2	6	0	-1.681895	1.249656	-0.082699
3	6	0	-2.428651	-0.048481	-0.256559
4	6	0	-1.581869	-1.261229	0.159770
5	6	0	-0.160471	-1.139421	-0.402767
6	6	0	0.510862	0.113574	0.167918
7	1	0	-2.267905	2.167151	-0.113039
8	1	0	-1.526870	-1.311541	1.254174
9	1	0	-2.048891	-2.190422	-0.185371
10	1	0	-0.194264	-1.059576	-1.496464
11	1	0	0.453957	-2.011299	-0.151069
12	1	0	0.137706	2.280945	0.272685
13	8	0	1.039412	-0.048001	1.433051
14	1	0	1.881203	-0.533301	1.293579
15	1	0	-3.361295	-0.014475	0.321731
16	1	0	-2.738066	-0.144047	-1.309742
17	8	0	1.677054	0.418806	-0.789477
18	8	0	2.769908	-0.201394	-0.404108

22TS23 C₁

Standard orientation:

Center Number	Atomic Number	Atomic Type	Coordinates (Angstroms)		
			X	Y	Z
1	6	0	-0.294574	-1.194932	-0.487624
2	6	0	-1.557056	-1.363278	-0.056934
3	6	0	-2.413708	-0.233129	0.449077
4	6	0	-1.895377	1.129294	-0.035107
5	6	0	-0.381269	1.256592	0.209063
6	6	0	0.369620	0.112640	-0.451727
7	1	0	-2.000382	-2.357305	-0.085820
8	1	0	-2.102561	1.230450	-1.108209
9	1	0	-2.424194	1.944057	0.471961
10	1	0	-0.187405	1.234714	1.288946

11	1	0	0.015381	2.198631	-0.180856
12	1	0	0.284715	-2.018525	-0.895873
13	8	0	1.322891	0.359212	-1.294485
14	1	0	2.282001	0.232953	-0.690969
15	1	0	-3.452726	-0.385811	0.130575
16	1	0	-2.433173	-0.261614	1.550778
17	8	0	1.729179	-0.295432	1.073075
18	8	0	2.829495	-0.071362	0.441282

23 C₁

Standard orientation:

Center Number	Atomic Number	Atomic Type	Coordinates (Angstroms)		
			X	Y	Z
1	6	0	-0.058830	-0.799839	0.059159
2	6	0	-1.184990	-1.537754	0.083285
3	6	0	-2.570520	-0.952750	0.083463
4	6	0	-2.581427	0.493595	-0.431044
5	6	0	-1.471159	1.323193	0.228287
6	6	0	-0.107676	0.668246	0.090540
7	1	0	-1.102704	-2.623695	0.109240
8	1	0	-2.426307	0.484916	-1.517718
9	1	0	-3.558030	0.956973	-0.253116
10	1	0	-1.668363	1.422723	1.307385
11	1	0	-1.410493	2.337947	-0.176220
12	1	0	0.932093	-1.249409	0.040583
13	8	0	0.914496	1.359187	0.053319
14	1	0	2.504852	0.703139	-0.040354
15	1	0	-3.237679	-1.583453	-0.517416
16	1	0	-2.969960	-0.997388	1.110288
17	8	0	3.253163	-1.002464	-0.057334
18	8	0	3.430367	0.315789	-0.089085

References

- (1) Anastas, P. T.; Warner, J. C. *Green Chemistry Theory and Practice*; Oxford University Press: New York, 1998.
- (2) Rogers, R. D.; Seddon, K. R. *Science* **2003**, *302*, 792-793.
- (3) Ranke, J.; Stolte, S.; Stormann, R.; Arning, J.; Jastorff, B. *Chem. Rev.* **2007**, *107*, 2183-2206.
- (4) Schaffner, B. *Chem. Rev.* **2010**, *110*, 4554-4581.
- (5) Jutz, F.; Andanson, J.-M.; Baiker, A. *Chem. Rev.* **2011**, *111*, 322-353.
- (6) Corma, A.; Garcia, H. *Chem. Rev.* **2003**, *103*, 4307-4365.
- (7) Brink, G.-J. t.; Arends, I. W. C. E.; Sheldon, R. A. *Chem. Rev.* **2004**, *104*, 4105-4123.
- (8) Tietze, L. F.; Ila, H.; Bell, H. P. *Chem. Rev.* **2004**, *104*, 3453-3516.
- (9) Min, B. K.; Friend, C. M. *Chem. Rev.* **2007**, *107*, 2709-2724.
- (10) Akiyama, R.; Kobayashi, S. *Chem. Rev.* **2009**, *109*, 594-642.
- (11) Kobayashi, S.; Makino, A. *Chem. Rev.* **2009**, *109*, 5288-5353.
- (12) Polshettiwar, V.; Luque, R.; Fihri, A.; Zhu, H.; Bouhrara, M.; Basset, J.-M. *Chem. Rev.* **2011**, *111*, 3036-3075.
- (13) Walsh, P. J.; Li, H.; Parrodi, C. A. d. *Chem. Rev.* **2007**, *107*, 2503-2545.
- (14) Marins, M. A. P.; Frizzo, C. P.; Moreira, D. N.; Buriol, L.; Machado, P. *Chem. Rev.* **2009**, *109*, 4140-4182.
- (15) Dallinger, D.; Kappe, C. O. *Chem. Rev.* **2007**, *107*, 2563-2591.

- (16) Herrerias, C. I.; Yao, X.; Li, Z.; Li, C.-J. *Chem. Rev.* **2007**, *107*, 2546-2562.
- (17) Chanda, A.; Fokin, V. V. *Chem. Rev.* **2009**, *109*, 725-748.
- (18) Sheldon, R. A.; Lau, R. M.; Sorgedraeger, M. J.; Rantwijk, F. v.; Seddon, K. R. *Green Chem.* **2002**, *4*, 147.
- (19) Gutowski, K. E. *J. Am. Chem. Soc.* **2003**, *125*, 6632.
- (20) Ohno, H. *Ionic Liquids: The Front and Future of Material Developments*; CMC: Tokyo, 2003.
- (21) Rogers, R. D.; Seddon, K. R. In *ACS Symp. Ser. 856*; American Chemical Society: Washington, DC, 2003.
- (22) Rogers, R. D.; Seddon, K. R. In *ACS Symp. Ser. 818*; American Chemical Society: Washington DC, 2002.
- (23) Wasserscheid, P.; T., W. *Ionic Liquids in Synthesis*; Wiley-VCH: Weinheim, Germany, 2003.
- (24) Freemantle, M. In *Chem. Eng. News* 1998; Vol. 76, p 32.
- (25) Head-Gordon, T.; Hura, G. *Chem. Rev.* **2002**, *102*, 2651.
- (26) Bellissent-Funnel, M. C.; Done, J. C. *Hydrogen Bond Networks*; Kluwer Academic Publications: Boston, 1994.
- (27) Narayan, S.; Muldoon, J.; Finn, M. G.; Fokin, V. V.; Kolb, H. C.; Sharpless, K. B. *Angew. Chem. Int. Ed.* **2005**, *44*, 3275.
- (28) Rideout, D. C.; Breslow, R. *J. Am. Chem. Soc.* **1980**, *102*, 7816.
- (29) Grieco, P. A.; Garner, P.; He, Z. *Tetrahedron Lett.* **1983**, *24*, 1897.
- (30) Grieco, P. A.; Yoshida, K.; Garner, P. *J. Org. Chem.* **1983**, *48*, 3137.

- (31) Rideout, D. C.; Moitra, U.; Breslow, R. *Tetrahedron Lett.* **1983**, *24*, 1901.
- (32) Attanasi, O. A.; Crescentinia, L. D.; Filipponea, P.; Fringuelli, F.; Mantellinia, F.; Matteuccib, M.; Piernattib, O.; Pizzo, F. *Helv. Chim. Acta.* **2001**, *84*, 513.
- (33) Loncaric, C.; Manabe, K.; Kobayashi, S. *Adv. Synth. Catal.* **2003**, *345*, 475.
- (34) Rispens, T.; Engberts, J. B. F. N. *J. Org. Chem.* **2003**, *68*, 8520.
- (35) Li, Z.; Seo, T. S.; Ju, J. *Tetrahedron Lett.* **2004**, *45*, 3143.
- (36) Butler, R. N.; Coyne, A. G.; Moloney, E. M. *Tetrahedron Lett.* **2007**, *48*, 3501.
- (37) Butler, R. N.; Coyne, A. G.; Cunningham, W. J.; Moloney, E. M.; Burke, L. A. *Helv. Chim. Acta.* **2005**, *88*, 1611.
- (38) Gonzalez-Cruz, D.; Tejedor, D.; de Armas, P.; Morales, E. Q.; Garcia-Tellado, F. *Chem. Commun.* **2006**, 2798.
- (39) Gonzalez-Cruz, D.; Tejedor, D.; De Armas, P.; Garcia-Tellado, F. *Chem.-Eur. J.* **2007**, *13*, 4823.
- (40) Bala, K.; Hailes, H. C. *Synthesis* **2005**, 3423.
- (41) Demko, Z. P.; Sharpless, K. B. *J. Org. Chem.* **2001**, *66*, 7945.
- (42) Himo, F.; Demko, Z. P.; Noodleman, L.; Sharpless, K. B. *J. Am. Chem. Soc.* **2002**, *124*, 12210.
- (43) Himo, F.; Demko, Z. P.; Noodleman, L.; Sharpless, K. B. *J. Am. Chem. Soc.* **2003**, *125*, 9983.
- (44) Nicolaou, K. C.; Xu, H.; Wartmann, M. *Angew. Chem. Int. Ed.* **2005**, *44*, 756.

- (45) Das Sarma, K.; Pirrung, M. C. *J. Am. Chem. Soc.* **2004**, *126*, 444.
- (46) Pirrung, M. C.; Das Sarma, K. *Tetrahedron* **2005**, *61*, 11456.
- (47) Lin, Q.; O'Neil, J. C.; Blackwell, H. E. *Org. Lett.* **2005**, *7*, 4455.
- (48) Shapiro, N.; Vigalok, A. *Angew. Chem. Int. Ed.* **2008**, *47*, 2849.
- (49) Converso, A.; Burow, K.; Marzinzik, A.; Sharpless, K. B.; Finn, M. G. *J. Org. Chem.* **2001**, *66*, 4386.
- (50) Converso, A.; Saaidi, P. L.; Sharpless, K. B.; Finn, M. G. *J. Org. Chem.* **2004**, *69*, 7336.
- (51) Cozzi, P. G.; Zoli, L. *Green Chem.* **2007**, *9*, 1292.
- (52) Cozzi, P. G.; Zoli, L. *Angew. Chem. Int. Ed.* **2008**, *47*, 4162.
- (53) Wu, J. L.; Yue, C. Y. *Synth. Commun.* **2006**, *36*, 2939.
- (54) El-Batta, A.; Jiang, C. C.; Zhao, W.; Anness, R.; Cooksy, A. L.; Bergdahl, M. *J. Org. Chem.* **2007**, *72*, 5244.
- (55) Zhang, H. B.; Liu, L.; Chen, Y. J.; Wang, D.; Li, C. J. *Eur. J. Org. Chem.* **2006**, 869.
- (56) Podgorsek, A.; Stavber, S.; Zupan, M.; Iskra, J. *Green Chem.* **2007**, *9*, 1212.
- (57) Podgorsek, A.; Stavber, S.; Zupan, M.; Iskra, J. *Tetrahedron Lett.* **2006**, *47*, 1097.
- (58) Pravst, I.; Zupan, M.; Stavber, S. *Tetrahedron Lett.* **2006**, *47*, 4707.
- (59) Bourhani, Z.; Malkov, A. V. *Chem. Commun.* **2005**, 4592.
- (60) Li, H. J.; Zhao, J. L.; Chen, Y. J.; Liu, L.; Wang, D.; Li, C. J. *Green Chem.* **2005**, *7*, 61.

- (61) Price, B. K.; Tour, J. M. *J. Am. Chem. Soc.* **2006**, *128*, 12899.
- (62) Postigo, A.; Ferreri, C.; Navacchia, M. L.; Chatgililoglu, C. *Synlett* **2005**, 2854.
- (63) Postigo, A.; Kopsov, S.; Ferreri, C.; Chatgililoglu, C. *Org. Lett.* **2007**, *9*, 5159.
- (64) Wu, X. F.; Liu, J. K.; Li, X. H.; Zanotti-Gerosa, A.; Hancock, F.; Vinci, D.; Ruan, J. W.; Xiao, J. L. *Angew. Chem. Int. Ed.* **2006**, *45*, 6718.
- (65) Metzger, J. O. *Angew. Chem. Int. Ed.* **1998**, *37*, 2975.
- (66) Wang, Y.; Teng, X.; Wang, J.-S.; Yang, H. *Nano Lett.* **2003**, *3*, 789.
- (67) Mahapatro, A.; Kumar, A.; Kalra, B.; Gross, R. A. *Macromolecules* **2004**, *37*, 35.
- (68) Doll, K. M.; Shogren, R. L.; Willett, J. L.; Swift, G. *J. Polym. Sci., Part A: Polym. Chem.* **2006**, *44*, 4259.
- (69) Metzger, J. O.; Mahler, R. *Angew. Chem. Int. Ed.* **1995**, *34*, 902.
- (70) Biermann, U.; Metzger, J. O. *Top. Catal.* **2004**, *27*, 119.
- (71) Peng, J.; Deng, Y. *Tetrahedron Lett.* **2001**, *42*, 5917.
- (72) Togo, H.; Hirai, T. *Synlett* **2003**, 702.
- (73) Huang, J.; Jiang, T.; Gao, H.; Han, B.; Liu, Z.; Wu, W.; Chang, Y.; Zhao, G. *Angew. Chem. Int. Ed.* **2004**, *43*, 1397.
- (74) Ji, S.; Jiang, Z. Q.; Lu, J.; Loh, T. P. *Synlett* **2004**, 831.
- (75) Duan, Z.; Gu, Y.; Deng, Y. *Synth. Commun.* **2005**, *35*, 1939.
- (76) Wang, H.; Cui, P.; Zou, G.; Yang, F.; Tang, J. *Tetrahedron* **2006**, *62*, 3985.

- (77) Bram, G.; Decodts, G.; Bensaïd, Y.; Farnoux, C. C.; Galons, H.; Miocque, M. *Synthesis* **1985**, 543.
- (78) Tanaka, K.; Toda, F. *Chem. Rev.* **2000**, *100*, 1025.
- (79) Kuroda, R.; Imai, Y.; Sato, T. *Chirality* **2001**, *13*, 588.
- (80) Parkin, I. P. *Transition Met. Chem.* **2002**, *27*, 569.
- (81) Ravinder, V.; Rani, P. U.; Balaswamy, G. *Indian J. Heterocycl. Chem.* **2004**, *14*, 73.
- (82) Wang, Y. M.; Wen, Z.; Chen, X. M.; Du, D. M.; Matsuura, T.; Meng, J. B. *J. Heterocycl. Chem.* **1998**, *35*, 313.
- (83) Nagendrappa, G. *Resonance* **2002**, *7*, 64.
- (84) Shailaja, J.; Karthikeyan, S.; Ramamurthy, V. *Tetrahedron Lett.* **2002**, *43*, 9335.
- (85) Jacobsen, E. N.; Pfaltz, A.; Yamamoto, H. *Comprehensive Asymmetric Catalysis*; Springer: Berlin, 1999.
- (86) Zhou, J.; Ye, M. C.; Huang, Z. Z.; Tang, Y. *J. Org. Chem.* **2004**, *69*, 1309.
- (87) Anslyn, E. V.; Dougherty, D. A. *Modern Physical Organic Chemistry*; University Science, 2005.
- (88) Li, Z.; Jablonski, C. *Chem. Commun.* **1999**, 1531.
- (89) Dey, S.; Powell, D. R.; Hu, C.; Berkowitz, D. B. *Angew. Chem. Int. Ed.* **2007**, *46*, 7010.
- (90) Pui, A.; Mahy, J.-P. *Polyhedron* **2007**, *26*, 3143.
- (91) Lue, Z.; Yuan, M.; Pan, F.; Gao, S.; Zhang, D.; Zhu, D. *Inorg. Chem.* **2006**, *45*, 3538.

- (92) Marzano, C.; Pellei, M.; Colavito, D.; Alidori, S.; Lobbia, G. G.; Gandin, V.; Tisato, F.; Santini, C. *J. Med. Chem.* **2006**, *49*, 7317.
- (93) Bregman, H.; Williams, D. S.; Atilla, G. E.; Carroll, P. J.; Meggers, E. *J. Am. Chem. Soc.* **2004**, *126*, 13594.
- (94) Doctrow, S. R.; Huffman, K.; Marcus, C. B.; Tocco, G.; Malfroy, E.; Adinolfi, C. A.; Kruk, H.; Baker, K.; Lazarowych, N.; Mascarenhas, J.; Malfroy, B. *J. Med. Chem.* **2002**, *45*, 4549.
- (95) Samsel, E. G.; Srinivasan, K.; Kochi, J. K. *J. Am. Chem. Soc.* **1985**, *107*, 7606.
- (96) Jha, S. C.; Joshi, N. N. *Tetrahedron: Asymmetry* **2001**, *14*, 2463.
- (97) Taylor, M. S.; Jacobsen, E. N. *J. Am. Chem. Soc.* **2003**, *125*, 11204.
- (98) Vanderwal, C. D.; Jacobsen, E. N. *J. Am. Chem. Soc.* **2004**, *126*, 14724.
- (99) Stewart, I. C.; Bergman, R. G.; Toste, F. D. *J. Am. Chem. Soc.* **2003**, *125*, 8696-8697.
- (100) Kisanga, P. B.; Ilankumaran, P.; Fetterly, B. M.; Verkade, J. G. *J. Org. Chem.* **2002**, *67*, 3555-3560.
- (101) Zhou, Z. H.; Li, Z. M.; Wang, Q. Y.; Liu, B.; Li, K. Y.; Zhao, G. F.; Zhou, Q. L.; Tang, C. C. *Journal of Organometallic Chemistry* **2006**, *691*, 5790.
- (102) Huang, W.; Song, Y. M.; Bai, C. M.; Cao, G. Y.; Zheng, Z. *Tetrahedron Lett.* **2004**, *45*, 4763.
- (103) Ilyashenko, G.; Motevalli, M.; Watkinson, M. *Tetrahedron: Asymmetry* **2006**, *17*, 1625.

- (104) Belokon, Y. N.; Ishibashi, E.; Nomura, H.; North, M. *Chem. Commun.* **2006**, 1775.
- (105) Sawada, D.; Kanai, M.; Shibasaki, M. *J. Am. Chem. Soc.* **2000**, *122*, 10521.
- (106) Yabu, K.; Masumoto, S.; Yamasaki, S.; Hamashima, Y.; Kanai, M.; W., D.; Curran, D. P.; Shibasaki, M. *J. Am. Chem. Soc.* **2001**, *123*, 9908.
- (107) Belokon, Y. N.; Caveda-Cepas, S.; Green, B.; Ikonnikov, N. S.; Khrustalev, V. N.; Larichev, V. S.; Moskalenko, M. A.; North, M.; Orizu, C.; Tararov, V. I.; Tasinazzo, M.; Timofeeva, G. I.; Yashina, L. V. *J. Am. Chem. Soc.* **1999**, *121*, 3968.
- (108) Gregory, R. J. H. *Chem. Rev.* **1999**, *99*, 3649.
- (109) North, M. *Tetrahedron: Asymmetry* **2003**, *14*, 147.
- (110) Brunel, J.-M.; Holmes, I. P. *Angew. Chem. Int. Ed.* **2004**, *43*, 2752.
- (111) Matthews, B. R.; Gountzos, H.; Jackson, W. R.; Watson, K. G. *Tetrahedron Lett.* **1989**, *30*, 5157.
- (112) Ziegler, T.; Horsch, B.; Effenberger, F. *Synthesis* **1990**, 575.
- (113) Jackson, W. R.; Jacobs, H. A.; Matthews, B. R.; Jayatilake, G. S.; Watson, K. G. *Tetrahedron Lett.* **1990**, *31*, 1447.
- (114) Effenberger, F.; Stelzer, U. *Angew. Chem. Int. Ed.* **1991**, *30*, 873.
- (115) Tanaka, T.; Saito, B.; Katsuki, T. *Tetrahedron Lett.* **2002**, *43*, 3259.
- (116) Chatterjee, A.; Bennur, T. H.; Joshi, N. N. *J. Org. Chem.* **2003**, *68*, 5668.
- (117) Dioos, B. M. L.; Jacobs, P. A. *Tetrahedron Lett.* **2003**, *44*, 8815.
- (118) Dioos, B. M. L.; Jacobs, P. A. *Tetrahedron Lett.* **2003**, *44*, 4715.

- (119) Kwiatkowski, P.; Asztemborska, M.; Jurczak, J. *Tetrahedron: Asymmetry* **2004**, *15*, 3189.
- (120) Kwiatkowski, P.; Chaladaj, W.; Jurczak, J. *Tetrahedron Lett.* **2004**, *45*, 5343.
- (121) Kwiatkowski, P.; Chaladaj, W.; Jurczak, J. *Tetrahedron* **2006**, *62*, 5116.
- (122) Kureshy, R. I.; Singh, S.; Khan, N. H.; Abdi, S. H. R.; Agrawal, S.; Jasra, R. V. *Tetrahedron: Asymmetry* **2006**, *17*, 1638.
- (123) Miller, A. W.; Nguyen, T. S. *Org. Lett.* **2004**, *6*, 2301.
- (124) Colca, J. R.; McDonald, W. G.; Waldon, D. J.; Thomasco, L. M.; Gadwood, R. C.; Lund, E. T.; Cavey, G. S.; Mathews, W. R.; Adams, L. D.; Cecil, E. T.; Pearson, J. D.; Bock, J. H.; Mott, J. E.; Shinabarger, D. L.; Xiong, L.; Mankin, A. S. *J. Biol. Chem.* **2003**, *278*, 21972.
- (125) Gawley, R. E.; Campagna, S. A.; Santiago, M.; Ren, T. *Tetrahedron: Asymmetry* **2002**, *12*, 29.
- (126) Phoon, C. W.; Abell, C. *Tetrahedron Lett.* **1998**, *39*, 2655.
- (127) Danishefsky, S. J.; Deninno, M. P. *Angew. Chem. Int. Ed.* **1987**, *26*, 15.
- (128) Danishefsky, S. J. *Aldrichimica Acta* **1986**, *19*, 59.
- (129) Zhang, W.; Loebach, J. L.; Wilson, S. R.; Jacobsen, E. N. *J. Am. Chem. Soc.* **1990**, *112*, 2801.
- (130) Katsuki, T.; Sharpless, K. B. *J. Am. Chem. Soc.* **1980**, *102*, 5976-5978.
- (131) Finn, M. G.; Sharpless, K. B. *J. Am. Chem. Soc.* **1991**, *113*, 113-126.
- (132) Martinez, A.; Hemmert, C.; Meunier, B. *Journal of Catalysis* **2005**, *234*, 250.

- (133) Krawczyk, E.; Koprowski, M.; Ska, A. S.; Luczak, J. *Tetrahedron: Asymmetry* **2004**, *15*, 2599.
- (134) Zhang, H. B.; LI, C. *Tetrahedron* **2006**, *62*, 6640.
- (135) Wang, D.; Wang, M.; Wang, X.; Chen, Y.; Gao, A.; Sun, L. *Journal of Catalysis* **2006**, *237*, 248.
- (136) Smith, K.; Liu, C. H. *Chem. Commun.* **2002**, 886.
- (137) Egami, H.; Onitsuka, S.; Katsuki, T. *Tetrahedron Lett.* **2005**, *46*, 6049.
- (138) Murakami, M.; Uchida, T.; Katsuki, T. *Tetrahedron Lett.* **2001**, *42*, 7071.
- (139) Uchida, T.; Tamura, Y.; Ohba, M.; Katsuki, T. *Tetrahedron Lett.* **2003**, *44*, 7965.
- (140) Tamura, Y.; Uchida, T.; Katsuki, T. *Tetrahedron Lett.* **2003**, *44*, 3301.
- (141) Hoffmann, R. W. *Angew. Chem. Int. Ed.* **2001**, *40*, 1411.
- (142) Maryanoff, B. E.; Reitz, A. B. *Chem. Rev.* **1989**, *89*, 863.
- (143) Sun, W.; Yu, B.; Kuhn, F. E. *Tetrahedron Lett.* **2006**, *47*, 1993.
- (144) Ready, J. M.; Jacobsen, E. N. *Angew. Chem. Int. Ed.* **2002**, *41*, 1374.
- (145) Greatrex, B. W.; Jenkins, N. F.; Taylor, D. K.; Tiekink, E. R. T. *J. Org. Chem.* **2003**, *68*, 5205.
- (146) Greatrex, B. W.; Taylor, D. K. *J. Org. Chem.* **2005**, *70*, 470.
- (147) Song, Y. M.; Chen, H.; Hu, X.; Bai, C.; Zheng, Z. *Tetrahedron Lett.* **2003**, *44*, 7081.
- (148) Uchida, T.; Saha, B.; Katsuki, T. *Tetrahedron Lett.* **2001**, *42*, 2521.
- (149) Uchida, T.; Katsuki, T. *Tetrahedron Lett.* **2001**, *42*, 6911.

- (150) Kim, H. J.; Kim, W.; Lough, A. J.; Kim, B. M.; Chin, J. *J. Am. Chem. Soc.* **2005**, *127*, 12776.
- (151) Das, S.; Punniyamurthy, T. *Tetrahedron Lett.* **2003**, *44*, 6033.
- (152) Sezen, B.; Sames, D. *Org. Lett.* **2003**, *5*, 3607.
- (153) Sezen, B.; Sames, D. *J. Am. Chem. Soc.* **2003**, *125*, 10580.
- (154) Cavazzini, M.; Quici, S.; Pozzi, G. *Tetrahedron* **2002**, *58*, 3943.
- (155) Niimi, T.; Uchida, T.; Irie, R.; Katsuki, T. *Tetrahedron Lett.* **2000**, *41*, 3647.
- (156) Solomon, E. I.; Chen, P.; Metz, M.; Lee, S.-K.; Palmer, A. E. *Angew. Chem. Int. Ed.* **2001**, *40*, 4570.
- (157) Solomon, E. I.; Jones, P. M.; May, J. A. *Chem. Rev.* **1993**, *93*, 2623.
- (158) Klinman, J. P. *Chem. Rev.* **1996**, *96*, 2541.
- (159) Klinman, J. P.; Mu, D. *Annu. Rev. Biochem.* **1994**, *63*, 299.
- (160) Tanizawa, K. *J. Biochem.* **1995**, *118*, 671.
- (161) Whittaker, J. W. *Metal Ions in Biological Systems*; Marcel Dekker: New York, 1993.
- (162) Knowles, P. F.; Ito, N. *Perspect. Bioinorg. Chem.* **1993**, *2*, 208.
- (163) Solomon, E. I.; Sundaram, U. M.; Machonkin, T. E. **1996**, *Chem. Rev.*
- (164) Mayer, A. M.; Harel, E. *Phytochemistry* **1979**, *18*, 193.
- (165) Anthony, C. *The Biochemistry of Methyotrophs*; Academic Press: London, 1982.
- (166) Hyman, M. R.; Murton, I. B.; Arp, D. J. *Appl. Environ. Microbiol.* **1988**, *54*, 3187.

- (167) Juliette, L. Y.; Hyman, M. R.; Arp, D. J. *Appl. Environ. Microbiol.* **1993**, *59*, 3718.
- (168) Pratt, R. C.; Stack, T. D. P. *Inorg. Chem.* **2005**, *44*, 2367-2375.
- (169) Pratt, R. C.; Stack, T. D. P. *J. Am. Chem. Soc.* **2003**, *125*, 8716.
- (170) Storr, T.; Verma, P.; Pratt, R. C.; Wasinger, E. C.; Shimazaki, Y.; Stack, T. D. P. *J. Am. Chem. Soc.* **2008**, *130*, 15448.
- (171) Stubbe, J.; van der Donk, W. A. *Chem. Rev.* **1998**, *98*, 705-762.
- (172) Wu, X.; Gorden, A. E. V.; Tonks, S. A.; Vilseck, J. Z. *J. Org. Chem.* **2007**, *72*, 8691-8699.
- (173) Wu, X.; Gorden, A. E. V. *Eur. J. Org. Chem.* **2009**, 503.
- (174) Guardiola, F.; Codony, R.; Addis, P. B.; Rafecas, M.; Boatella, J. *Food Chem. Toxicol.* **1996**, *34*, 193-211.
- (175) Schroepfer, G. J. J. *Physiol. Rev.* **2000**, *80*, 361-544.
- (176) Guardiola, F.; Dutta, P. C.; Codony, R.; Savage, G. P. *Cholesterol and Phytosterol Oxidation Products: Analysis, Occurrence, and Biological Effects*; AOCS Press: Champaign, IL, 2002.
- (177) Parish, E. J.; Kizito, S. A.; Qiu, Z. *Lipids* **2004**, *39*, 801-804.
- (178) Arsenou, E. S.; Koutsourea, A. I.; Fousteris, M. A.; Nikolaropoulos, S. S. *Steroids* **2003**, *68*, 407-414.
- (179) Lee, J. W.; Fuda, H.; Javitt, N. B.; Strott, C. A.; Rodriguez, I. R. *Exp. Eye Res.* **2006**, *83*, 465.

- (180) Berthier, A.; Lemarie-Ewing, S.; Prunet, C.; Monier, S.; Athias, A.; Bessade, G.; Paisde Barros, J.-P.; Laubriet, A.; Gambert, P.; Lizard, G.; Nacel, D. *Cell Death Differ.* **2004**, *11*, 897.
- (181) Deckert, V.; Duverneuil, L.; Poupon, S.; Monier, S.; de Guen, N.; Lizard, G.; Masson, D.; Lagrost, L. *Br. J. Pharmacol.* **2002**, *137*, 655.
- (182) Steffen, Y.; Wiswedel, I.; Peter, D.; Schewe, T.; Sies, H. *Free Radicals Biol. Med.* **2006**, *41*, 1139.
- (183) Javitt, N. B. *Curr. Opin. Lipidol.* **2007**, *18*, 283.
- (184) Kasal, A. *Tetrahedron* **2000**, *56*, 3559.
- (185) Bora, U.; Chaudhuri, M. K.; Dey, D.; Kalita, D.; Kharmawphlang, W.; Mandal, G. C. *Tetrahedron* **2001**, *57*, 2445.
- (186) Salvador, J. A. R.; Silvestre, S. M.; Moreira, V. M. *Curr. Org. Chem.* **2006**, *10*, 2227-2257.
- (187) Liu, J.; Zhu, H. Y.; Cheng, X. H. *Synth. Commun.* **2009**, *39*, 1076-1083.
- (188) Parish, E. J.; Sun, H.; Kizito, S. A. *J. Chem. Res. Synop.* **1996**, *12*, 544-545.
- (189) Manahan, S. E. *Environmental Chemistry 7th ed.*; Lewis Pub.: Boca Raton, FL, 2000.
- (190) Silvestre, S. M.; Salvador, J. A. R. *Tetrahedron* **2007**, *63*, 2439.
- (191) Choi, H.; Doyle, M. P. *Org. Lett.* **2007**, *9*, 5349-5352.
- (192) Miller, R. A.; Li, W.; Humphrey, G. R. *Tetrahedron Lett.* **1996**, *37*, 3429-3432.
- (193) Salvador, J. A. R.; Silvestre, S. M. *Tetrahedron Lett.* **2005**, *46*, 2581-2584.

- (194) Salvador, J. A. R.; Clark, J. H. *Chem. Commun.* **2001**, 33-34, 33.
- (195) Yu, J. Q.; Corey, E. J. *Org. Lett.* **2002**, 4, 2727.
- (196) Shing, T. K. M.; Yeung, Y.-Y.; SU, P. L. *Org. Lett.* **2006**, 8, 3149-3151.
- (197) McLaughlin, E. C.; Choi, H.; Wang, K.; Chiou, G.; Doyle, M. P. *J. Org. Chem.* **2009**, 74, 730-738.
- (198) Ballini, R.; Bosica, G. *Tetrahedron* **1995**, 51, 4213.
- (199) Danishefsky, S.; Kahn, M. *Tetrahedron Lett.* **1981**, 22, 489.
- (200) *Comprehensive Organic Synthesis*; Page, P. C. B.; McCarthy, T. J., Eds.; Pergamon: Oxford, 1991; Vol. 7.
- (201) Trost, B. M.; Pergamon Press: Oxford, 1991; Vol. 7.
- (202) Salva, J.; Faulkner, D. J. *J. Org. Chem.* **1990**, 55, 1941.
- (203) Bollinger, P.; Zardin-Tartaglia, T. *Helv. Chim. Acta.* **1976**, 59, 1809.
- (204) Chexal, K. K.; Tamm, C.; Clardy, J. *Helv. Chim. Acta.* **1979**, 62, 1129.
- (205) Webb, J. S.; Cosulich, D. B.; Mowat, J. H.; Patrick, J. B.; Broschard, R. W.; Meyer, W. E.; Williams, R. P.; Wolf, C. F.; Fulmor, W.; Pidacs, C.; Lancaster, J. E. *J. Am. Chem. Soc.* **1962**, 84, 3185.
- (206) Seto, H.; Cary, L. W.; Tanabe, M. *J. Chem. Soc., Chem. Commun.* **1973**, 867.
- (207) Ballini, R.; Astolfi, P. *Liebigs Ann.* **1996**, 1879.
- (208) Dohi, T.; Takenaga, N.; Goto, A.; Fujioka, H.; Kita, Y. *J. Org. Chem.* **2008**, 73, 7365.
- (209) Ochiai, M.; Ito, T.; Takahashi, H.; Nakanishi, A.; Toyonari, M.; Sueda, T.; Goto, S.; Shiro, M. *J. Am. Chem. Soc.* **1996**, 118, 7716.

- (210) Zhao, Y.; Yeung, Y.-Y. *Org. Lett.* **2010**, *12*, 2128-2131.
- (211) Muzart, J. *Chem. Rev.* **1992**, *92*, 113.
- (212) Fousteris, M. A.; Koutsourea, A. I.; Nikolaropoulos, S. S.; Riahi, A.; Muzart, J. *J. Mol. Catal., A* **2006**, *250*, 70.
- (213) Yu, J. Q.; Corey, E. J. *Org. Lett.* **2002**, *4*, 2727.
- (214) Yu, J. Q.; Corey, E. J. *J. Am. Chem. Soc.* **2003**, *125*, 3232.
- (215) Yu, J. Q.; Corey, E. J. *Org. Lett.* **2005**, *7*, 1415.
- (216) Catino, A. J.; Forslund, R. E.; Doyle, M. P. *J. Am. Chem. Soc.* **2004**, *126*, 13622.
- (217) Catino, A. J.; Nichols, J. M.; Choi, H.; Gottipamula, S.; Doyle, M. P. *Org. Lett.* **2005**, *7*, 5167.
- (218) McLaughlin, E. C.; Doyle, M. P. *J. Org. Chem.* **2008**, *73*, 4317.
- (219) Jurado-Gonzalez, M.; Sullivan, A. C.; Wilson, J. R. H. *Tetrahedron Lett.* **2003**, *44*, 4283.
- (220) Salvador, J. A. R.; Clark, J. H. *Chem. Commun.* **2001**, *6*, 33.
- (221) Barton, D. R. H.; Le Gloahec, V. N. *Tetrahedron* **1998**, *54*, 15457.
- (222) Salvador, J. A. R.; Sa e Melo, M. L.; Campos Neves, A. S. *Tetrahedron Lett.* **1997**, *38*, 119.
- (223) Srinivasan, K.; Perrier, S.; Kochi, J. K. *J. Mol. Catal.* **1986**, *36*, 297.
- (224) Whittaker, J. W. *Chem. Rev.* **2003**, *103*, 2347-2363.
- (225) Whittaker, J. W. *Arch. Biochem. Biophys.* **2005**, *433*, 227-239.
- (226) Li, Y.; Wu, X.; Lee, T. B.; Isbell, E. K.; Parish, E. J.; Gordon, A. E. V. *J. Org. Chem.* **2010**, *75*, 1807.

- (227) Achord, J. M.; Hussey, C. L. *Anal. Chem.* **1980**, *52*, 601.
- (228) Rothenberg, G. *Catalysis: Concepts and Green Applications*; Wiley-VCH, 2008.
- (229) Kornblum, N.; DeLaMare, H. E. *J. Am. Chem. Soc.* **1951**, *73*, 880.
- (230) Kitajima, N.; Katayama, T.; Fujisawa, K.; Iwata, Y.; Moro-oka, Y. *J. Am. Chem. Soc.* **1993**, *115*, 7872.
- (231) Chen, P.; Fujisawa, K.; Solomon, E. I. *J. Am. Chem. Soc.* **2000**, *122*, 10177.
- (232) Holm, R. H.; Kennepohl, P.; Solomon, E. I. *Chem. Rev.* **1996**, *96*, 2239.
- (233) Solomon, E. I.; Tucek, F.; Root, D. E.; Brown, C. A. *Chem. Rev.* **1994**, *94*, 827.
- (234) Itoh, S. *Curr. Opin. Chem. Biol.* **2006**, *10*, 115.
- (235) Chen, P.; Solomon, E. I. *Proc. Natl. Acad. Sci* **2004**, *101*, 13105-13110.
- (236) Klinman, J. P. *J. Biol. Chem.* **2006**, *281*, 3013-3016.
- (237) Chen, P.; Solomon, E. I. *J. Am. Chem. Soc.* **2004**, *126*, 4991-5000.
- (238) Kodera, M.; Kita, T.; Miura, I.; Nakayama, N.; Kawata, T.; Kano, K.; Hirota, S. *J. Am. Chem. Soc.* **2001**, *123*, 7715-7716.
- (239) Crespo, A.; Marti, M. A.; E., R. A.; Amzel, L. M.; Estrin, D. A. *J. Am. Chem. Soc.* **2006**, *128*, 12817-12828.
- (240) Yoshizawa, K.; Kihara, N.; Kamachi, T.; Shiota, Y. *Inorg. Chem.* **2006**, *45*, 3034-3041.
- (241) Decker, A.; Solomon, E. I. *Curr. Opin. Chem. Biol.* **2005**, *9*, 152-163.

- (242) Lucas, H. R.; Li, L.; Narducci Sarjeant, A. A.; Vance, M. A.; Solomon, E. I.; Karlin, K. D. *J. Am. Chem. Soc.* **2009**, *131*, 3230-3245.
- (243) Mirica, L. M.; Ottenwaelder, X.; Stack, T. D. P. *Chem. Rev.* **2004**, *104*, 1013-1045.
- (244) Lewis, E. A.; Tolman, W. B. *Chem. Rev.* **2004**, *104*, 1047-1076.
- (245) Hatcher, L. Q.; Karlin, K. D. *J. Biol. Inorg. Chem.* **2004**, *9*, 669-683.
- (246) Liang, H. C.; Dahan, M.; Karlin, K. D. *Curr. Opin. Chem. Biol.* **1999**, *3*, 168-175.
- (247) Ghosh, P.; Tyeklar, Z.; Karlin, K. D.; Jacobsen, R. R.; Zubieta, J. *J. Am. Chem. Soc.* **1987**, *109*, 6889-6891.
- (248) Jacobsen, R. R.; Tyeklar, Z.; Farooq, A.; Karlin, K. D.; Liu, S.; Zubieta, J. *J. Am. Chem. Soc.* **1988**, *110*, 3690-3692.
- (249) Karlin, K. D.; Ghosh, P.; Cruse, R. W.; Farooq, A.; Gultneh, Y.; Jacobsen, R. R.; Blackburn, N. J.; Strange, R. W.; Zubieta, J. *J. Am. Chem. Soc.* **1988**, *110*, 6769-6780.
- (250) Karlin, K. D.; Cruse, R. W.; Gultneh, Y. *Chem. Commun.* **1987**, 599-600.
- (251) Karlin, K. D.; Cruse, R. W.; Gultneh, Y.; Hayes, J. C.; Zubieta, J. *J. Am. Chem. Soc.* **1984**, *106*, 3372-3374.
- (252) Pate, J. E.; Cruse, R. W.; Karlin, K. D.; Solomon, E. I. *J. Am. Chem. Soc.* **1987**, *109*, 2624-2630.
- (253) Kitajima, N.; Fujisawa, K.; Fujimoto, C.; Morooka, Y.; Hashimoto, S.; Kitagawa, T.; Toriumi, K.; Tatsumi, K.; Nakamura, A. *J. Am. Chem. Soc.* **1992**, *114*, 1277-1291.

- (254) Wada, A.; Harata, M.; Hasegawa, K.; Jitsukawa, K.; Masuda, H.; Mukai, M.; Kitagawa, T.; Einaga, H. *Angew. Chem. Int. Ed.* **1998**, *37*, 798-799.
- (255) Yamaguchi, S.; Nagatomo, S.; Kitagawa, T.; Funahashi, Y.; Ozawa, T.; Jitsukawa, K.; Masuda, H. *Inorg. Chem.* **2003**, *42*, 6968-6970.
- (256) Yamaguchi, S.; Wada, A.; Nagatomo, S.; Kitagawa, T.; Jitsukawa, K.; Masuda, H. *Chem. Lett.* **2004**, *33*, 1556-1557.
- (257) Fujii, T.; Naito, A.; Yamaguchi, S.; Wada, A.; Funahashi, Y.; Jitsukawa, K.; Nagatomo, S.; Kitagawa, T.; Masuda, H. *Chem. Commun.* **2003**, 2700-2701.
- (258) Ohta, T.; Tachiyama, T.; Yoshizawa, K.; Yamabe, T.; Uchida, T.; Kitagawa, T. *Inorg. Chem.* **2000**, *39*, 4358-4369.
- (259) Ohtsu, H.; Itoh, S.; Nagatomo, S.; Kitagawa, T.; Ogo, S.; Watanabe, Y.; Fukuzumi, F. *Inorg. Chem.* **2001**, *40*, 3200-3207.
- (260) Osako, T.; Nagatomo, S.; Tachi, Y.; Kitagawa, T.; Itoh, S. *Angew. Chem. Int. Ed.* **2002**, *41*, 4325-4328.
- (261) Cheruzel, L. E.; Cecil, M. R.; Edison, S. E.; Mashuta, M. S.; Baldwin, M. J.; Buchanan, R. M. *Inorg. Chem.* **2006**, *45*, 3191-3202.